Synthesis, characterization & bioactivities of chemically and biologically generated nanoparticles with special emphasis on antiproliferative potential in MCF 7 breast cancer cell line

Thesis submitted to
University of Calicut in partial fulfillment of
the requirement for the award of

DOCTOR OF PHILOSOPHY IN BIOTECHNOLOGY

By

SUHANA KOOTHRADAN

DEPARTMENT OF BIOTECHNOLOGY
UNIVERSITY OF CALICUT
KERALA, INDIA- 673 635
APRIL 2025

Synthesis, characterization & bioactivities of chemically and biologically generated nanoparticles with special emphasis on antiproliferative potential in MCF 7 breast cancer cell line

Ph.D. Thesis in Biotechnology under the School of Bioscience

Author

SUHANA KOOTHRADAN
Research Scholar
Department of Biotechnology
University of Calicut
Thenhipalam, Kerala- 673 635
E-mail: Suhana.k6@gmail.com

Supervising Teacher

Dr. Elyas K.K
Professor
Department of Biotechnology
University of Calicut
Thenhipalam, Kerala- 673 635
E-mail: kkelyas@yahoo.com

Department of Biotechnology
University of Calicut
Thenhipalam, Kerala- 673 635
April 2025

കാലിക്കറ്റ് സർവ്വകലാശാല
ജൈവ സാങ്കേതികവിദ്യാ പഠനവിഭാഗം
കാലിക്കറ്റ് യൂണിവേഴ്സിറ്റി പി.ഒ., മലപ്പുറം
കേരള - ഇന്ത്യ - 673 635

ഫോൺ നമ്പർ
വകുപ്പ് തലവൻ - 0494 2407403
ഓഫീസ് - 0494 2407404

UNIVERSITY OF CALICUT
DEPARTMENT OF BIOTECHNOLOGY
Calicut University (P.O.), Malappuram (Dist.),
Kerala - India - 673 635

Tel. No : Head - 0494 2407403
Office - 0494 2407404
e-mail : biotechhod@uoc.ac.in

Re-Accredited by NAAC with "A" Grade

No.DBT/104/Research/2026 – 27 **30.05.2026**

Regarding the submission of the corrected thesis of Ms Suhana Koothradan (Ref: U. O. No. 8539/2019/Admn)

Certificate

This is to certify that all corrections, as suggested by the Thesis adjudicators, have been incorporated in the thesis being resubmitted. Also, the contents in the thesis and the soft copy are the same.A detailed report on the corrections, including page number, is attached herewith. Please do the needful for conducting the Viva-Voce examination.

CU Campus

Prof (Dr). K. K. Elyas

Research Supervisor

Dr. ELYAS. K.K
PROFESSOR, DEPT. OF BIOTECHNOLOGY
UNIVERSITY OF CALICUT
KERALA, INDIA-673 635

Forwarded

Dr. Gopinathan.C
Professor & Head
Department of Biotechnology
University of Calicut
Malappuram-673 635, Kerala

DEPARTMENT OF BIOTECHNOLOGY
Date.....

UNIVERSITY OF CALICUT

CERTIFICATE ON PLAGIARISM CHECK

1.	Name of the Research Scholar	Suhana Koothradan	
2.	Title of thesis / dissertation	Synthesis, characterization & bioactivities of chemically and biologically generated nanoparticles with special emphasis on antiproliferative potential in MCF 7 breast cancer cell line	
3.	Name of the Supervisor	Dr. Elyas. K.K	
4.	Department/Institution	Department of Biotechnology, University of Calicut	
5.	Similar content (%) identified	Non Core **Introduction/ Theoretical overview/Review of literature/ Materials & Methods/ Methodology**	Core **Analysis/Result/Discussion / Summary/Conclusion/ Recommendations**
		5	**3**
	Acceptable maximum limit (%)	10	10
6.	Software used	iThenticate	
7.	Date of verification	15.04.25	

**Report on plagiarism check, specifying included/excluded items with % of similarity to be attached.*

Checked by (with name , designation & signature) Dr. Nasirudheen. T
Assistant Librarian
University of Calicut, Kerala.

Name and signature of the Researcher Suhana Koothradan

Name and signature of the Supervisor. 23/4/25
Prof.(Dr.)K.K ELYAS
Department of Biotechnology
University of Calicut,Kerala 673635

The Doctoral Committee* has verified the report on plagiarism check with the contents of the thesis, as summarized above and appropriate measures have been taken to ensure originality of the Research accomplished herein.

Name & Signature of the HoD/HoI (Chairperson of the Doctoral Committee)
Dr. Anu Joseph
Associate Professor & Head
Department of Biotechnology
University of Calicut
Malappuram-673635, Kerala

Date. 23.04.25

**In case of languages like Malayalam, Tamil etc..on which no software is available for plagiarism check, a manual check shall be made by the Doctoral Committee, for which an additional certificate has to be attached.*

UNIVERSITY OF CALICUT
DEPARTMENT OF BIOTECHNOLOGY

Dr. Elyas K.K
Professor

University of Calicut
Kerala, India- 673 635

Date: 23. 04. 2025

Certificate

This is to certify that the thesis entitled **"Synthesis, characterization & bioactivities of chemically and biologically generated nanoparticles with special emphasis on antiproliferative potential in MCF 7 breast cancer cell line''** is a report of the original work carried out by **Ms. Suhana Koothradan** under my supervision and guidance in the Department of Biotechnology, University of Calicut, Kerala and that no part thereof has been presented for the award of any other degree. The candidate has passed the coursework of the Ph.D. program in accordance with the UGC regulations.

C.U. Campus

Prof. (Dr.) Elyas K.K
(Research Supervisor)

UNIVERSITY OF CALICUT
DEPARTMENT OF BIOTECHNOLOGY

Date: 23. 04. 2025

Certificate

This is to certify that **Ms. Suhana Koothradan** has carried out the research work embodied in this thesis under the supervision and guidance of **Prof. (Dr.) Elyas K.K,** Department of Biotechnology, University of Calicut, Kerala for the full period prescribed under the Ph.D. ordinance of this University. I recommend her thesis entitled **"Synthesis, characterization & bioactivities of chemically and biologically generated nanoparticles with special emphasis on antiproliferative potential in MCF 7 breast cancer cell line''**, for submission for the degree of **Doctor Philosophy in Biotechnology** of the University of Calicut.

C.U. Campus

Head of the Department

DECLARATION

I hereby declare that the work presented in this Thesis entitled **"Synthesis, characterization & bioactivities of chemically and biologically generated nanoparticles with special emphasis on antiproliferative potential in MCF 7 breast cancer cell line''** submitted to the University of Calicut, as partial fulfillment of Ph.D. program for the award of the degree of Doctor of Philosophy in Biotechnology, is original and carried out by me under the supervision of **Prof. (Dr.) Elyas K.K**, Department of Biotechnology, University of Calicut. This has not been submitted earlier either in part or full for any degree or diploma of any University. The contents of the thesis have undergone a plagiarism check using 'iThenticate' software at C.H.M.K. Library, University of Calicut, and the similarity index found within the permissible limit. I also declare that the thesis is free from AI-generated content.

C.U. Campus
23rd April, 2025

Suhana Koothradan

Prof.(Dr.) Elyas K.K
Department of Biotechnology
University of Calicut.

ACKNOWLEDGEMENTS

I bow down before God Almighty for his blessings of health and happiness, but above all, I am thankful to him for the wisdom, skill, bravery, opportunity, tenacity, and inspiration bestowed upon me throughout my studies, among other things. I thank God for keeping the doors open and giving me the fortitude to go through life's challenges and crises.

I am incredibly grateful to Prof. (Dr.) Elyas.K. K, my research supervisor and teacher, for providing me with this esteemed opportunity to work under him. His enthusiasm for teaching and meticulousness are lessons I will carry with me as a researcher for the rest of my life. He allowed us to conduct any experiment related to our research without ever placing any pressure on us to complete our task. His extensive background and expertise influenced my papers and thesis. He helped me at every stage of the research process. I value him as a wonderful human being and an ideal research guide.

I would like to thank Dr. Anu Joseph, the department head, for the department's facilities as well as for her support and generosity. I appreciate the assistance of Acknowledgement: Dr. C. Gopinathan and Dr. V. B. Smitha, who are part of the department's teaching faculty. Thanks to the guest faculties, Dr. Anusha T S and Dr. Lakshmi Priya for their company and suggestions. I would like to express my profound gratitude to the department's non-teaching staff, including our librarian Santhosh, Iqbal, and Sreelatha, Technical assistant

Dr. K. M. Thara, Section assistant Sunanda, and Sudheesh, Typing assistant Sree Vidya, Lab attenders Jameela, Murali, Shambhu (late) and Lalitha, for all of the technical assistance during my research period.

Then, I want to express my gratitude to the University Grants Commission, Government of India for funding my studies through the junior and senior research fellowships. I am grateful to the UGC, for the timely disbursal of the fellowships, which enabled me to sustain my livelihood during the years of my research.

Now, I would like to express my sincere gratitude to my dear colleague, Dr. Safia, for introducing me to the realm of nanoparticles and providing me with fresh perspectives that enabled me to better organize my research. I appreciate her help at the beginning of my work. I acknowledge CSIF – University of Calicut, FACS facility – RGCB Trivandrum, NIT Calicut, and Care Keralam, and the technical assistants for all the help provided. I thank department of Chemistry, University of Calicut for providing the FTIR facility. I thank Athira from the Chemistry department for her patience in handling my numerous samples. Also, I extend my gratitude to the Department of Lifesciences, University of Calicut for providing space in their deep freezer to keep our samples. I thank the research scholars, especially Merin, from the Department of Lifesciences for their cooperation. I thank all other sister departments at the University of Calicut. I am grateful to Ms. Indhu Ramachandran and Ms. Arya Anoop, FACS facility RGCB Trivandrum, for technical assistance with flow

cytometry I also acknowledge Mr. Rajesh of Bina Photostat for technical assistance during the preparation of this Thesis.

To my favorite friends and seniors, Dr. Megha K. B. and Dr. Tancia Rosalin, I am so grateful for your warmth and support. I am deeply grateful for our friendship and for the wonderful experiences, we have shared. Thank you and love to all of my lab partners: Surya, Anju, Jesna, Reshma, and Jobish. I am grateful to Dr. Faisal, Remya, and Meghna for training me to do the animal cell culture effortlessly. You made it lighter for me. I thank the support from the other research scholars, Mubashira, Archana, Hana, Keerthy, Reshma, and Arya for all the encouragement and academic support extended to me.

I'm grateful for the affection and support I received from my university neighbors and all the other friends I made there at the convent. For their direct or indirect assistance in helping me finish this thesis, I would like to express my gratitude to all of my friends and their families. I owe a debt of gratitude to everyone in my life who helped make this thesis a reality; I am so grateful to have met you all.

Last but not least, I would like to thank my family for believing in me. To my beloved parents, it was not possible without your love, prayers, and physical and emotional support. I remember my father-in-law, who was so proud of me for pursuing a PhD. To my dear husband, you are the driving force behind each of my achievements. To my kids, Amlu, Allu, and Hadi, it was quite hard for you to be a PhD scholar's kid, but we persevered through it all. Thank you for understanding your mom.

ABSTRACT

This study aimed to develop novel nanoparticle-based treatment strategies for breast cancer. For that, we used both the chemical and biological synthesis approaches; The first approach created an effective drug delivery system using chemically synthesized Iron oxide Gold core-shell-nanoparticles (IONPs). A bacterial macrolide-derived compound, Rapamycin, which has already proven anti-proliferative ability in breast cancer cells, is used here to check the efficiency of the chemically synthesized nanocarrier system. In the second approach, the cell-free supernatant of the soil bacterial isolates was used to synthesize Gold nanoparticles with anti-proliferative properties in the human breast adenocarcinoma cell line, MCF-7. We also characterized the AuNPs and assessed their anti-oxidant, anti-fungal, and anti-bacterial properties.

The results documented the first report on the successful delivery of Rapamycin using the Au-IONP delivery system that successfully delivered and enhanced the anti-cancer activity of Rapamycin. And also, the first-ever production of gold nanoparticles from *Enterobacter hormaechei* soil isolates with exceptional anticancer and anti-bacterial potentials. This research successfully constituted two different methodologies for the synthesis of nanoparticles with comparable anti-proliferative effects in breast cancer cells.

Keywords: Iron oxide nanoparticles, Gold nanoparticles, Rapamycin, *Enterobacter hormaechei*, Fluoroquinolones, Breast Cancer,

സാരാംശം

സ്തനാർബുദത്തിനുള്ള നാനോപാർട്ടിക്കിൾ അടിസ്ഥാനമാക്കിയുള്ള പുതിയ ചികിത്സാ തന്ത്രങ്ങൾ വികസിപ്പിക്കുന്നതിനാണ് ഈ പഠനം ലക്ഷ്യമിടുന്നത്. അതിനായി ഞങ്ങൾ രാസപരവും ജൈവശാസ്ത്രപരവുമായ പ്രക്രിയകൾ ഉപയോഗിച്ചു; ആദ്യ സമീപനം രാസപരമായി സമന്വയിപ്പിച്ച അയൺ ഓക്സൈഡ് ഗോൾഡ് കോർ-ഷെൽ-നാനോപാർട്ടിക്കിൾസ് (Au-IONPs) ഉപയോഗിച്ച് ഫലപ്രദമായ മരുന്ന് വിതരണ സംവിധാനം സൃഷ്ടിച്ചു. സ്തനാർബുദ കോശങ്ങളിലെ ആൻ്റി-പ്രൊലിഫെറേറ്റീവ് കഴിവ് ഇതിനകം തെളിയിച്ചിട്ടുള്ള റാപാമൈസിൻ എന്ന ബാക്ടീരിയൽ മാക്രോലൈഡിൽ നിന്ന് ഉരുത്തിരിഞ്ഞ സംയുക്തം രാസപരമായി സംശ്ലേഷണം ചെയ്ത നാനോകാരിയർ സിസ്റ്റത്തിൻ്റെ കാര്യക്ഷമത പരിശോധിക്കാൻ ഇവിടെ ഉപയോഗിച്ചു. രണ്ടാമത്തെ സമീപനത്തിൽ, മനുഷ്യ സ്തന അഡെനോകാർസിനോമ സെൽ ലൈൻ ആയ MCF-7 ഇൽ ആൻ്റി-പ്രൊലിഫെറേറ്റീവ് ഗുണങ്ങളുള്ള സ്വർണ്ണ നാനോപാർട്ടിക്കിളുകളെ (AuNP) നിർമ്മിക്കാൻ മണ്ണിലെ ബാക്ടീരിയൽ ഐസൊലേറ്റുകളുടെ സെൽ-ഫ്രീ സൂപ്പർനാറ്റൻ്റ് ഉപയോഗിച്ചു. ഞങ്ങൾ AuNP-കളുടെ സ്വഭാവവും അവയുടെ ആൻറി-ഓക്സിഡൻ്റ്, ആൻറി ഫംഗൽ, ആൻറി ബാക്ടീരിയൽ ഗുണങ്ങളും വിലയിരുത്തി.

Au-IONP ഡെലിവറി സിസ്റ്റം ഉപയോഗിച്ച് റാപാമൈസിൻ വിജയകരമായി വിതരണം ചെയ്തതിൻ്റെ ആദ്യ റിപ്പോർട്ട് ഫലങ്ങൾ രേഖപ്പെടുത്തി, അത് റാപാമൈസിന്റെ കാൻസർ വിരുദ്ധ പ്രവർത്തനം വിജയകരമായി നൽകുകയും

മെച്ചപ്പെടുത്തുകയും ചെയ്തു. കൂടാതെ, മണ്ണിൽ നിന്ന് വേർതിരിച്ച *Enterobacter hormaechei* ബാക്ടീരിയ ഉപയോഗിച്ച് ആദ്യമായി സ്വർണ്ണ നാനോകണങ്ങളുടെ (AuNP) ഉത്പാദനം നടത്തുകയും അവയുടെ അസാമാന്യമായ ആൻറി-കാൻസർ, ആൻറി ബാക്ടീരിയൽ ഗുണങ്ങൾ തെളിയിക്കുകയും ചെയ്തു. ഈ ഗവേഷണം സ്തനാർബുദ കോശങ്ങളിലെ താരതമ്യപ്പെടുത്താവുന്ന ആൻ്റി-പ്രൊലിഫെറേറ്റീവ് ഇഫക്ടുകളുള്ള നാനോപാർട്ടിക്കിളുകളുടെ ഉത്പാദനത്തിനായി രാസപരവും ജീവശാസ്ത്രപരവുമായ രണ്ട് വ്യത്യസ്ത രീതികൾ വിജയകരമായി രൂപീകരിച്ചു.

സൂചകപദങ്ങൾ: അയൺ ഓക്സൈഡ് നാനോകണങ്ങൾ, ഗോൾഡ് നാനോകണങ്ങൾ, റാപാമൈസിൻ, ഇ. ഹോർമേച്ചെ, ഫ്ലൂറോക്വിനോലോണുകൾ, സ്തനാർബുദം,

Dedicated to…

My Parents, Husband, and Kids

"When you want something, all the universe conspires in helping you to achieve it"

Paulo Coelho

GRAPHICAL ABSTRACT

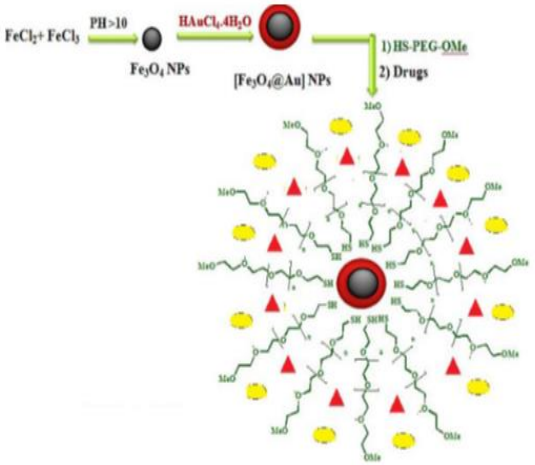

R-Au-IONPs

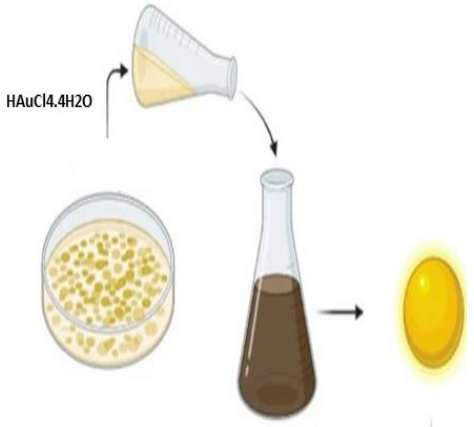

Au NPs

Nanoparticle characterization

Cytotoxicity assays in MCF 7 cells

CONTENTS

LIST OF TABLES

LIST OF FIGURES

ABBREVIATIONS

%	:	Percentage
°C	:	Degree Celsius
µg	:	Microgram
µL	:	Microliter
µm	:	Micrometer
ABTS	:	2,2'-azino-bis(3-ethylbenzothiazoline-6- sulfonic acid)
AFM	:	Atomic Force Microscopy
$AgNO_3$	:	Silver nitrate
Ag-NPs	:	Silver nanoparticles
ANOVA	:	Analysis of variance
AO	:	Acridine orange
AP	:	Aprotinin
Apaf	:	Apoptotic Protease Activating Factor
APS	:	Ammonium persulphate
ATCC	:	*American Type Culture Collection*
ATP	:	Adenosine triphosphate
Au-IONPs	:	Gold core-shell iron oxide nanoparticles
AuNPs	:	Gold nanoparticles
Bax	:	Bcl-2-associated X protein
Bcl-2	:	*B-cell leukemia/lymphoma 2*
BET	:	Brunauer-Emmett-Teller
BLAST	:	Basic local alignment search tool
BSA	:	Bovine serum albumin
BSS	:	Balanced salt solution
$CaCl_2$	:	Calcium chloride
$CHCl_3$	:	Chloroform

cm	:	Centimeter
cm−1	:	Wave number
CO_2	:	Carbon dioxide
cryo-TEM	:	Cryogenic Transmission Electron Microscopy
DAB	:	*3, 3'-Diaminobenzidine*
DCS	:	Differential Centrifugal Sedimentation
DLS	:	Dynamic Light Scattering
DMEM	:	Dulbecco's Modified Eagle's Medium
DMSO	:	Dimethyl sulfoxide
DNA	:	Deoxyribonucleic acid
DPPH	:	*2,2-diphenyl-1-picrylhydrazyl*
DTA	:	Differential Thermal Analysis
DTT	:	*Dithiothreitol*
EtBr	:	Ethidium bromide
EBSD	:	Electron Backscatter Diffraction
EDTA	:	Ethylenediaminetetraacetic acid
EELS	:	Electron Energy-Loss Spectroscopy
EPLS	:	Elliptically Polarized Light Scattering
EPM	:	Electrophoretic Mobility
EXAFS	:	Extended X-ray Absorption Fine Structure
FACS	:	*Fluorescence-activated cell sorting*
FBS	:	Fetal bovine serum
$FeCl_2$	:	Ferrous chloride
$FeCl_3$	:	Ferric chloride
FESEM	:	Field-emission scanning electron microscopy
FITC	:	*Fluorescein isothiocyanate*
FMR	:	Ferromagnetic Resonance
FTIR	:	Fourier transform infrared spectroscopy
g	:	Gram, gravity
GenBank	:	Genetic sequence database
GYE	:	Glycerol yeast extract agar

h, hr	:	hour
H_2O_2	:	Hydrogen peroxide
HCl	:	*H*ydrogen chloride *or hydrochloric acid*
HCT 116	:	Human colorectal carcinoma cell line
HEK	:	Human embryonic kidney cell line
HEPES	:	4-(2-hydroxyethyl)-1- piperazineethanesulfonic
hPBLs	:	Human peripheral blood lymphocytes
HRP	:	Horseradish peroxidase
HRTEM	:	High-resolution transmission electron microscopy
HSPEG-OMe	:	Thiol-Poly ethylene glycol
IARC	:	International Agency for Research on Cancer
IC	:	Inhibitory concentration
ICMR	:	Indian Council for Medical Research
ICP-MS	:	Inductively Coupled Plasma Mass Spectrometry
ICP-OES	:	Inductively Coupled Plasma Optical Emission Spectrometry
IgG	:	Immunoglobulin G
IONP	:	Iron oxide nanoparticles
$K_3Fe(CN)_6$	:	*Potassium hexacyanoferrate*
KBr	:	Potassium bromide
kDa	:	Kilodalton
Kg	:	Kilogram
Kv	:	Kilovolt
LC	:	Liquid chromatography
LC-QTOF-MS	:	Liquid chromatography-quadrupole time of flight - mass spectrometry
LEIS	:	Low-Energy Ion Scattering Spectroscopy
LP	:	Leupeptin
LSM	:	Lymphocyte separation medium
M	:	Molar
mA	:	Milli ampere

MALDI	:	Matrix-Assisted Laser Desorption/Ionization
MAPK	:	Mitogen-activated protein kinase
MCF-7	:	Human breast adenocarcinoma cell line
MEGA	:	Molecular evolutionary genetics analysis
MFM	:	Magnetic Force Microscopy
mg	:	Milligram
MGYPA	:	Malt Extract, Glucose, Yeast Extract, and Peptone agar
MIC	:	Minimum inhibitory concentration
Min	:	Minutes
mL	:	Milliliter
mm	:	Millimeter
mM	:	Millimolar
MMP	:	Mitochondrial membrane potential
MRI	:	Magnetic resonance imaging
MS	:	Mass spectrometry
mTOR	:	Mammalian target of rapamycin
MTT	:	3-(4, 5- dimethylthiazol-2-yl)-2, 5-diphenyltetrazolium bromide
MW	:	Molecular weight
Na_2CO_3	:	Sodium carbonate
Na_2HPO_4	:	Disodium hydrogen phosphate
NaCl	:	Sodium chloride
$NaHCO_3$	:	Sodium bicarbonate
NaOH	:	Sodium hydroxide
NaV	:	Sodium vanadate
NCBI	:	National center for biotechnology information
NCCS	:	National Centre for Cell Science
NCIM	:	National Collection of Industrial Microorganisms
ng	:	Nanogram
NH_4HCO_3	:	Ammonium bicarbonate

NIR	:	Near-infrared ray
nm	:	Nanometer
nM	:	Nanomolar
NMR	:	Nuclear magnetic resonance
NPs	:	Nanoparticles
NTA	:	Nanoparticle Tracking Analysi
^{o}C	:	Degree Celsius
OD	:	Optical density
P	:	Probability value
PAGE	:	*Polyacrylamide gel electrophoresis*
PARP	:	*Poly (ADP-ribose) polymerase*
PBS	:	Phosphate buffered saline
PDA	:	Potato dextrose agar
PEG	:	Polyethylene glycol
PI	:	Propidium iodide
PI3K	:	Phosphoinositide 3-kinase
PL	:	Photoluminescence
PS	:	Phosphatidylserine
PTA	:	Particle Tracking Analysis
PVDF	:	Polyvinylidene fluoride
Raf	:	Rapidly accelerated fibrosarcoma
Ras	:	Rat sarcoma
R-Au-I ONP	:	Rapamycin-loaded pegylated gold core-shell iron oxide nanoparticles
RBC	:	Red blood cell
RNA	:	Ribonucleic acid
RNase	:	Ribonuclease
RNase	:	Ribonuclease
ROS	:	Reactive oxidative species
rpm	:	*Revolutions per minute*
RPMI	:	Roswell Park Memorial Institute medium

RT	:	Room temperature, Retention time
SANS	:	Small-Angle Neutron Scattering
SAXS	:	Small-Angle X-ray Scattering
SC	:	Starch casein agar
SD	:	Standard deviation
SDS	:	*Sodium dodecyl sulfate*
SDS-PAGE	:	Sodium dodecyl sulfate-polyacrylamide gel electrophoresis
SEM	:	Scanning Electron Microscopy
SEM-EDX	:	Scanning Electron Microscopy with Energy-Dispersive X-ray Spectroscopy
SIMS	:	Secondary Ion Mass Spectrometry
Sp-ICP-MS	:	Single-Particle Inductively Coupled Plasma Mass Spectrometry
SQUID	:	Superconducting QUantum Interference Device
STEM	:	Scanning Transmission Electron Microscopy
T	:	Temperature
TBE	:	Tris Borate EDTA
TBS	:	Tris buffered saline
TBST	:	Tris buffered saline
TCA	:	Trichloroacetic acid
TEM	:	Scanning Transmission Electron Microscopy
TEMED	:	N,N,N',N'-Tetramethylethylenediamine
TGA	:	Thermogravimetric analysis
T*HP-1*	:	*Leukemia monocytic cell line*
Thr	:	Threonine
TOF	:	Time of flight
Tris-HCl	:	*Tris(hydroxymethyl)aminomethane*
Trp	:	Tryptophan
TRPS	:	Tunable Resistive Pulse Sensing
TRPS	:	Tunable Resistive Pulse Sensing

Tyr	:	Tyrosine
UV	:	Ultraviolet
UV-Vis	:	Ultraviolet-Visible Spectroscopy
v/v	:	Volume/volume
VEGFR	:	Vascular endothelial growth factor
VIS	:	Visible
VSM	:	Vibrating Sample Magnetometer
W	:	Watt
w/v	:	Weight/volume
WBC	:	White Blood cells
WCL	:	Whole cell lysis buffer
WHO	:	World Health Organization
XAS	:	X-ray Absorption Spectroscopy
XMCD	:	X-Ray Magnetic Circular Dichroism
XPS	:	X-ray Photoelectron Spectroscopy
XRD	:	X-ray diffraction
$\Delta\psi M$	:	Change in mitochondrial membrane potential

1. INTRODUCTION

1.1. Breast cancer; statistics and treatment

According to the WHO's 2022 GLOBOCAN registry data, breast cancer leads among females with over 2 million new cases globally. (Organization, 2024) According to the ICMR-NICPR, breast cancer prevails among Indian women and for every 2 women newly diagnosed with breast cancer, one woman dies of it in India. The data underlined the significant global burden of breast cancer, appealing to the development of more effective treatment options for it. At present, breast cancer is treated mainly by surgery, radiation therapy, and chemotherapy. Apart from surgery, chemotherapy remains the most favored treatment option even though it has many side effects. Throughout the years, Chemotherapeutic agents/pharmaceuticals persisted as the lead drugs for the treatment of many malignancies (Anand et al., 2023). Since they are Large-sized, these drugs/therapeutics have to deal with several barriers such as in-vivo stability, poor bioavailability/solubility/absorption, and may not get delivered to the target. These hurdles can be overcome by Bionanotechnology approaches in which the combination of biology and nanotechnology is employed.

1.2. Bionanotechnology in cancer treatment

'Bionanotechnology' is an interdisciplinary field comprising biology and nanotechnology in which, organisms or their components

are used to develop new nanomaterials or devices for application in medical, environmental, and industrial purposes. (Mishra et al., 2020) The key attributes of this field are; drug delivery, diagnostics, and therapeutics. (Lee & Moon, 2020) Metallic Nanoparticles (MNPs) are preferred in biological applications due to their unique surface properties which enhance their mechanical, magnetic, optical, and catalytic properties. They can rapidly circulate through the bloodstream and absorb large amounts of drugs. (Haleem et al., 2023) Generated from Gold, Silver, Iron, Copper, and other metals, they are being developed for use in the biomedical field, including cancer therapy, biosensing platforms, immunotherapy, regenerative medicine, tissue treatment, wound healing, and diagnostics. (Vijayaram et al., 2024)

1.3. Synthesis of metallic nanoparticles

Mainly three methods are in use for the production of MNPs; physical, chemical, and biological/green synthesis. The physical methods include pyrolysis, plasma arcing, sputter deposition, electrolysis, diffusion, laser ablation, evaporation-condensation, and high-energy ball milling. (Iravani et al., 2014) Chemical synthesis of NPs involves using different chemical precursors to produce nanoparticles under controlled reaction conditions. (Thanki et al., 2013) Chemically synthesized nanoparticles can be used for targeted drug delivery, which transports a known drug to desired locations of the body with enhanced bioavailability, biodistribution, and the ability to elude the immune system. (Di Stefano, 2023) These nanoparticle-

directed drugs/medicines are intended to act on a specific protein or mediator involved in cancer cell proliferation, thereby retarding their growth or inducing apoptosis of the cells. (Min & Lee, 2022)

In the biological/green synthesis of MNPs, natural or renewable materials such as plants and plant products, algae, fungi, yeast, bacteria, and viruses are used. Here, metal salts are mixed with the biological precursors to initiate the synthesis of nanoparticles. (Kuppusamy et al., 2016). The biosynthesized MNPs are capped with natural anti-cancer molecules produced by the natural resources used.

1.4. Iron Oxide Gold-core shell Nanoparticles (Au-IONPs)

Iron oxide (Fe3O4 and -Fe2O3) nanoparticles are biocompatible and Superparamagnetic with applications in drug delivery, magnetofection, hyperthermia, and magnetic resonance imaging. Even though they possess few limitations such as rapid agglomeration, oxidation in the tumor environment, chemical reactivity, and high superficial energy, which may result in the depletion of magnetic properties (Cândido et al., 2023). To overcome this, the Gold coating is used, it provides a shielding effect for the magnetic core, and serves as an active layer for loading bioactive molecules (Lau et al., 2023). By gold coating, the IONPs' colloidal stability and compatibility under physiological conditions are increased (Tonthat et al., 2023). Nanoparticle core–shells, with a ferrous core and a gold shell (Au-IONPs), have an inert surface and improved physical, chemical, and optical properties(Cândido et al., 2023).

Polyethylene glycol (PEG) is a linear polymer with chemically active hydroxyl groups at both ends. Biomolecules or nanoparticles can be conjugated to PEG through functional groups by a process called PEG-ylation. PEG-ylation improves the pharmacokinetic attributes of the molecules, drugs, or nanoparticles, such as less toxicity, increased half-life, escape from immune attack, and increased hydrophilicity. NPs can be PEG-ylated by covalent bonding to avoid the separation of PEG from the NP surface. (L. Shi et al., 2021)

1.5. Rapamycin as a breast cancer drug

Rapamycin is an mTOR (mammalian Target of Rapamycin) inhibitor and a bacterial macrolide-derived compound produced by *Streptomyces hygroscopicus.* (J. Li et al., 2014)(Guertin & Sabatini, 2009)(Betz & Hall, 2013). It possesses immunosuppressive and anti-proliferative properties in mammalian cells, and it was shown to be a potent inhibitor of S6K1 activation (Foster & Fingar, 2010). Rapamycin has been found effective in Primary Effusion Lymphoma (PEL) in culture and murine xenograft models. (Sin et al., 2007). Rapamycin also enhanced the ability of cisplatin, an alkylating agent, to induce apoptosis in the human promyelocytic leukaemia cell line HL-60 and the human ovarian cancer cell line SKOV3 (Y. Shi et al., 1995), mTOR pathway takes part in many signaling pathways such as phosphoinositide-3-kinase (PI3K)/AKT, tuberous sclerosis complex subunit 1 (TSC1)/tuberous sclerosis complex subunit 2 (TSC2)/Rheb, LKBL/adenosine 5′monophosphate-activated protein kinase (AMPK), VAM6/Rag GTPases and many more (Dowling et al., 2010). Thus,

mTOR inhibitors are extensively used in research including various tumors/cancers, organ transplantation, rheumatoid arthritis, etc. The Rapamycin analogs, Temsirolimus, and Everolimus are approved by the FDA for treating many cancers including breast and renal cancers (Zhu et al., 2019)..

1.6. Bacterial cultures in the synthesis of metallic nanoparticles

Microbial cells or cell-free supernatants are extensively used to synthesize MNPs due to their being harmless and cost-effective(Kapoor et al., 2021). The bacterial cell-free supernatants are excellent candidates for the production of metallic nanoparticles as they can be produced continuously and are renewable. Bacterial enzymes or secondary metabolites catalyze the synthesis of MNPs under suitable physiologic conditions and decide the morphology, size, and biological properties of the NPs(Kapoor et al., 2021). Microbial enzymes, proteins, reducing co-factors, and organic molecules act as capping agents in the synthesized NPs. (Asmathunisha & Kathiresan, 2013) Since gold is biocompatible and inert, its nanoparticles (AuNPs) find wide applications in surface modification, imaging, detection, and therapy (Hammami et al., 2021). When administered orally, the AuNP molecules are absorbed via passive/active diffusion in the gastrointestinal tract and distributed in the body through the venous system, they can also be administered straight to the organs or tissues of interest. (Ansari, 2019) Hence, Au NPs can be regarded as a potential candidate in cancer therapy.

1.7. MCF-7 cells as a breast cancer model

MCF-7 is a human breast adenocarcinoma cell line. It was isolated from a pleural effusion of a patient with metastatic breast cancer in 1970 and established as a cell line in 1973. (Comşa et al., 2015) It is a widely used model for studying breast cancer, particularly estrogen-dependent breast cancer, due to its estrogen receptor expression and ability to retain characteristics of differentiated mammary epithelium.

1.8. Regarding the doctoral research

This study aimed to develop novel nanoparticle-based treatment strategies for breast cancer. For that, we used both the chemical and biological synthesis approaches;

The first approach created an effective drug delivery system using chemically synthesized Iron oxide Gold core-shell-nanoparticles (IONPs). A bacterial macrolide-derived compound, Rapamycin, which has already proven anti-proliferative ability in breast cancer cells, is used here to check the efficiency of the chemically synthesized nanocarrier system.

In the second approach, the cell-free supernatant of the soil bacterial isolates was used to synthesize Gold nanoparticles with anti-proliferative properties in the human breast adenocarcinoma cell line, MCF-7. We also characterized the AuNPs and assessed their anti-oxidant, anti-fungal, and anti-bacterial properties.

1.9. About the Thesis

1.9.1. Objectives

1. To chemically synthesize gold-coated Iron Oxide nanoparticles and their characterization.
2. To load Rapamycin, a breast cancer drug, to the chemically synthesized gold-coated Iron Oxide nanoparticles and check the drug loading efficiency.
3. To biologically synthesize nanoparticles using the cell-free supernatants of soil bacterial isolates and screen for cytotoxicity.
4. To identify the bacterial strain involved in the production of the NPs through 16s rRNA sequencing.
5. To characterize the biologically synthesized nanoparticles for their structural and compositional analysis
6. To assess the anti-oxidant and anti-microbial activities of the biologically produced nanoparticles.
7. To elucidate the antiproliferative ability of the chemically and biologically generated nanoparticles using different viability, apoptosis, and cell cycle assays.

1.9.2. Thesis Layout

This doctoral Thesis is divided into seven chapters. The first chapter is the introduction, which briefly discusses the context, theme,

and objectives of the research work. Fig. 1.1 represents an outline of the study. The second chapter analyses the literature relative to the topic. A detailed description of all the materials and methods involved in this research is given in the third chapter. The results are divided into two chapters viz; 4, and 5. The nanoparticle synthesis and characterization data are covered in the fourth chapter; it gives a detailed description of the chemical synthesis of Iron oxide Gold-core-shell nanoparticles; loading of the bacterial-derived drug, Rapamycin to it (R-Au-IONPs), and the biological synthesis of Gold nanoparticles using a soil bacterial isolate (KDY2 NPs). It also describes the LC/Q-TOF/MS analysis and the anti-microbial effects of KDY2 NPs. The improved anti-cancer activity of Rapamycin in MCF-7 cells employing the Au-IONP drug delivery approach is discussed in chapter five. This chapter also describes the cellular and molecular evidence supporting KDY2 NPs' ability to inhibit MCF-7 cell proliferation by triggering apoptosis. In the sixth chapter, 'Conclusions', the results of the entire study are highlighted. In the seventh and last chapter, 'Recommendations', the applications and future perspectives of the study are discussed. An appendix with recipes for making the reagents and solutions and a thorough bibliography of all citations are discussed later. All of the acronyms, figures, and tables used in the thesis are listed in the pre-pages.

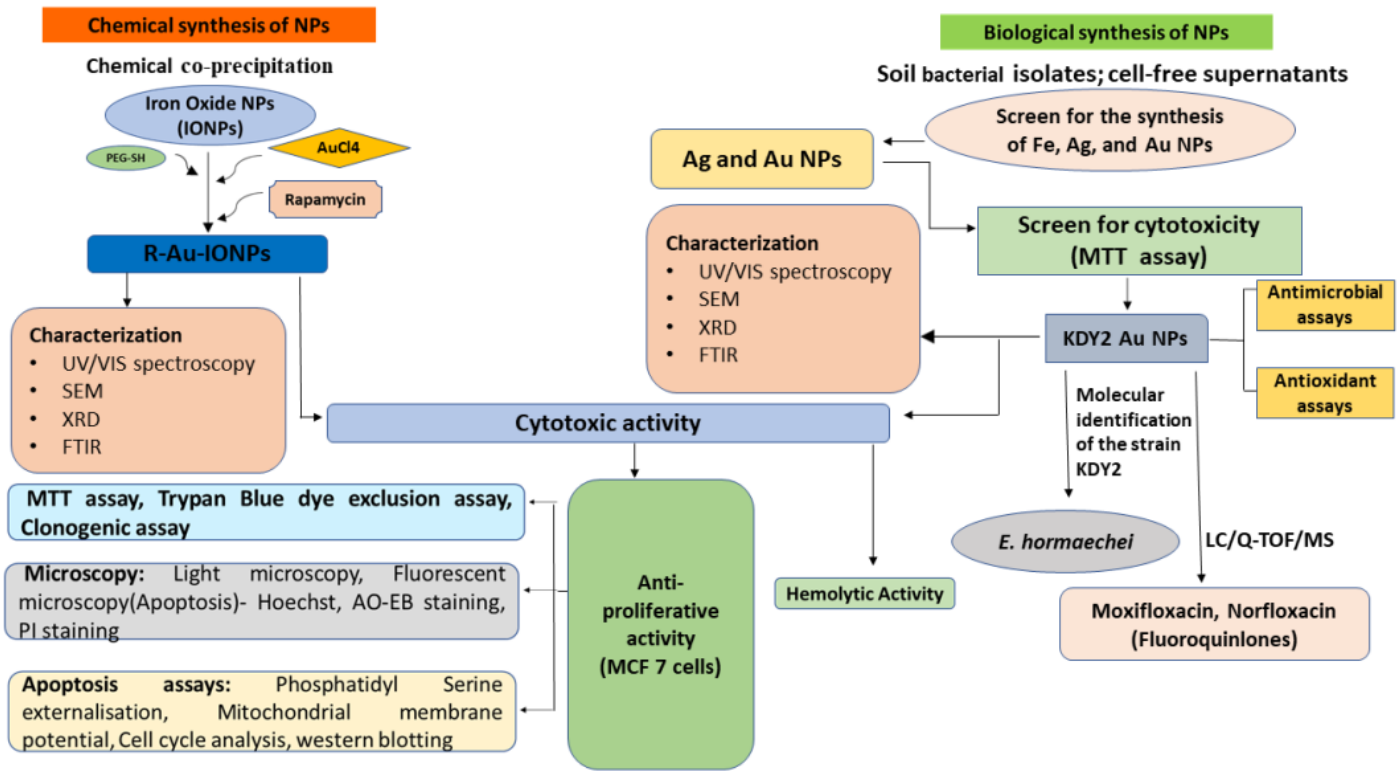

Fig. 1.1. Flowchart summarizing the research work carried out

2. REVIEW OF LITERATURE

2.1. Breast cancer; global statistics and treatment strategies

According to the GLOBOCAN 2022 survey conducted by the International Agency for Research on Cancer (IARC), there were 9.7 million cancer deaths with 20 million new cancer cases in 2022 worldwide. Almost half of the latest cases and deaths were reported from Asia. Among the various cancer types, breast cancer predominated among women while in males, lung cancer took the lead. (Organization, 2024) A recent study forecasted a 40% rise in new breast cancer cases up to 3 million per year and a 50% rise, i.e., more than 1 million deaths due to it annually by 2040. (Arnold et al., 2022) This scenario increases the urge to develop effective treatments for breast cancer.

Breast cancer is generated from the milk duct epithelium and it is developed in women at any time after puberty with increasing instances over aging. (Chavda et al., 2023) It is primarily classified based on the expression of Estrogen receptor (ER), Progesterone receptor (PR), and Human Epidermal growth factor receptor 2 (HER 2). It is reported that 80% of breast cancers reported in women are ER-positive (ER+). (Kohler et al., 2015) (Bonnie, 2020)

Neoadjuvant and adjuvant chemotherapy refers to drug administration before and after surgery to reduce the size of the tumor

and inhibit further cancer growth. (Kerr et al., 2022) Hormone therapy and chemotherapy are the neoadjuvant therapies opted for ER+ breast cancer. Hormone inhibitors like Tamoxifen, Fulvestrant, and Aromatase and the CDK4/6 inhibitors such as palbociclib, ribociclib, and abemaciclib are used in combination here. (Rodriguez et al., 2023) However, there exists the occurrence of resistance to these therapeutics over time, and it is mainly due to the modifications in survival mechanisms including RAS/MAPK/ERK and PI3K/AKT/mTOR pathways. (Xi & Ma, 2020) (Hanker et al., 2020) Many PI3K/AKT/mTOR inhibitors have been tested for their efficacy against ER + breast cancer, and the first mTOR inhibitor approved for the treatment of ER + HER2- breast cancer with resistance to hormone therapy was Everolimus. (Beaver & Park, 2012) Everolimus is a Rapamycin derivative that can be applied orally. Other survival mechanism inhibitors used are Polyadenosine diphosphate-ribose polymerase inhibitors, angiogenesis inhibitors, histone deacetylase (HDAC) inhibitors, poly (adenosine di-phosphate-ribose) polymerase (PARP) inhibitors, p53/mouse double minute 2 homolog (MDM2) inhibitors, hedgehog pathway blockers, tyrosine kinase inhibitors, and proteasome inhibitors. (Sawyers, 2004)

2.2. Limitations of current cancer treatment

Current cancer chemotherapeutics have many limitations including acquired resistance (Zugazagoitia et al., 2016), tumor heterogeneity (Parker et al., 2022), immune escape (Sterner & Sterner, 2021), low drug penetration (B. Liu et al., 2024), and accumulation of

mutation (Lee Ventola, 2017). Oral and intravenous administration of chemotherapeutic agents for the treatment of cancer remains common. However, the oral route has many challenges such as low bioavailability, gastrointestinal side effects, and first-pass metabolism. (Chaurasia et al., 2023) Also, these drugs are applied at very high concentrations resulting in various side effects to the body. (Torino et al., 2013) Most of this chemotherapeutics lack specificity, i.e., they are not able to act on the target cancer cells. (Anand et al., 2023) To improve the targeted delivery of chemotherapeutics, many strategies including nanoparticle-based drug delivery have been executed. (Chaurasia et al., 2023)

2.3. Nanotechnology in cancer diagnosis and treatment

Nanotechnology is the field of science and engineering where materials, structures, devices, and systems are designed, characterized, manufactured, and applied using materials that occur at nanoscale dimensions (10^{-9}). It is considered the most promising technology of the twenty-first century. In recent years, we have seen an unanticipated increase in the usage of nanoparticles in various domains, including molecular biology, physics, organic and inorganic chemistry, medicine, and material science (Chandrakala et al., 2022).

Nanoparticles are tiny structures with two or three dimensions ranging from 1 to 100 nm. (Sajid & Płotka-Wasylka, 2020). Their larger surface-to-volume ratio imparts them a distinct intrinsic reactivity. (Elahi et al., 2018) They include materials that are close in size to biomolecules and open up novel candidates in cell perturbation, patient

treatment, biological monitoring and identification, agriculture, and the food industry. The nanoformulations consisting of these nanoparticles loaded with different drug candidates have several favorable effects such as controlled drug release (Xie et al., 2016), targeted delivery of the drug (Cheng et al., 2023), enhanced bioavailability and circulation time of the therapeutics (N. Ahmad et al., 2022).

2.4. Nanoparticle classification

Nanoparticles are broadly classified into different groups based on their composition, structure, and chemical reactivity.

2.4.1. Carbon nanoparticles

These are carbon-based nanoparticles. Graphene Oxide, fullerenes, and carbon nanotubes are the major subgroups of this category. (Kadhum et al., 2024) (Holmannova et al., 2022) Stability, heat and electrical conductivity, strength, less toxicity, and biocompatibility make them favorable in applications like diagnostics and drug delivery. (Choudhary et al., 2014)

2.4.2. Metallic nanoparticles

Metallic Nanoparticles (MNPs) are generated from Gold, Silver, Iron, Copper, and other metals. They are being developed for use in the biomedical field, including biosensing platforms, immunotherapy, regenerative medicine, tissue treatment, wound healing, and diagnostics. (Vijayaram et al., 2024) Their unique surface properties enhance their mechanical, magnetic, optical, and catalytic

properties. MNPs can rapidly circulate through the bloodstream and absorb large amounts of drugs. (Haleem et al., 2023) Compared to traditional methods, nanoparticles made the non-invasive imaging and drug delivery systems more effective. (Mody et al., 2009)

2.4.3. Lipid-based nanoparticles

Lipid-based nanoparticles are ionizable lipids assembled in a spherical shape, they enter the cells by endocytosis, at physiological pH, they are not charged and at lower pH, they are positively charged. ("Let's Talk about Lipid Nanoparticles," 2021) These NPs are being extensively used in clinical imaging, nutrition, cosmetics, and agriculture. Also, as an mRNA carrier in RNA-based vaccines. (Tenchov et al., 2021)

2.4.4. Polymeric nanoparticles

Polymeric NPs are made up of different natural and synthetic polymers with sizes ranging from 1-1000nm. (Zielinska et al., 2020) Due to their biocompatibility, drug loading capacity, and biodegradability, they are widely used as drug nanocarriers. (Bhardwaj & Jangde, 2023) Chitosan, cellulose, gelatin, Polyethylene glycol (PEG), Polyhydroxyalkanoates (PHA), poly (lactic-co-glycolic acid) (PLGA), Polyvinyl alcohol (PVA), and Polycaprolactone (PCL) are the common polymers used in the generation of polymeric NPs.(Spirescu et al., 2021)

2.5. Metallic nanoparticles synthesis and characterization

Metallic nanoparticles are synthesized mainly by three different methods; top-down or physical method, bottom-up or chemical, and biological/green method. (Altammar, 2023) Figure 2.1 summarizes the different approaches adopted for metallic nanoparticle synthesis.

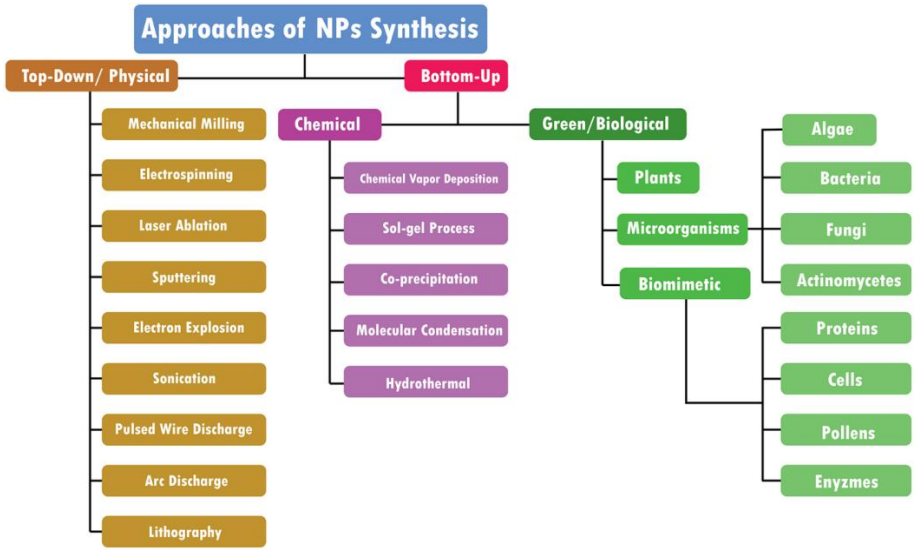

Fig. 2.1. Summarizing the physical, chemical, and biological methods employed for the synthesis of metallic nanoparticles. (Altammar, 2023)

2.5.1. Physical/ top-down method

This method converts larger or bulk materials into nano-sized particles by different physical processes. (Baig et al., 2021) The different techniques involved are, Laser ablation (Baig et al., 2021), mechanical milling (Lyu et al., 2017), electrospinning (R. Kumar et al., 2013), sputtering (Baig et al., 2021), electron explosion (Lyu et al.,

2017), sonication (Zheng et al., 2010), and Pulsed wire discharge method. (Patil et al., 2021)

2.5.2. Bottom-up method; chemical synthesis

In the bottom-up approach, small molecules or atoms are utilized to construct nanoparticles. (S. Kumar et al., 2018) Both chemical and biological methods come under this approach.

The chemical synthesis of nanoparticles is achieved by different methods such as Chemical vapor deposition (Machac et al., 2020), sol-gel process (Parashar et al., 2020), co-precipitation (Patil et al., 2021), Inert gas condensation/molecular condensation (Pérez-Tijerina et al., 2008), and Hydrothermal synthesis (Banerjee et al., 2008).

2.5.3. Bottom-up method; biological synthesis

In the biological/green synthesis approach, different metal nanoparticles are synthesized using various biological precursors including plant parts, fungi, algae, bacteria, and different biological wastes. (Kumari et al., 2021) This synthesis approach poses many benefits such as the NPs' biocompatibility, affordability, and stability with fast production time, less toxic by-products, and ease of scaling up for large-scale production. (Malhotra & Alghuthaymi, 2021) Figure 2.2 summarizes the different biological agents employed in the green synthesis of nanoparticles.

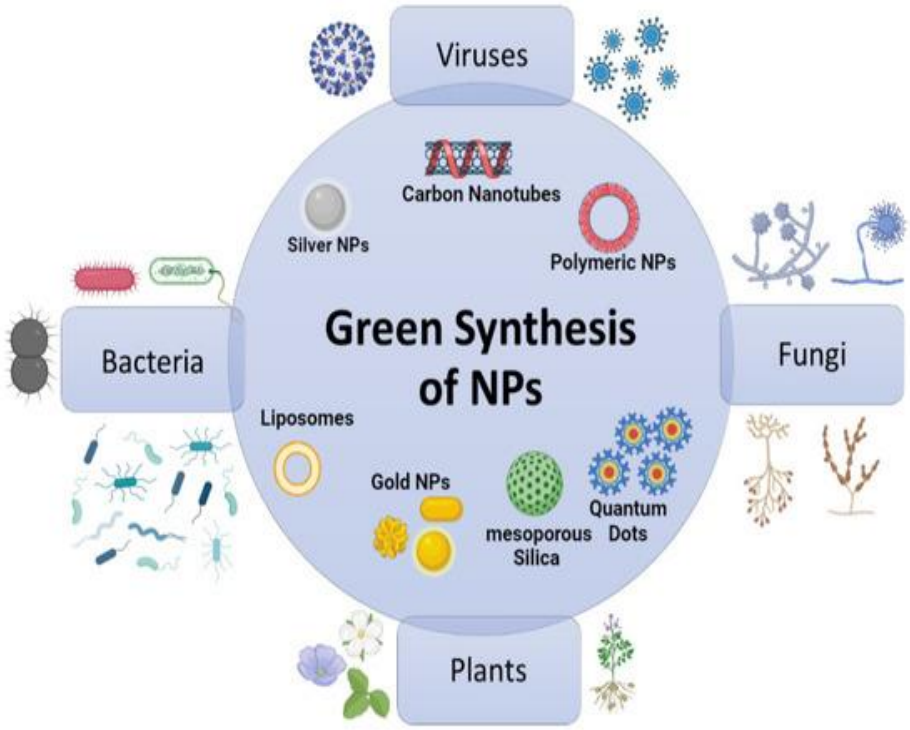

Fig. 2.2. Representation depicting the biological/green synthesis of different NPs using different organisms such as plants, bacteria, fungi, and viruses. (Venkatas et al., 2022)

2.6. Functionalization of metallic nanoparticles

The metallic nanoparticles have many limitations to be used in medical applications including targeted drug delivery. The major limitation is, low stability due to the tendency to agglomerate and rapid oxidization (Upadhyay et al., 2023a). Low targeting potential and high toxicity are the other limitations. (Thiruppathi et al., 2017) These can be overcome by the surface functionalization of the nanoparticles. Functionalization refers to the modification of the nanoparticle surface by different chemical or biological molecules to improve their stability, biocompatibility, and other pharmacokinetic attributes. (Comanescu, 2023) The NPs are usually modified using inert metals like gold and silver, polymers, organic molecules, and drug molecules. (Upadhyay et al., 2023b)

2.6.1. Methods of Functionalization

Nanoparticle surfaces are modified using organic and inorganic compounds for the desired effects. (F. Ahmad et al., 2022) Figure 2.3 illustrates the common materials used for nanoparticle functionalization. Different organic molecules such as thiols, amines, citrates, phosphates, and polymers like PEG, PLGA, PVA, polyacrylic acid, dextran, and chitosan are employed for this purpose. (Laurent et al., 2008) Insitu modification and post-annealing coating are the two methods used for the surface medication of nanoparticles. (F. Ahmad et al., 2022) in the Insitu modification method, the synthesis and surface modification of the NPs take place simultaneously. In the post-annealing modification, the NPs are modified after their synthesis. Ligand addition, ligand exchange, and encapsulation are used here.

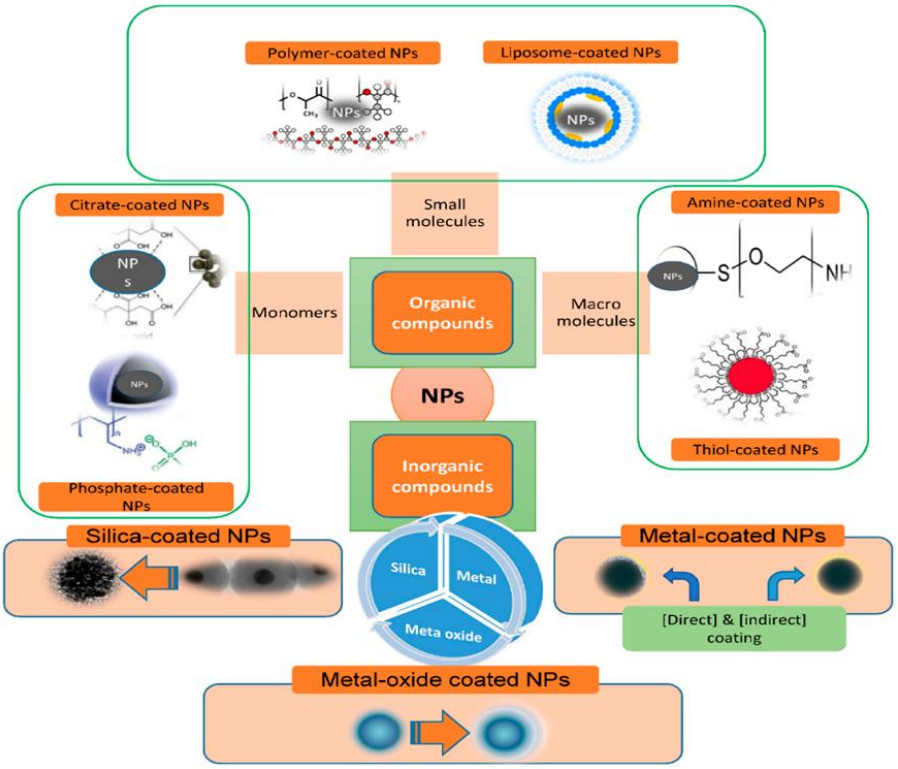

Fig.2.3. The functionalization of nanoparticles using different molecules such as Different organic and inorganic materials. (F. Ahmad et al., 2022)

In ligand addition, the functional group is added to the surface of the NPs without removing any ligand from its surface. In ligand exchange, one of the ligand molecules present on the NP surface is replaced with the added ligand of interest. (F. Ahmad et al., 2022) The ligands are attached via covalent interactions, hydrophobic interactions, ionic interactions, and adsorption. (F. Ahmad et al., 2022) Encapsulation enables the NPs to convert their hydrophobic surface to hydrophilic by covering them with amphiphilic molecules. (F. Ahmad et al., 2022)

2.6.2. PEG ylation of nanoparticles

PEG ylation is the process of attaching a polymer, polyethylene glycol (PEG), to therapeutic agents or nanoparticles to improve their pharmacological characteristics such as stability, hydrophilicity, increased circulation time, and escape from host immune responses. (Padín-González et al., 2022) PEG is a non-ionic polymeric molecule that can increase the molecular weight of the drugs, increase their solubility, decrease the excretion rates, and reduce the immunogenicity of the drugs. (Padín-González et al., 2022)

Thiol PEG is a modified form of polyethylene glycol with a thiol (SH) functional group at both ends (figure 2.4). (Wang et al., 2013) It is used for the surface modification of Gold nanoparticles to prevent flocculation of Au NPs. (Cobley et al., 2011) The Au-SH bond formed between Au NPs and thiol PEG stabilizes their interaction and helps to functionalize the Au NPs with different molecules/ compounds. (Han et al., 2020)

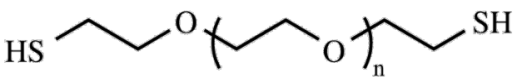

Fig. 2.4. Structure of Thiol-PEG (SH-PEG-SH)

2.7. Targeted drug delivery using nanoparticles.

To improve the stability, bioavailability, and biodistribution of the various therapeutic agents, nanoparticle-mediated delivery of them is utilized. (Di Stefano, 2023) These are particularly applied for targeting the drug candidates to the desired organs or tissues. (Marinelli et al., 2022) Figure 2.5 illustrates the targeted delivery of drugs into organs by the nanoparticles.

The therapeutics are delivered by passive or active targeting, passive targeting involves the nanocarrier transport via the body's physiological activity, while active targeting involves the use of ligand-receptor interactions. (A. Kumar et al., 2017) (Rani & Paliwal, 2014) Active targeting also involves the use of magnetic targeting and photothermal targeting. (Chitgupi et al., 2017)

Magnetic targeting makes use of the paramagnetic property of the metallic nanoparticles, especially Iron oxide nanoparticles and nanoparticles modified with iron oxide, and delivers the drug-loaded NPs to the targeted organs using external magnetic fields. (Rarokar et al., 2024) Photothermal therapy consists of light-responsive NPs like gold nanoparticles and laser radiations are used to accumulate the drug into the target tissue. (Aboeleneen et al., 2022)

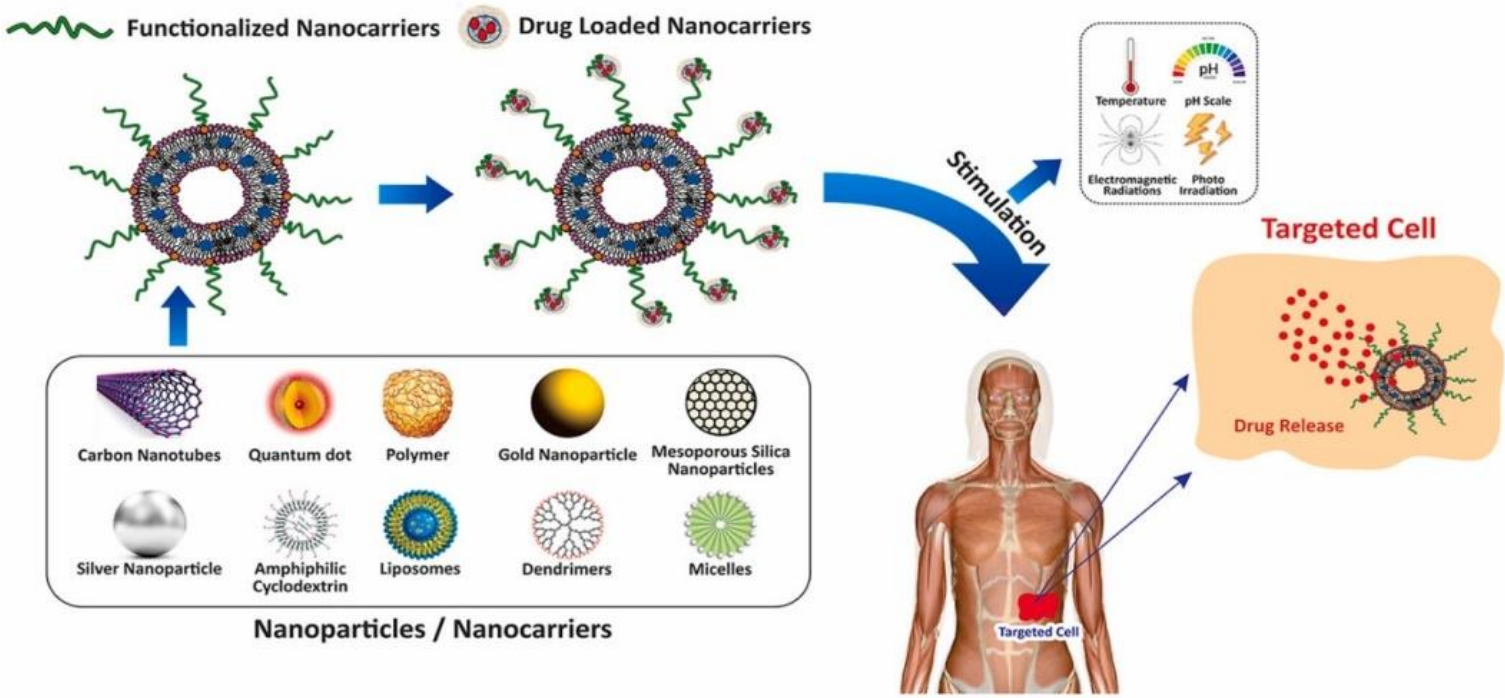

Fig.2.5. Illustration depicting the targeted delivery of drugs using nanocarrier systems employing magnetic, photothermal, and other methods. (Shah et al., 2021)

2.8. Iron oxide nanoparticles (IONPs)

Iron is regarded as an essential element with many biological roles in the human body. (Ling & Hyeon, 2013) Iron oxide nanoparticles possess unique characteristics such as paramagnetic properties, biocompatibility, cost-effectiveness, and environmental safety. (Salehirozveh et al., 2024) This makes them eligible for many applications including Magnetic resonance imaging (MRI), drug delivery, and tissue engineering. (Colombo et al., 2012)

2.8.1. Synthesis of Iron oxide nanoparticles

IONPs can be synthesized by physical, chemical, and biological methods. Common chemical methods used are chemical co-precipitation, hydrothermal synthesis, sol-gel process, thermal breakdown, sonochemical method, polyol method, and microemulsion method. (Salehirozveh et al., 2024)The chemical co-precipitation method is the most common approach as it is easy to synthesize IONPs and the precursors are harmless. (Osial et al., 2018) This involves the coprecipitation of Fe^{2+} and Fe^{3+} ions under low-temperature and alkaline pH yielding high purity IONPs with lower particle size. (Yazdani & Seddigh, 2016) The chemical reaction of the formation of Fe_3O_4 NPs is as follows,

$$Fe^{2+} + 2\ Fe^{3+} + 8\ OH^- \rightarrow Fe_3O_4 + 4H_2O$$

This method yields Magnetite nanoparticles (Fe_3O_4 NPs) effortlessly with preferable size, shape, and magnetic properties. (Lassoued et al., 2017) However, the Iron oxide nanoparticles exhibit certain drawbacks such as rapid oxidization, invitro toxicity at higher doses, and agglomeration. (Jun et al., 2008) Hence, they should be

modified to improve their pharmacological attributes. Different functionalization strategies are employed in iron oxide nanoparticles to make them useful in biomedical applications.

2.8.2. Iron oxide gold-core shell nanoparticles

The functionalization of IONPs is important as they tend to agglomerate, get oxidized, increase chemical reactivity, and high superficial energy, and consequently lose their magnetic property. (Cândido et al., 2023) Nanoparticles with an iron core coated with a gold shell will be more stable and easily functionalized with different drug molecules as the gold coating imparts a shielding effect on IONPs (Sanad et al., 2021) and improves the biological attributes of the nanoformulation without losing its properties. The gold coating prevents enzymatic degradation of the IONPs. (L. Wang et al., 2005) It also acts as a docking site for further modifications. (Huang et al., 2011)

2.9. Metallic nanoparticle synthesis using bacteria

The synthesis of metallic nanoparticles using microbes is considered more economical and eco-friendlier. (Castillo-Henríquez et al., 2020) Microbial cells are called nano factories and the synthesis of NPs using these helped in the development of nanobiotechnology. (Singh et al., 2023) The nanoparticle synthesis using bacteria can be done in three ways, by using living cells, using cell free supernatants, or by using cell lysates. (Campaña et al., 2023) The nanoparticle synthesis using the cell free supernatants has some added advantages such as easy downstream purification, direct visualization of the NP synthesis, and simpler characterization, also controlled synthesis is

possible as it is driven by the compounds and functional groups present in the cell free supernatant rather than the bacterial cells. (Campaña et al., 2023) These NPs are capped with bio-molecules which are bio compatible and no-toxic compounds with different biological activities, these molecules also act as stabilizing agents by preventing degradation and agglomeration of the NPs. (F. Ahmad et al., 2019) Table 2.1 summarizes some of the reported metallic nanoparticle produced using bacteria.

Table 2.1. Different metallic nanoparticles produced using various bacterial strains

Organism	**NP**	**Size**	**Morphology**	**Localization**	**References**
Bifidobacterium lactis	Au	5-40 nm	Hexagonal	Intracellular	(Chen et al., 2021)
Bacillus cereus	Au	20-50 nm	Spherical/Hexagonal/ Octagonal	Extracellular	(Pourali et al., 2017)
Caldicellulosiruptor changbaiensis	Au	1-20 nm	Not reported	Membrane	(Bing et al., 2018)
Escherichia coli	Au	6-60 nm	Spherical	Extracellular	(Chen et al., 2021)
Lactobacillus casei	Au	7-56 nm	Not reported	Membrane	(Kikuchi et al., 2016)
Pseudomonas stutzeri	Au	10-20 nm	Spherical	Not reported	(Desai et al., 2020)
Bacillus brevis	Ag	22-60 nm	Spherical	Supernatant	(Saravanan et al., 2021)
Bacillus cereus	Ag	5-7 nm	Not reported	Spherical	(Ibrahim et al., 2021)
Lactobacillus Acidophilus	Ag	10-20 nm	Spherical	Supernatant	(Abishad et al., 2022)
Pseudomonas aeruginosa	Ag	25 nm	Spherical	Supernatant	(Quinteros et al., 2019)
Pseudomonas stutzeri	Ag	22-46 nm	Spherical	Membrane/ Supernatant Extracellular	(Gopinath et al., 2017)
Escherichia coli	Pt	2.3-4.5 nm	Spherical	Not reported	(Attard et al., 2012)
Bacillus megaterium	Pd	10-40 nm	Anisotropic Spherical	Intracellular	(Omajali et al., 2019)
Bacillus cereus	Fe3O4	18-29 nm	Spherical	Supernatant	(Fatemi et al., 2018)
Escherichia coli	Fe3O4	18 nm	Spherical	Intra/Extracellular	(Crespo et al., 2017)

2.10. *E. hormaechei* as a potential candidate in nanoparticle synthesis

Enterobacter hormaechei is a Gram-negative opportunistic pathogenic bacterium found all over the environment. (Cao et al.,2022)

Monowar et al., 2021 demonstrated the production of Silver nanoparticles with significant anti-bacterial and anti-fungal activity using endophytic *E. hormaechei* strain. Also, the production of Tin nanoparticles with anti-bacterial, anti-larvicidal, anti-inflammatory, and anti-aging properties was reported using the soil isolate of *E. hormaechei* EAF63 strain. (Rizwan et al., 2023)

The mechanism of nanoparticle formation by *E. hormaechei* is not well known, the reducing enzymes present in the culture, pH, and temperature may play crucial roles in the generation of nanoparticles with optimum size, and the biological activities are supposed to be contributed by the capping molecules from the bacterial cells/culture supernatant. (Rai et al., 2009)

2.11. Characterization of nanoparticles

The characterization of the synthesized nanoparticles is crucial to determine and quantify their properties such as size, shape, composition, and behavior. (Mourdikoudis et al., 2018) The size distribution, surface area, surface charge, degree of aggregation, and surface chemistry can also be examined by different techniques. The major characterization techniques used are summarized in Table 2.2.

Table. 2.2. Different characterization methods to determine nanoparticle properties (Mourdikoudis et al., 2018)

Entity characterized	**Characterization techniques suitable**
Size (structural properties)	TEM, XRD, DLS, NTA, SAXS, HRTEM, SEM, AFM, EXAFS, FMR, DCS, ICP-MS, UV-Vis, MALDI, NMR, TRPS, EPLS, magnetic susceptibility
Shape	TEM, HRTEM, AFM, EPLS, FMR, 3D-tomography
Elemental-chemical composition	XRD, XPS, ICP-MS, ICP-OES, SEM-EDX, NMR, MFM, LEIS
Crystal structure	XRD, EXAFS, HRTEM, electron diffraction, STEM
Size distribution	DCS, DLS, SAXS, NTA, ICP-MS, FMR, superparamagnetic relaxometry, DTA, TRPS, SEM
Chemical state–oxidation state	XAS, EELS, XPS, Mössbauer
Growth kinetics	SAXS, NMR, TEM, cryo-TEM, liquid-TEM
Ligand binding/composition/density/arrangement/mass, surface composition	XPS, FTIR, NMR, SIMS, FMR, TGA, SANS
Surface area, specific surface area	BET, liquid NMR
Surface charge	Zeta potential, EPM
Concentration	ICP-MS, UV-Vis, RMM-MEMS, PTA, DCS, TRPS
Agglomeration state	Zeta potential, DLS, DCS, UV-Vis, SEM, Cryo-TEM, TEM
Density	DCS, RMM-MEMS
Single particle properties	Sp-ICP-MS, MFM, HRTEM, liquid TEM
3D visualization	3D-tomography, AFM, SEM
Dispersion of NP in matrices/supports	SEM, AFM, TEM
Structural defects	HRTEM, EBSD
Detection of NPs	TEM, SEM, STEM, EBSD, magnetic susceptibility
Optical properties	UV-Vis-NIR, PL, EELS-STEM
Magnetic properties	SQUID, VSM, Mössbauer, MFM, FMR, XMCD, magnetic susceptibility

2.12. Rapamycin; discovery and characteristics

Rapamycin, a bacterial macrolide-derived compound, produced by *Streptomyces hygroscopicus,* was discovered in 1975 from the soil sample of Rapa Nui (Easter Island) as an antifungal agent (J. Li et al., 2014)(Guertin & Sabatini, 2009)(Betz & Hall, 2013). It possesses immunosuppressive and anti-proliferative properties in mammalian cells, and it was shown to be a potent inhibitor of S6K1 activation, a serine/threonine kinase (Foster & Fingar, 2010). Rapa, the so-called Sirolimus, allosterically inhibits mTOR (mammalian target of Rapamycin) by binding with the cellular protein FKBP12, this FKBP12 – Rapa complex directly binds to the FRB domain (FKBP12-rapamycin-binding domain) and inhibits its intrinsic kinase activity (Guertin & Sabatini, 2009). 4EBP1 and p70s6k are the two main targets of the mTOR signaling pathway and rapamycin is a prominent suppressor of their function (Law, 2005). Acute exposure to Rapamycin only inhibits the mTORC1 complex. Chronic exposure inhibits mTORC2 in a few cell types by seizing newly synthesized mTOR molecules (Laplante & Sabatini, 2012).

Rapamycin (Sirolimus) analogs, commonly known as rapalogs are, Temsirolimus, Everolimus, Ridaforolimus (Deforolimus), and Zotarolimus (Feng et al., 2021). (figure 2.6). Rapamycin has been found effective in Primary Effusion Lymphoma (PEL) in culture and murine xenograft models (Sin et al., 2007). Rapamycin also enhanced the ability of cisplatin, an alkylating agent, to induce apoptosis in the human promyelocytic leukemia cell line HL-60 and the human ovarian cancer cell line SKOV3 (Y. Shi et al., 1995).

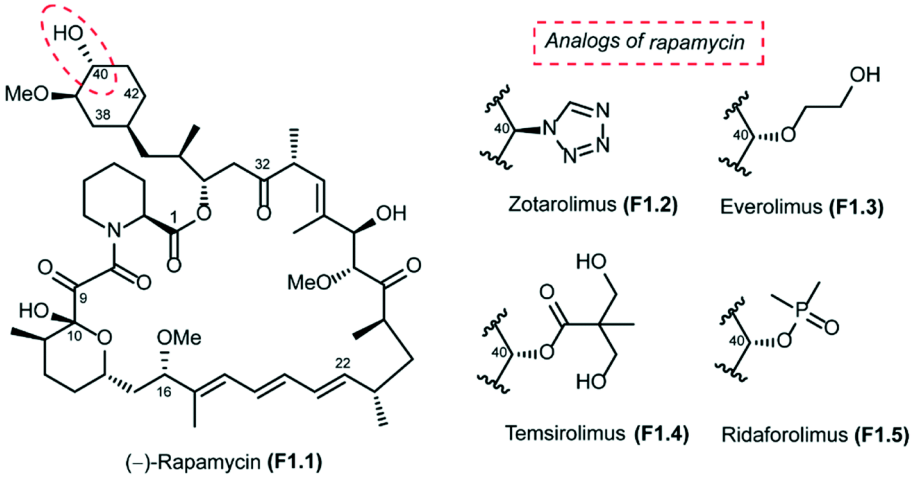

Figure 2.6. Structure of Rapamycin and its analogs (Guduru & Arya, 2018)

2.12.1. TOR and mTOR

The discovery of a Ser/Thr protein kinase, known as TOR (target of rapamycin), took place through the observations of the capacity of an antifungal agent, Rapamycin, to inhibit S6K1 activation and PI3kinase signaling (Laplante & Sabatini, 2012). It is the focal part of a highly conserved signaling pathway that controls cell growth in response to nutrients, hormones, and stresses (Foster & Fingar, 2010)(Soulard et al., 2009). The TOR complex 1 (TORC1) and TOR complex 2 (TORC2), which are individually functional, constitute its catalytic core (Jacinto & Lorberg, 2008). They carry unique and shared protein partners and administer numerous cellular activities in feedback to diverse environmental cues (Foster & Fingar, 2010). Higher eukaryotes like mammals, drosophila, and *C. elegans* contain one *TOR* gene *i.e. mTOR*, *dTOR*, and *ceTOR*. Yeast

(*Saccharomyces cerevisiae*, *Schizosaccharomyces pombe*) contains two *TOR* genes, Tor1 (or) Tor2 in the absence of Tor1. Tor1forms TORC1 and Tor2 forms TORC2 in *S. cerevisiae* (Jacinto & Lorberg, 2008).

The mTORC1 components are; mTOR, RAPTOR (regulatory associated protein of TOR), and mLST8 (mammalian lethal with sec-13 protein 8). Other components include DEPTOR (DEP-domain containing mTOR interacting protein) and PRAS40 (Proline-rich Akt substrate 40kDa). The mTOR complex 2 (mTORC2) consists of mTOR, the rapamycin-insensitive companion of mTOR (RICTOR), stress-activated protein kinase-interacting protein 1 (mSIN1), and mLST8. Proteins observed with RICTOR 1/2 (PROTOR 1/2) and DEPTOR are the additional regulatory components (Cornu et al., 2013) (figure 2.7).

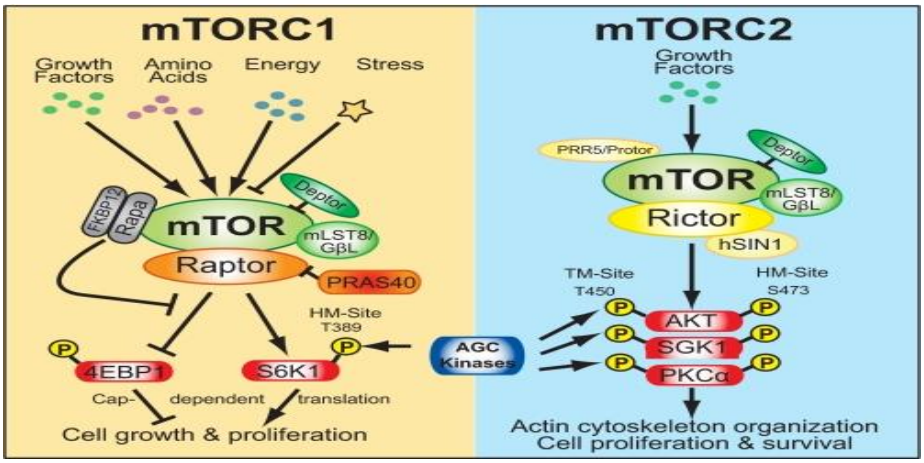

Figure 2.7. mTOR C1 and mTOR C2 complexes and their unique protein partners, susceptibility to Rapamycin, substrates, and cellular mechanisms. (© 2010 by The American Society for Biochemistry and Molecular Biology, Inc.)

The major function of mTORC1 is in the regulation of cell growth and metabolism, and mTORC2 regulates cell proliferation and survival (Unni & Arteaga, 2019). mTORC1 responds to signals from growth factors, nutrients, and energy supply to promote cell growth and catabolism according to the demands of the body and it accomplishes its functions by coordinating protein synthesis (Averous & Proud, 2006)(Ma & Blenis, 2009), biosynthesis of nucleotides (Ben-Sahra et al., 2013) lipogenesis, glycolysis (Peterson et al., 2011), and autophagy (Nao Hosokawa et al., 2009). mTORC2 regulates cell growth by lipid synthesis, glucose metabolism (Hagiwara et al., 2012), and apoptosis (Datta et al., 1997) (figure 2.8).

It is interpreted experimentally that mTOR is taking part in many signaling pathways such as phosphoinositide-3-kinase (PI3K)/AKT, tuberous sclerosis complex subunit 1 (TSC1)/tuberous sclerosis complex subunit 2 (TSC2)/Rheb, LKBL/adenosine 5′monophosphate-activated protein kinase (AMPK), VAM6/Rag GTPases and many more(Dowling et al., 2010). It influences transcription and protein synthesis by integrating various signal stimulations and finally regulates apoptosis, growth, and autophagy of cells (Neufeld, 2010). Hence, mTOR inhibitors are extensively used in the research of various tumors/cancers, organ transplantation, rheumatoid arthritis, etc.

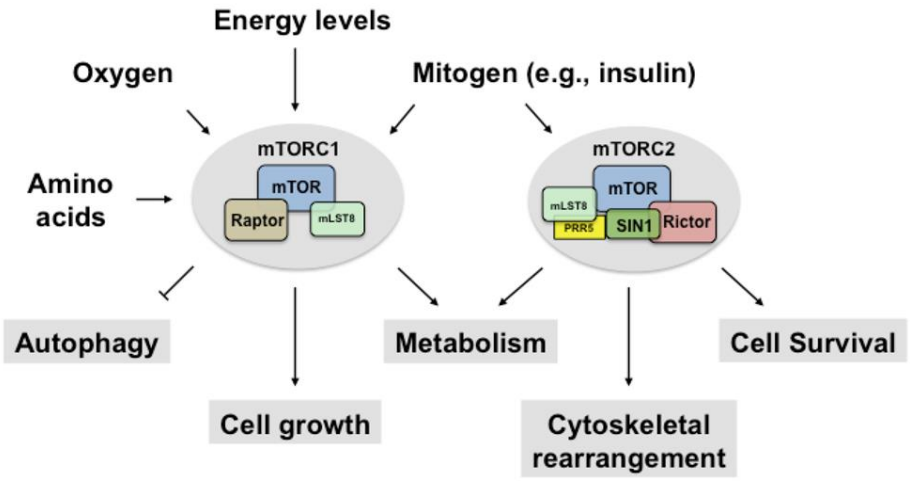

Figure 2.8. Flowchart describing the mTOR C1 and C2 responses to different signals (Yoon, 2017)

2.12.2. mTOR Pathway

mTOR C1 pathway:

RAPTOR complexes with mTOR with the aid of a protein, GßL, in response to nutrient signals (Kim et al., 2003). RAPTOR also functions as a bridging molecule in the phosphorylation of p70S6 Kinase 1 (S6K1) and eIF4E Binding Protein (4EBP) by mTOR for facilitating protein synthesis. The phosphorylation of S6K1 promotes its activation by PDK1. Active S6K1 phosphorylates and activates many other intermediates that promote mRNA translation (Holz et al., 2005) (figure 2.9).

mTORC1 stimulates lipid biosynthesis through the SREBP (sterol-responsive element binding protein) transcription factors (Porstmann et al., 2008). although SREBP is usually triggered in response to low lipid availability, mTORC1 signaling also activates the

SREBP transcription factor solely through an S6K1-dependent mechanism (Düvel et al., 2010) also, through the phosphorylation of Lipin1, an inhibitor of SREBP (Peterson et al., 2011).

mTORC1 also assists in nucleotide synthesis needed for DNA replication and ribosome development in cells. mTORC1 boosts the expression of ATF4-dependent MTHFD2, which is an essential unit of the mitochondrial tetrahydrofolate cycle that supplies C1 units for purine biosynthesis (Ben-Sahra et al., 2016). Further, S6K1 activates carbamoyl-phosphate synthetase (CAD), a key factor in the de novo pyrimidine synthesis pathway (Ben-Sahra et al., 2016).

mTORC1 enhances glucose metabolism by switching from oxidative phosphorylation to glycolysis through the increased synthesis of HIF1α, a transcription factor that promotes the expression of many glycolytic enzymes, thereby promoting cell growth (Saxton & Sabatini, 2017)(Düvel et al., 2010). In addition, mTORC1-mediated SREBP activation results in a rise in the oxidative pentose phosphate pathway (PPP), in which cells produce NADPH and other metabolites needed for proliferation and growth (Saxton & Sabatini, 2017).

mTORC1 also supports cell growth by inhibiting protein catabolism and autophagy. In a nutrient-sufficient situation, it phosphorylates the crucial kinase involved in autophagy, ULK1, and prevents its AMPK-mediated phosphorylation and activation (J. Kim et al., 2011).

mTOR C2 pathway:

mTORC2 regulates cell proliferation and survival by phosphorylating several protein kinases such as PKA, PKG, and PKC. The mTORC2 substrates include PKCα, PKCδ, PKCζ, and PKCγ, and PKCε, all of these kinases take part in cytoskeletal modification and cell migration (Dos et al., 2004)(Gan et al., 2012)(X. Li & Gao, 2014)(Thomanetz et al., 2013). mTORC2 also phosphorylates and activates Akt, a key precursor in insulin/PI3K signaling (Sarbassov et al., 2005). As well, mTORC2 phosphorylates and activates SGK1, an AGC kinase that modulates ion transport as well as cell survival (García-Martínez & Alessi, 2008) (figure 2.9)

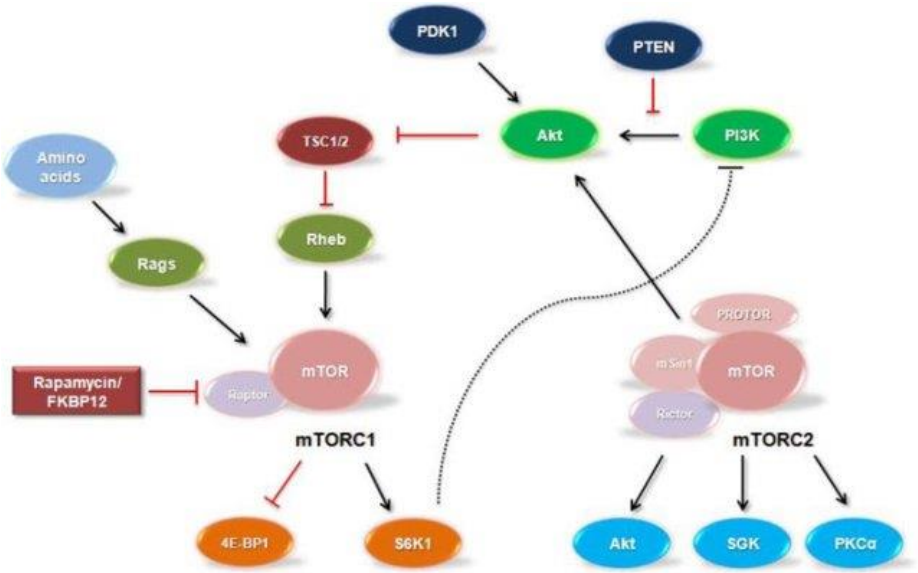

Figure 2.9. Figure illustrating both mTOR C1 and mTOR C2 pathways (Hwang & Kim, 2011)

2.12.3. Role of mTOR signaling in cancer

Cancer cells grow with abnormal signaling and metabolic remodeling (Vander Heiden & DeBerardinis, 2017). In nutrient-limited and exhausting conditions, cancer cells alter their cellular mechanisms to ensure their growth and survival. This alteration is frequently dealt with by oncogenic signaling (Mossmann et al., 2018). specifically, mTOR signaling is often triggered in tumors and checks the metabolic pathways of cancer cells via reprogramming the activity of several key metabolic enzymes (Saxton & Sabatini, 2017).

2.12.4. Rapamycin as an anti-cancer agent

Rapamycin is a well-established chemotherapeutic agent for its anti-proliferative properties in different cancer cells including renal and breast. (Blagosklonny, 2023) (Din et al., 2014) Rapamycin initiates apoptosis in cancer cells and prevents cancer progression. (Mathew et al., 2004) The long-term use of Rapamycin suppresses aging which is a risk factor concerning cancer occurrence. (Blagosklonny, 2022) The effect of rapamycin on ER+ breast cancer cells has been studied widely and reported to induce apoptosis in MCF-7 cells with G0/G1 cell cycle arrest. (Din et al., 2014)

2.13. Fluoroquinolones; anti-cancer and anti-bacterial properties

Fluoroquinolones (FQs) are widely used anti-bacterial compounds with better bioavailability, and half-life. (Idowu & Schweizer, 2017) They act by inhibiting DNA Gyrase and Topoisomerase IV and affect bacterial replication and transcription.

(Pham et al., 2019) (Kloskowski et al., 2023). Even though fluoroquinolones are synthetic molecules, many bacteria have been reported to create their analogs. (Karatay et al., 2023). Figure 2.10 depicts the applications of fluoroquinolone molecules.

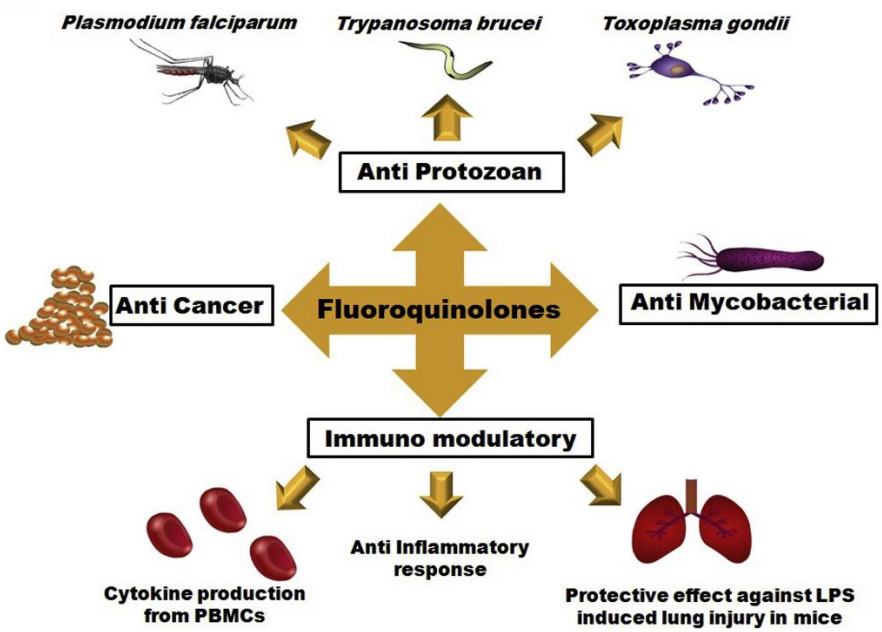

Fig. 2.10. Multiple applications of fluoroquinolone molecules including anti-cancer, anti-mycobacterial anti-protozoan, and immune modulatory effects. (Yadav & Talwar, 2019)

In cancer cells, they induce apoptosis by increasing BAX expression, mitochondrial depolarization, PARP cleavage, and the induction of Caspase-8, -9, and -3. They also induce cell cycle arrest by targeting Cyclin-CDK complexes. (Aranha et al., 2000) (Aranha et al., 2003)(Sousa et al., 2013) (Mukherjee et al., 2005) (Herald et al., 2002). Also, they can cause mitochondrial malfunction, oxidative stress, and decreased glutathione levels. (Beberok, Rzepka, et al.,

2018). Table 2.3 summarizes the mechanism of action by some of the fluoroquinolone compounds with anti-cancer activities.

Table. 2.3. Fluoroquinolone molecules with anticancer activity and their mechanism of action

Fluoroquinolone	Cell Line	Mechanism of Anticancer Activity	Reference
Ciprofloxacin	COLO829 melanoma	Cell cycle arrests in the S phase, induction of mitochondrial membrane breakdown leading to apoptosis	(Beberok, Wrześniok, Minecka, et al., 2018)
	MDA-MB-231 breast cancer	Cell cycle arrests in S phase, induction of apoptosis	(Beberok, Wrześniok, Rok, et al., 2018)
	LOVO colon cancer	Induction of apoptosis	(Jemel-Oualha et al., 2016)
	T24 bladder cancer	Cell cycle arrests in S phase, induction of apoptosis	(Kloskowski et al., 2021)
	Huh7/HepG2 liver cancer	Increased expression of CD86+CD206- macrophages leading to inhibition of cell growth	(Fan et al., 2020)
Norfloxacin	NCI-H460 lung cancer	The antiproliferative effect, generation of apoptosis	(Mondal et al., 2004)
Lomefloxacin	HeLa S3 epithelial cancer	The antiproliferative effect, generation of photocleavage of plasmid DNA associated with high photoreactivity of the compound	(Perucca et al., 2014)
	HL-60	Induction of	(Nakai et al.,

	leukemia	apoptosis in combination with UVA radiation	2017)
Levofloxacin	HepG2 hepatocellular carcinoma	Cell cycle arrests in the G2/M phase and induction of apoptosis	(He et al., 2022)
	MCF-7	Inhibition of cell proliferation, induction of apoptosis	(M. Yu et al., 2016)
Gatifloxacin	PaCa-2/Panc-1 pancreatic cancer	Cell cycle arrests in phases S and G2 without induction of apoptosis	(Yadav et al., 2012)
Moxifloxacin	C32/COLO829 Melanoma cells	Apoptosis induction and DNA fragmentation	(Beberok et al., 2019)

2.13.1. Moxifloxacin and Norfloxacin as anti-cancer agents

Moxifloxacin and Norfloxacin are Fluoroquinolone molecules with anti-bacterial properties. Also, they have exhibited anti-proliferative effects in certain types of cancers. Moxifloxacin has been reported to inhibit the proliferation of human pancreatic cancer cell lines (MIA PaCa-2 and Panc-1) by apoptosis induction and S-phase cell cycle arrest. This was achieved through the activation of caspases and Bcl-xL and Bak expression. Also, Moxifloxacin upregulated the apoptotic potential of Cisplatin suggesting a synergistic effect. (Kassab et al., 2024) (Yadav et al., 2015) Moxifloxacin modified with fatty acids such as oleic acid, and stearic acid exhibited enhanced anti-proliferative activity compared to Moxifloxacin alone in prostate and colorectal cancer cell lines. (Kassab et al., 2024)

Norfloxacin also demonstrated anti-proliferative potential in different cancers including breast and bladder cancers with G2/M cell cycle arrest, induction of apoptosis, reduction in metalloproteinase expression, and inhibition of topoisomerase II and histone deacetylases. (Ferrario et al., 2024) Although the production of these compounds by bacteria, their conjugation onto bacterial-derived nanoparticles is to be extensively studied.

MATERIALS AND METHODS

This study involved the production of nanoparticles using chemical and biological methods. The synthesized nanoparticles were characterized and their ability to interfere with cell proliferation was checked.

3.1. Chemicals and reagents

Starch, Casein, Ammonia, Glycerol, Yeast Extract, Tris Base, Sodium Hydroxide, Silver nitrate, SDS, triton-X-100, EDTA, Acridine Orange, Ethidium Bromide, ethanol, acetone, methanol HCL, DMSO, and Trypsin were purchased from SRL (Sisco Research Laboratories Pvt. Ltd., India). Dulbecco's Modified Eagle Medium (DMEM), 3-(4, 5-dimethylthiazol-2-yl)-2, 5-diphenyltetrazolium bromide (MTT), HiKaryo XL™ RPMI medium, Hi-Sep™ Lymphocyte separation medium (LSM), Streptomycin, Penicillin, Gentamicin, Gluteraldehyde, Tween 20, Formaldehyde, skimmed milk, LB broth, BSA, DPPH, and DAB were purchased from Hi-Media Laboratories (India). Rapamycin was purchased from TCI (Japan). Gold Chloride, HSPEG-OMe, dialysis tube, Rhodamine-123, Hoechst 33258, and Acridine Orange were obtained from Sigma (USA). $FeCl_3$, $FeCl_2$, PVDF membrane, PEG, and H_2O_2 were purchased from Merck Life Sciences, Mumbai, India. Propidium Iodide, and Alexa Fluor®488 Annexin V/ Dead cell Apoptosis Kit were procured from Invitrogen, USA. Fetal Bovine Serum (FBS) was purchased from Gibco, Germany. Protein molecular

weight marker (medium range), and Goat anti-rabbit Ig G-HRP conjugate was purchased from Genei Laboratories, Bangalore, India. Anti- β actin and anti-PARP antibodies were obtained from Cell Signaling Technologies, USA. RNase A was purchased from Thermo Fisher Scientific. All the other reagents and chemicals used in this study are of analytical grade.

3.2. Cell lines and cell cultures

The human breast adenocarcinoma cell line MCF-7 was purchased from the National Center for Cell Sciences (Pune, India). HCT 116, HEK, and L929 cell lines were maintained in the Molecular Oncology Lab, Department of Biotechnology, University of Calicut. The cells were cultured in Dulbecco's modified Eagle's medium (DMEM) (Himedia, India) containing 10% fetal bovine serum with 55 µg/mL gentamicin, 100 µg/mL streptomycin, 50 U/mL penicillin, and 2 µg/mL amphotericin B. The cells were incubated at 37º C in a humidified incubator with a 5% CO_2 atmosphere and passaged over two times a week and confirmed mycoplasma-free regularly. Exponentially growing cells were taken for all the analysis. Cells were dissociated using 0.53 mM EDTA in phosphate-buffered saline (PBS) and 0.25% trypsin.

Human peripheral blood lymphocytes (hPBLs) were isolated from freshly drawn human blood. The blood was diluted by an equal volume of phosphate-buffered saline (PBS) and carefully overlaid on a Hi-Sep^{TM} Lymphocyte separation medium (LSM) in a centrifuge tube. After centrifugation at 400 x g for 30 min at room temperature, the

buffy coat at the fluid interface was aspirated using a sterile Pasteur pipette and washed twice with PBS. The cells were then cultured in HiKaryo XL™ RPMI medium by incubating at 37 °C in a humidified incubator with a 5% CO_2 atmosphere

3.3. Chemical Synthesis of Iron Oxide Gold core-shell Nanoparticles (Au-IONPs)

For designing a nanoparticle-based drug-delivery system using the chemical synthesis method, we preferred Iron Oxide Nanoparticles (IONPs) as they are biocompatible and superparamagnetic, which would benefit the targeted delivery of medicines. The Gold coating imparts a shielding effect on the IONPs, it improves the IONPs' bioavailability and stability. And aids in the loading of different chemotherapeutic agents on them. To check the effectiveness of the Nanocarrier system, Rapamycin, an anti-proliferative, anti-fungal, immunosuppressant drug was chosen.

3.3.1. Standardization of the synthesis of Iron Oxide Nanoparticles (IONPs)

Fe_3O_4 NPs were synthesized using the chemical co-precipitation method, which was standardized using four different protocols as described below. the synthesized Fe_3O_4 NPs were subjected to Scanning Electron Microscopy (SEM) to obtain their morphological characteristics, and XRD analysis was done to determine their compositional structure. The method that produced

IONPs with lower particle size and better XRD analysis scores was chosen for developing the Nano-drug-carrier system.

Method 1: The synthesis was done by the protocol described in (Arshad et al., 2018), with slight modifications; 2 g $FeCl_3$ and 2 g $FeCl_2$ were dissolved in 50 mL of deionized water and stirred to maintain a homogenous solution. 1 M NaOH was added dropwise to the homogenous solution under vigorous stirring in which 8 mL PEG (0.0025 M) was added quickly before heating the solution to 80 °C for 1 hour. The black solution was refluxed for 1 hour and cooled at room temperature. The precipitate was washed at 12000 g with deionized water 5 times and finally with 70 % ethanol**.** The NPs were obtained as a black powder after drying overnight in a hot air oven at 80 °C.

Method 2: The synthesis was done by the protocol described in (Schwaminger et al., 2020), with slight modifications; 3.5 g $FeCl_3$ and 8.64 g $FeCl_2$ were dissolved in 20 mL of deionized water each and stirred to maintain a homogenous solution. 7.2 g NaOH was dissolved in 100 mL water and made the reaction volume to 140 mL. The stirring temperature was set to 55 °C. The precipitate was washed at 12000 g with deionized water for 5 times. The NPs were obtained as a black powder after drying overnight in a hot air oven at 80 °C.

Method 3**:** The synthesis was done in the protocol described in *Method 1* with slight modifications; 2 g $FeCl_3$ and 2 g $FeCl_2$ were dissolved in 50 mL of deionized water and stirred to maintain a homogenous solution. Ammonia water was added dropwise to the homogenous solution under vigorous stirring in which 8 mL PEG (0.0025 M) was

added quickly before heating the solution to 80 °C for 1 hour. The black solution was refluxed for 1 hour and cooled at room temperature. The precipitate was washed at 12000 g with deionized water 5 times and finally with 70 % ethanol. The NPs were obtained as a black powder after drying overnight in a hot air oven at 80 °C.

Method 4: The synthesis was done in the protocol described in *Method 1* with slight modifications. 2 g $FeCl_3$ and 2 g $FeCl_2$ were dissolved in 50 mL of deionized water and stirred to maintain a homogenous solution. Ammonia water was added dropwise to the homogenous solution under vigorous stirring in which 10 mL EDTA (2 mM) was added quickly before heating the solution to 80 °C for 1 hour. The black solution was refluxed for 1 hour and cooled at room temperature. The precipitate was washed at 12000 g with deionized water 5 times and finally with 70 % ethanol**.** The NPs were obtained as a black powder after drying overnight in a hot air oven at 80 °C.

3.3.2. Preparation of Iron oxide Gold-core shell nanoparticles (Au-IONPs)

To improve the stability and pharmaceutical attributes of the IONPs, it was coated with Gold nanoparticles to form a core-shell structure with an iron core and gold shell. The Gold shell coating on IONPs was done by adopting the standard protocol (Kheiri Manjili et al., 2016) with slight modifications. A 2 % solution of IONPs was prepared in sodium citrate (10 mM). This solution was sonicated for 3 hours and slowly heated to 70 °C on a stirrer. 0.1 M solution of $HAuCl_4.4H_2O$ was dropped into the solution and stirred vigorously for

approximately 30 min, allowing Au^{3+} to attach to the surface of the IONPs. Cooled by stirring at RT, magnetically separated Au - IONPs from Au NPs. Freeze-dried and stored.

PEGylation on Au-IONPs was done by adopting the protocol described (Kheiri manjili et al., 2016). 0.04 g of Au - IONPs dispersed in 5 mL of Chloroform was added to 0.03 g thiolated polyethylene glycol (HSPEG-OMe) in Chloroform. The mixture was stirred for 2 h in the dark at RT. The particles were then collected by centrifugation and washed with $CHCl_3$ and hexane (1:5 V/V). Solvents were air-dried and the resulting product was dialyzed for 24 hours.

3.3.3. Preparation of Rapamycin loaded Iron oxide Gold core-shell nanoparticles (R - Au – IONPs)

The drug Rapamycin was loaded onto the Iron oxide gold core-shell nanoparticles to improve the bioavailability, half-life, and solubility/absorption, and R-Au-IONPs were formed. Rapamycin loading onto the Au-IONPs was done by the physical adsorption method as described before (Kheiri Manjili et al., 2016) With slight modifications. Drug solution with the primary concentration of 1.4 mg/mL was mixed with 4 mg of PEG - ylated Au - IONPs in Tris/HCl buffer (pH 7) and kept at 4 °C . After 24 hours, the NPs were magnetically separated (which may contain the drug) and the drug concentration in the solution was determined. Drug concentrations were obtained using a UV-visible spectrophotometer at 280 nm. The difference between initial and residual drug concentrations was used to determine the loading efficiency. (Danafar et al., 2018). The

magnetically separated R - Au - IONPs were dispersed in distilled water and freeze-dried.

$$\text{Loading efficiency} = \frac{\text{Obtained drug concentration in nanoformulation}}{\text{Concentration of drug used}} \times 100$$

3.3.4. Invitro drug release assay of R-Au-IONPs

To assess the invitro release profile of the loaded drug Rapamycin from the Au-IONPs, the dialysis method was used. The release of Rapamycin from R -Au - IONPs was measured for 2-100 hours in PBS at a pH of 7.4. 0.6 mg of R - Au - IONPs dissolved in 2 mL of PBS and added into the dialysis bags (molecular weight cut-off of 3.5 kDa) and kept at 37 °C and 100 rpm. After each 6-hour interval, 2 mL of samples were collected and replaced with 2 mL of fresh PBS. Drug releases at different time intervals (4 days) were measured using a UV-visible spectrophotometer at 280 nm (Perkin Elmer, Lambda 25) (Danafar et al., 2018).

3.4. Biological Synthesis of Nanoparticles

To explore the possibility of generating metallic nanoparticles with the same properties as the chemically synthesized drug-loaded ones using biological methods, we employed cell-free supernatants of soil bacterial isolates. Since soil bacteria comprises a variety of species capable of producing many secondary metabolites with remarkable bio-activities, their nanoparticles capped with these molecules could be an excellent choice for replacing the drug-loaded chemically synthesized NPs

3.4.1. Isolation of pure bacterial colonies from soil samples

Soil samples from different terrains; Paddy field (11°07'16.8"N 75°51'04.8" E), normal (11°06'54.3"N 75°49'54.4" E), and coastal (11°07'23.75" N 75°49'01.32" E); of Calicut, Kerala, India, were collected in sterile polythene bags and stored at 4 ^{o}C until further use. For isolating pure bacterial colonies, Starch Casein Agar (SC Agar) and Glycerol Yeast Extract Agar (GYE Agar) were used. Starch casein agar was used to isolate soil actinomycetes and the GYE agar was used to isolate mesophilic and thermophilic strains. The soil samples were air dried at RT, and sieved, 1 gram of each sample was resuspended in 100 mL sterile deionized water and then left to settle down. Serial dilutions up to 10^{-4} were prepared. 100 µL of 10^{-3} and 10^{-4} dilutions were spread evenly on both SC and GYE plates and incubated at RT for 5 days. Pure Colonies were obtained by streaking the different isolates on the respective agar plates, each colony was given a code number.

3.4.2. Screening of isolates for extracellular biosynthesis of metallic NPs

The seven different isolates acquired were screened for their ability to produce metallic nanoparticles of iron, gold, and silver using different metallic precursors; each isolate was cultured in the respective culture broth (50 mL) and kept at RT with shaking at 200 rpm for 7 days. The culture supernatant was harvested via centrifugation at 8,000 rpm for 15 min.

3.4.2.1. Screening for the Synthesis of Iron Oxide Nanoparticles (IONPs)

For the biogenesis of Iron oxide nanoparticles, equal amounts of $FeCl_3 \cdot 6H_2O$ (1 mM) were added to the cell-free supernatants, which were then incubated for 48 hours at room temperature and 120 rpm in the dark. The formation of IONPs was observed by the change in color of the reaction mixture from yellow to dark brown or black. (Jacob et al., 2017)

3.4.2.2. Screening for the Synthesis of Gold Nanoparticles

To generate Gold Nanoparticles, a 10^{-3} M Gold Chloride aqueous solution ($HAuCl_4.3H_2O$) was added to the cell-free supernatant. The reactants were adjusted to neutral pH using 0.1 M NaOH solution. For 48 hours, the entire combination was left in the dark. The progressive change in the color of the reaction solution from pale yellow to ruby red to deep purple indicated the production of AuNPs. (Sadhasivam et al., 2012)

3.4.2.3. Screening for the Synthesis of Silver Nanoparticles

For the green synthesis of Ag-NPs, the culture supernatants were mixed with equal volumes of 0.1 mM Silver nitrate ($AgNO_3$), and pH was adjusted to 8 using 0.1 M NaOH solution. The mixture was incubated at RT for 5 days in the dark. The change in the color of the mixture to dark brown indicated the production of Silver NPs. (S. S. et al., 2021)

3.4.3. Screening of the biologically synthesized NPs for cytotoxic potential

MTT assays were performed to assess the effects of the synthesized NPs on cell proliferation and viability. HCT 116 and MCF-7 cells were cultivated (3000 cells/well) in 96-well plates with 100 µL DMEM. Following 12 hours, cells were treated with fresh media that contained varying concentrations of NPs (in DMEM) and incubated at 37 ºC with 5% CO2. 100 µL of MTT solution (5 mg/mL) was added after 72 hours, and the plates were then incubated for two hours at 37 °C. DMSO (100 µL/well) was then added to dissolve the formazan crystals, and the mixture was maintained at 37 °C for 30 minutes. Using a microplate reader (Biotek, USA), the optical density was determined at 570 nm. Every experiment was run in triplicate. The percentage viability of cells in each tested concentration was calculated using the formula,

$$\% \text{ viability} = \frac{\text{OD of Test}}{\text{OD of negative control}} \times 100$$

The IC 50 concentrations of each NPs were determined from the graph.

3.5. Characterization experiments

The NPs were characterized by UV-VIS spectroscopy, in which the absorption spectra were taken in the 280-700 nm range. Morphological characteristics of the synthesized NPs were obtained by FESEM analysis (Carl Zeiss Gemini 300 Germany) using Smart SEM Software. The particle size distribution of the NPs was obtained from

the SEM images using the Image J software. The compositional structure of NPs was determined by X-ray diffraction (XRD). which was measured by PANanalytical (XPert3 Powder) with Cu Kα radiations (l = 1.5406 Å) operated at a voltage of 40 kV and current of 30 mA. The Fourier transform infrared spectroscopy (FTIR) spectra were taken using an FTIR spectrometer (Jasco 4100) in the 4000 to 400 cm−1 regions.

3.6. Molecular identification of the selected strain KDY2

Molecular identification of the KDY2 strain was carried out using 16S rRNA sequencing. Bacterial DNA was extracted and 16S rDNA was amplified using 1492R (5′TACGGYTACCTTGTTA CGACTT3′) and 27F (5′AGAGTTTGATCMTGGCTCAG 3′) universal primers. The Sanger technique was used to sequence the DNA and was then compared for percent similarity in BLAST sequence similarity search on the NCBI website and the sequence was deposited in the GenBank for accession number. The phylogenetic tree was constructed using the neighbor-joining method in MEGA 11.

3.7. Anti-oxidant assays of KDY 2 Au NPs

3.7.1. Anti-oxidant activity evaluation by DPPH free radical scavenging assay

The antioxidant activity of the KDY2 NPs was measured according to the method described by Brand-Williams et al. 1995). This method is based on the scavenging activity of the stable 2,2-diphenyl-1-picrylhydrazyl (DPPH) free radical. DPPH solution

(0.1 mM) in methanol was mixed with 1 mL of KDY2 NP solution of different concentrations. The reaction mixture was incubated at room temperature in the dark for 30 minutes. Absorbance was recorded at 517 nm. Ascorbic acid served as the reference standard. The inhibition % was calculated using the following formula.

$$\% \text{ Inhibition } = \frac{\text{Absorbance}_{\text{control}} - \text{Absorbance}_{\text{test}}}{\text{Absorbance}_{\text{control}}} \times 100$$

3.7.2. ABTS radical scavenging activity

The ABTS (2, 2‘-azinobis (3-ethylbenzthiazoline-6-sulphonic acid) cation scavenging activity was adapted from (Nitha et al., 2010) and (S. Kumar et al., 2014)). The ABTS stock solution with equal volumes of 7 mM ABTS and 2.45 mM potassium persulfate was prepared and incubated at room temperature for 12 hours in the dark. A dark-colored solution containing ABTS radical cation was formed. Before each assay, a fresh working solution was by diluting the stock solution with methanol (50%). The initial absorbance at 745 nm and 30°C was about 0.700 (± 0.02). The ABTS free radical scavenging activity was obtained by mixing 100 µL of different concentrations of KDY2 Au NPs (100.0 µg/mL – 1.0 mg/mL) with 1.0 mL of ABTS working solution. After 1 min, the absorbance was measured at 745nm (Lambda 25, Perkin Elmer, UK) and the final absorbance was noted up to 6 min. Ascorbic acid was used as positive control. Based on the percentage of ABTS radicals scavenged, the scavenging activity was calculated by using the formula:

$$\% \text{ ABTS scavenging } = \frac{\text{Absorbance}_{\text{control}} - \text{Absorbance}_{\text{test}}}{\text{Absorbance}_{\text{control}}} \times 100$$

3.7.3. Metal chelating activity of Ferrous ion

The Fe^{2+} chelating activity of the KDY2 Au NPs was evaluated using the method described by (Hazra et al., 2008) with few modifications.12.5 µM Ferrous sulfate and 75 mM Ferrozine were prepared in 20 mM HEPES buffer (pH 7.2). Each of the two reagents (75 µL) was mixed with 75 µL of varying concentrations of the KDY 2 Au NPs (100 µg/mL – 1.0 mg/mL) and stirred vigorously. After incubating at room temperature for 20 min, the absorbance was read at 562 nm. EDTA (concentrations ranging from 25– 250 µg/mL) was used as the positive control. The percentage of ferrozine-Fe^{2+} complex formation inhibition was calculated using the formula:

$$\% \text{ metal chelation} = \frac{\text{Absorbance}_{\text{control}} - \text{Absorbance}_{\text{test}}}{\text{Absorbance}_{\text{control}}} \times 100$$

3.8. Anti-microbial activity of KDY2 Au NPs

Antibacterial and antifungal activities of the KDY2 Au NPs were assessed by Microwell dilution and Agar well diffusion methods respectively (Mogana et al., 2020) (Tortora et al., 2010) (Lalitha, 2007). Two Gram-positive bacteria (*Staphylococcus aureus*-ATCC 29213, *Enterococcus faecalis*- ATCC 29212), three Gram-negative bacteria (*Escherichia coli*- ATCC 25922, *Klebsiella pneumoniae*- ATCC 700603, *Pseudomonas aeruginosa*- ATCC 27853), and two pathogenic fungi (*Aspergillus niger*- NCIM 1004, *Candida albicans*-

NCIM 3102) were used. Chloramphenicol, clotrimazole, and nystatin were employed as the positive controls for bacteria and fungi respectively. The KDY2 NPs were dissolved in sterile PBS (pH 7.4).

The agar well diffusion method was used to check the antifungal activity of different concentrations (260, 500, 750 µg/mL) of KDY2 NPs. PDA plates and MGYPA plates were used for A. niger and C. albicans respectively. Each Petri plate was dug with four wells of 6 mm diameter. The wells were filled with 100 µL of NP formulations, Positive and negative controls. The plates containing A. niger were incubated in an inverted position at 25 °C for 5 days and the MGYPA plates containing C. albicans were kept at 25 °C for 48 hours. The antifungal activity was measured in millimeters (mm) with the help of a calibrated transparent scale.

In the anti-bacterial assay, diluted bacterial cultures from 0.5 McFarland standards were used. Serial dilutions of the KDY2 NPs (0.5-2.5 mg/mL) and the standard antibiotic chloramphenicol (0-10 µg/mL) were made and added to the cultures. Sterility control without culture and growth control without the drug were also employed. The assays were performed in sterile, 96-well microtiter plates with Mueller-Hinton broth. To control the NP solution's color, absorbance at 600 nm (OD_{600}) measurements were taken before incubation at 37 °C and after 12 hours. The IC 50 values were calculated from the average OD_{600} value.

3.9. LC/Q-TOF/MS analysis of KDY2 cell-free supernatant

To identify the composition involved in the bioactivities of KDY 2 Au NPs, the KDY2 cell-free supernatant was subjected to LC/Q-TOF/MS analysis. The Agilent 6545 Accurate-Mass Quadrupole Time-of-Flight (Q-TOF) LC/MS system combined with an Agilent Jet Stream dual electrospray ionization (ESI) source was used. The Agilent MassHunter qualitative analysis software was used for the library search (version 10.0).

3.10. Cytotoxicity assays

3.10.1. MTT Assay

The nanoparticle's effects on cell survival and proliferation were evaluated using MTT assays in HEK, L929, and MCF-7 cells as described earlier. The IC 50 concentrations of each NPs were determined. Additionally, the cytotoxicity of the NPs on healthy human peripheral blood cells was assessed using the MTT assay. (Van Meerloo et al., 2011)

3.10.2. Trypan Blue Dye Exclusion Assay

The trypan blue dye exclusion assay was also used to assess the viability of cells treated with various doses of R-Au-NPs (chemically synthesized) and KDY2 Au NPs (biologically synthesized). Dead cells absorb the stain and become blue, whereas living cells don't absorb the dye, hence they appear transparent. In 12-well plates, 10^4 cells/mL were seeded, and treated with the Nanoparticles for 24 hours. A

hemocytometer was used to count the cells after they were collected and stained with a 0.4 % trypan blue solution. (Strober, 2015)

3.10.3. Hemolytic assay

When evaluating the cytotoxicity of chemicals or drugs, hemolysis is critical. Erythrocytes are a good choice as typical human cells due to their quantity, accessibility, and simplicity of separation from plasma. Here, the NPs' capacity to trigger erythrocyte membrane breakdown and the release of cellular content is assessed. (Sæbø et al., 2023) Fresh human blood (5.0 mL, heparinized) was centrifuged at 1500 rpm for 10 min to obtain an erythrocyte pellet (the plasma and the buffy coat were removed). The pellet was then washed thrice with sterile PBS and resuspended in PBS to get approximately 10^8 cells/mL. 0.5 mL of cell suspension was incubated with different concentrations of R-Au-NPs and KDY2 Au NPs for 1 h at 37 °C followed by centrifugation at 1500 x g for 10 min. The absorbance of the supernatant was measured at 540 nm. 1% Triton X-100 and PBS were used as positive and negative controls respectively. Conventionally, hemolysis readings below 10 % are regarded as non-hemolytic. (Amin & Dannenfelser, 2006).

3.11. Microscopic examination

Using phase contrast and fluorescence microscopy (Leica DM6 B), cytomorphological changes triggered by R-Au-NPs and KDY2 Au NPs were observed and recorded by photography. After collecting, the treated and untreated MCF-7 cells (3000 cells/mL) were washed with

ice-cold PBS. The resulting cells were examined under a phase contrast microscope and stained with appropriate fluorescent dyes like AO-EtBr (100 µg/mL) (K. Liu et al., 2015), Propidium Iodide (20 µg/mL) (Baskić et al., 2006), and Hoechst 33258 (1.0 mg/mL) (Zhang et al., 2016), dropped to glass slides, incubated for ten minutes at room temperature in the dark, and observed under a fluorescence microscope.

3.12. Clonogenic Assay

Clonogenic assay, an invitro cell survival assay, examines a single cell's ability to proliferate into a colony. Both treated and untreated cells were seeded to create colonies in a complete medium, cultured for six days. Glutaraldehyde was used to fix the colonies, followed by crystal violet staining and counting. (Franken et al., 2006)

3.13. Apoptosis Assays

3.13.1. Assessment of mitochondrial membrane potential (ΔψM).

Depletion in mitochondrial membrane potential is regarded as an initial event in apoptosis induction in some organisms. By staining the cells with the lipophilic cationic dye Rhodamine 123 (5 µg/mL) for 30 minutes at 37°C, the mitochondrial membrane potential of the control and treated cells is observed. After being washed with PBS, the cells were centrifuged, resuspended in PBS, placed on slides, and examined using a fluorescence microscope. (Leica DM6 B) (Kari et al., 2022)**.**

3.13.2. Assessment of phosphatidylserine (PS) externalization.

Phosphatidylserine (PS) is generally found on the inner leaflet of the plasma membrane bilayer and is translocated to the cell surface at the onset of apoptosis. (Martin et al., 1995) Using Alexa Fluor 488 annexin V (Apoptosis kit, Invitrogen, USA) following the manufacturer's instructions, the externalization of PS in the R-Au-IONPs and KDY2 Au NPs-treated MCF-7 cells was assessed. Together with fluorescence microscopy, flow cytometry using BD FACS ARIA III equipment with BD FACS Diva software version 8.0.3 was used to evaluate the fluorescence intensity.(Kari et al., 2022)

3.13.3. Immunoblotting

Western blotting was performed following SDS PAGE basically as depicted in (Howland, 1996) for the detection of an apoptosis-associated protein, PARP (Poly (ADP) Ribose Polymerase), an enzyme that facilitates the poly ADP ribosylation of nuclear proteins. Its cleavage is regarded as the hallmark of apoptosis. (Boulares et al., 1999)

5×10^5 cells were seeded and treated with different concentrations of R-Au-IONPs and KDY2 Au NPs for 24 hours. Following SDS-PAGE of the whole-cell lysates prepared (70µg), the proteins were transferred to polyvinylidene difluoride membranes (PVDF: Merck Millipore IPVH00010). Each membrane was then blocked for one hour at room temperature using 5% skim milk prepared in TBST (TBS with 0.1% Tween 20). Separate

immunostaining against β-actin and PARP (CST) was done overnight at 4 °C using rabbit-derived primary antibodies (dilution 1:1000). Following a TBST wash, the membranes were incubated with anti-rabbit HRP-conjugated secondary antibodies (dilution1:5000) for two hours at room temperature. After another TBST wash, the bands were stained with 3, 3'-diaminobenzidine (DAB) to make them visible.

3.14. cell cycle Analysis

Cell cycle analysis is done to examine the different phases of a cell's cycle. Here we used flow cytometry to evaluate the effect of apoptosis on the R-Au-IONPs and KDY2 Au NPs treated MCF-7 cells' cell cycle distribution. Propidium iodide (PI), a DNA intercalating dye, was used to stain the cells. The percentage of cells distributed within the sub-groups of the total cell population representing sub-G0/G1, G0/G1, S, and G2/M phases of the cell cycle was then calculated using BD FACS Diva software version 8.0.3(Gousias et al., 2022) on a BD FACS-ARIA III Flow cytometer. Briefly, the treated and control cells were isolated, fixed in 70% ice-cold ethanol, rinsed twice with PBS, and stored at -20 °C until needed. A 20 µg/mL PI solution containing 200 µg/mL DNase-free RNase A was used to stain the cells for 30 minutes before data collection and analysis.

3.15. Statistical analysis

The mean ± SD of three separate experiments expresses all experimental results. BD FACS Diva software version 8.0.3 was utilized for the flow cytometry data. Microsoft Office Excel 2019 was

used to do a one-way ANOVA on the results to determine their significance.

3.16. Ethics statement

Blood samples used for erythrocyte-based hemolytic assay and isolation of lymphocytes for hPBL culture and MTT assay were willingly self-donated by the scholar. It may be noted that according to the Indian Council for Medical Research, New Delhi, India ((National ethical guidelines for biomedical and health research involving human participants) the ethical approval for the use of self-donated blood by the researcher was deemed unnecessary. According to this guideline, proposals with less than minimal risks are exempt from the ethical review process.

RESULTS I

4. CHEMICALLY AND BIOLOGICALLY GENERATED NANOPARTICLES; SYNTHESIS & CHARACTERIZATION

The chemical synthesis of Iron oxide gold core-shell nanoparticles loaded with Rapamycin, the biological synthesis of Gold nanoparticles from the cell-free supernatant of soil bacterial isolate, and their characterization are described in this chapter.

4.1. Chemically synthesized Iron Oxide Gold-core shell Nanoparticles in the tumor-targeted delivery of Rapamycin; synthesis and characterization

Here, we aimed to develop a drug delivery system using chemically synthesized nanoparticles for the delivery of a pure breast cancer drug, Rapamycin, which has already proven its effectiveness in treating estrogen receptor-positive (ER+) breast cancer. The iron oxide nanoparticles were chosen due to their biocompatibility, low toxicity, and super paramagnetic properties. These IONPs were modified with Gold and PEG to improve their stability, functionalization, and hydrophilicity. The synthesis of IONPs, functionalization, loading of the drug Rapamycin, drug loading efficiency, and the characterization of the NPs are described in this section.

4.1.1. Synthesis of IONPs

The Iron oxide nanoparticles were synthesized using the chemical co-precipitation method. The NPs were analyzed using SEM and XRD. Fig 4.1.1 gives the SEM images and XRD patterns of the IONPs produced through the different methods. Table 4.1.1 depicts the JCPDS (Joint Committee on Powder Diffraction Standards) analysis score of IONPs from each method and Table 4.1.2 gives the particle size of the NPs. The third one of the 4 different methods used gave IONPs with better particle size (10.3 nm) and a JCPDS analysis score of 77.

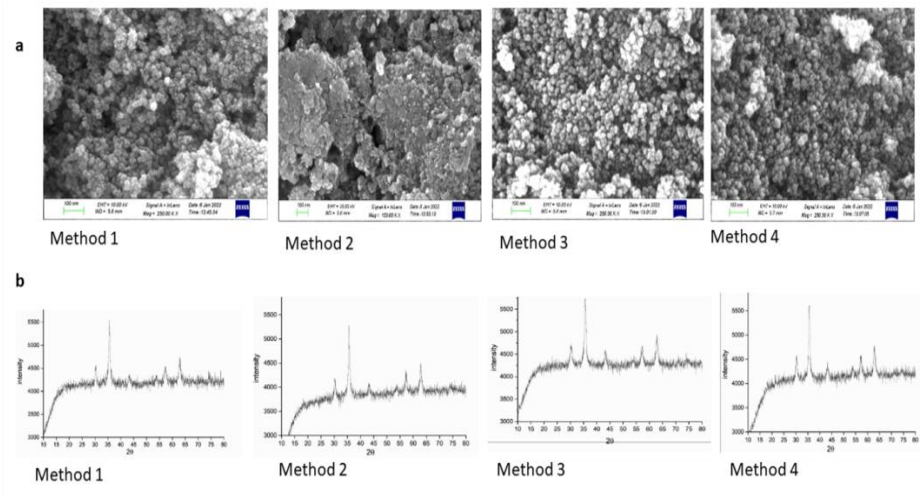

Fig. 4.1.1. (a) SEM images of IONPs synthesized using the four different methods, **(b)** XRD patterns of the IONPs obtained from different synthesis methods

Table 4.1.1. The JCPDS analysis scores of IONPs produced from different methods. JCPDS (joint committee on powder diffraction standards)/ ICDD (international center for diffraction data)

Method	Ref. code	Score	Compound name	Chemical formula
1	01-084-2782	75	Iron Oxide	Fe_3O_4
2	01-084-2782	73	Iron Oxide	Fe_3O_4
3	**01-084-2782**	**77**	**Iron Oxide**	**Fe_3O_4**
4	01-084-2782	68	Iron Oxide	Fe_3O_4

Table 4.1.2. The Peak list and crystallite size in A^o of the synthesized IONPs obtained from XRD analysis. Peak height, width, and area are also given.

Method	Pos. (2θ)	d-spacing [A^o]	FWHM-Left[*2θ]	Height [cts]	Area [cts*2θ]	Back gr.[cts]	Relative int. [%]	Crystallite size only [A^o]
1	35.5962	2.52008	0.5724	868.03	732.18	4191.06	100	120
2	35.6003	2.5198	0.6039	906.77	805.21	3826.9	100	113
3	**35.5982**	**2.51995**	**0.7242**	**956.31**	**914.31**	**4283.87**	**100**	**103**
4	35.5865	2.52075	0.6932	1003.51	976.83	4088.39	100	101

4.1.2. Synthesis of Au-IONPs, PEG-Au-IONPs, and R-Au - IONPs

The synthesized IONPs needed modifications to overcome the drawbacks such as rapid agglomeration, oxidization, etc., and to improve their surface properties to achieve binding of different molecules onto them. The Gold coating acts as a protective layer for the IONPs and provides an active layer for loading different molecules onto them. PEG-ylation again improves the pharmacokinetic attributes of the Au-IONPs by increasing hydrophilicity, escaping from immune attack, and increasing half-life.

The gold-coated IONPs (Au – IONPs), PEG - ylated Au -IONPs, and Rapamycin-loaded PEG ylated Au-IONPs (R - Au – IONPs) were synthesized as described in the methods section. All were separated magnetically using their magnetic property. (Fig 4.1.2)

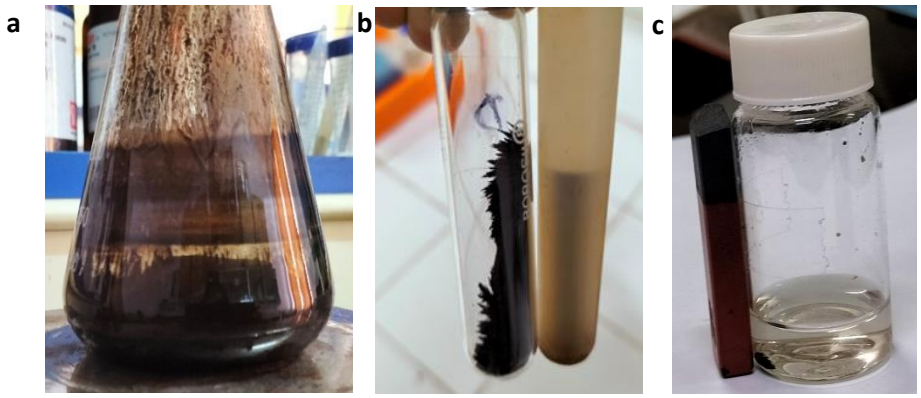

Fig. 4.1.2. Synthesis of IONPs, Au IONPs, and R-Au-IONPs: (a) The formation of IONPs as a black precipitate, **(b)** The Au-IONPs with magnetic properties, **(c)** The R-Au-IONPs separated from free drug solution using a magnet.

4.1.3. Characterization of the chemically synthesized IONPs. Au-IONPs and R-Au-IONPs

The synthesized NPs were characterized by different characterization techniques such as UV-VIS spectroscopy, XRD, FTIR, and SEM.

Scanning Electron Microscopy (SEM):

IONPs and Au-IONPs were subjected to Scanning electron microscopy to determine their morphology and size distribution. The SEM images provided information on the NP's spherical morphology and size, which is less than 100 nm in diameter. (Fig 4.1.3)

UV-Visible spectroscopy:

The IONPs and Au-IONPs were characterized by UV-visible spectroscopy to confirm the coating of gold nanoparticles onto the

IONPs. Bare IONPs showed a peak at 290 nm and the Au - IONPs showed an additional peak at 545 nm. Gold NPs have a peak at approximately 525 nm; the peak observed at 545 nm is broad and shifted away from this wavelength due to the dielectric effect of the iron oxide NPs. (Fig 4.1.4 a)

XRD analysis:

The IONPs and Au-IONPs were again characterized further to obtain the particle size and to confirm the formation of Iron oxide and iron oxide gold core-shell NPs via peak analysis and library search using the JCPDS data.

IONPs had a peak at 36^{o} (2θ) and the Au-IONPs showed an additional peak at 38^{o} (2θ), confirming the formation of IONPs and the coating of Au onto the IONPs. The size of the synthesized IONPs was found to be 10 nm. After coating with Au, the size of the IONPs was increased to 52 nm. (Fig 4.1.4 b), (table 4.1.3)

FTIR analysis:

To identify the compositional structure of the IONPs, Au - IONPs, Rapamycin, and R-Au-IONPs, they were subjected to FTIR spectroscopy to confirm the conjugation of each component. The peaks obtained evidence for the successful synthesis of PEG - ylated Au – IONPs. The coating of Rapamycin onto the PEG - ylated Au-IONPs was evidenced by the common peaks observed at 1030, 1290,1460, and 1630 cm^{-1} between pure Rapamycin and R-AU-IONPs ((Fig 4.1.5).

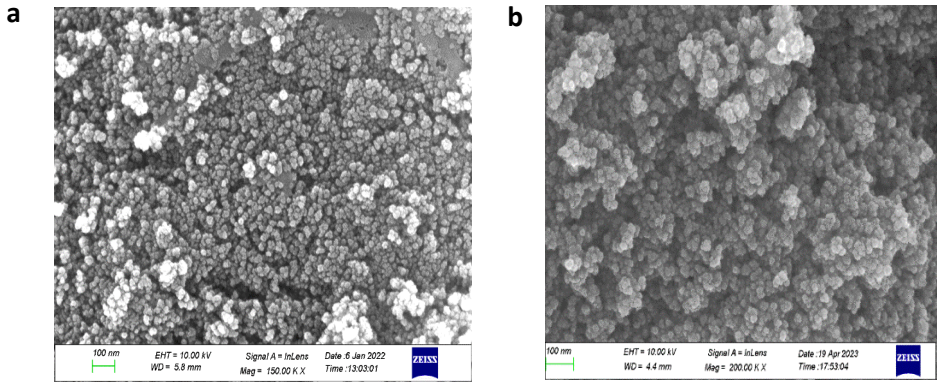

Fig. 4.1.3. SEM images of the synthesized NPs: (a) bare IONPs **(b)** Gold coated IONPs(Au-IONPs). Scale bars represent 100nm.

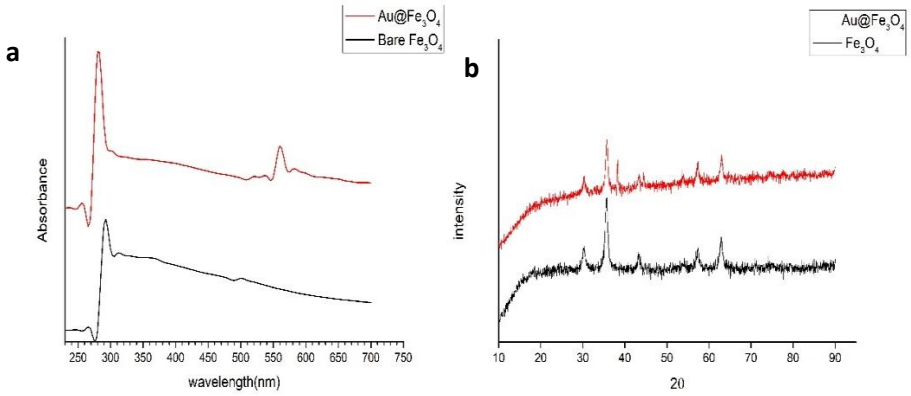

Fig. 4.1.4. Characterization of IONPs and Au-IONPs by UV-vis spectroscopy and XRD: (a) UV-vis spectra of the NPs **(b)** XRD pattern of the NPs

Table 4.1.3. The crystallite size of the IONPs and Au-IONPs in A^o

Sl. No	**NPs**	**Crystallite size [A^O]**
1	Iron oxide nanoparticles (IONPs)	103
2	Gold-coated IONPs (Au-IONPs)	517

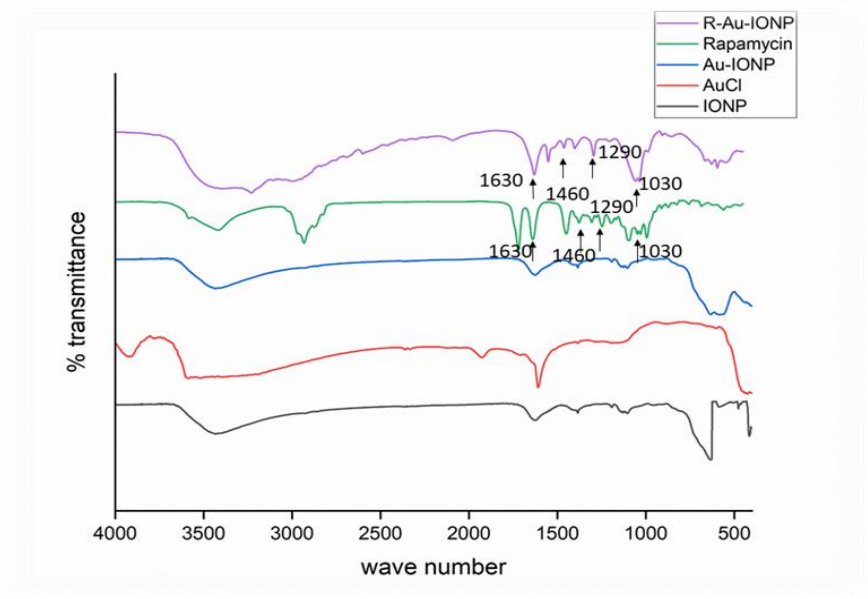

Fig. 4.1.5. FTIR spectra of IONPs, AuCl, Au - IONPs, pure Rapamycin, and R – Au – IONPs: Arrows represent significant peaks shared by pure Rapamycin and R - Au – IONPs. The shared peaks gave evidence for the successful synthesis of PEG - ylated Au - IONPs and the coating of Rapamycin onto it.

4.1.4. Drug loading efficiency

The Rapamycin loading efficiency onto the PEG-ylated Au - IONPs was determined at 24 hours. The drug loading efficiency of the formulation was approximately 70 %. The amount of Rapamycin loaded was found to be 1.36 µg/mL per 100 µg/mL of the nanoparticles.

4.1.5. Invitro drug release assay

Invitro Rapamycin release was assessed using a dialysis bag method at pH 7.4. the cumulative release of the drug was calculated

and plotted. The results showed a release of approximately 30 % from Au - IONPs at the first 5 hours, which uniformly increased and reached approximately 50 % after 20 hr. Again, the drug release gradually increased up to 80 % at 60 hours and no further increase in release was observed then. (Fig 4.1.6)

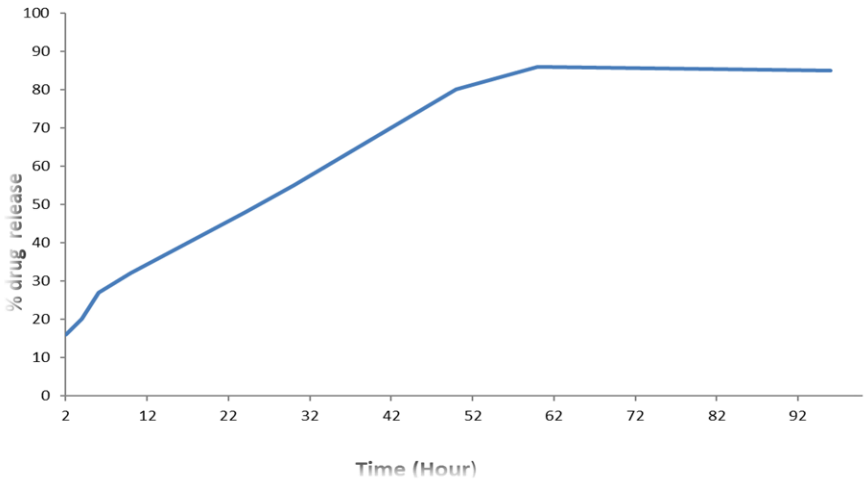

Fig. 4.1.6. Invitro drug release profile of R - Au – IONPs: Approximately 30% of Rapamycin was released within the first 5 hours, which uniformly increased and reached approximately 50 % after 20 hr. Again, the drug release gradually increased up to 80 % at 60 hours and no further increase was observed then.

4.2. Biologically produced Gold nanoparticles containing a Fluoroquinolone molecule from the cell-free extract of *E. hormaechei* soil isolates

To check the possibility of replacing the chemical methods. We attempted to develop a natural compound-capped metallic nanoparticle formulation with cytotoxic potential using different soil bacterial cell-free supernatants. For that, soil samples were collected from different

geographical regions and screened for their nanoparticle-producing capability using different metallic precursors. From the different metallic nanoparticles formed, the one with considerable cytotoxicity was selected for further investigations in MCF-7 cells. Also, the respective bacterial strain was identified by 16s rRNA sequencing and the constituents of the NPs were identified.

4.2.1. Isolation of pure bacterial colonies from soil samples

From soil samples collected from the different terrains, 7 morphologically different bacterial colonies were isolated. They were streaked onto respective agar plates (SC/GYE) and stored on slants. (Fig. 4.2.1). All the colonies were given a code number corresponding to their place of collection which was used in further studies.

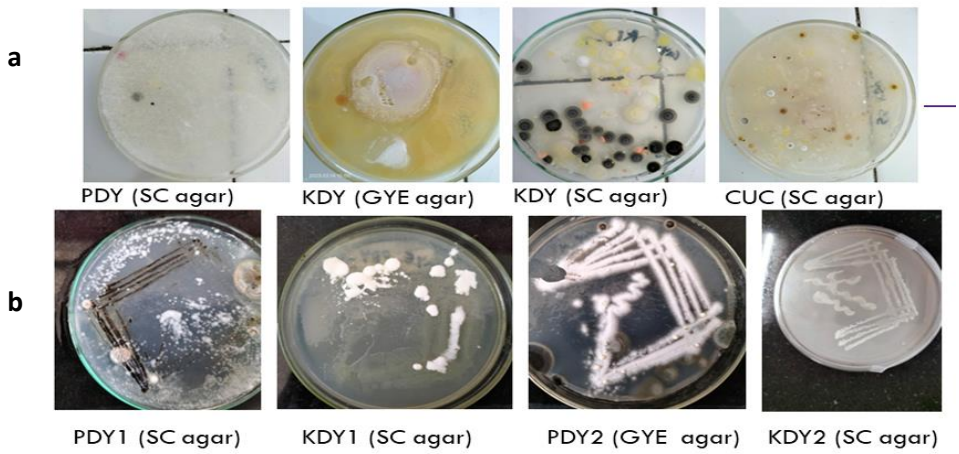

Fig. 4.2.1. Isolation of pure bacterial colonies from soil samples: (a) Bacterial colonies were obtained by spreading soil samples onto SCN and GYE agar plates and incubating at room temperature **(b)** Pure bacterial cultures Bacterial were obtained by streaking onto respective agar plates and incubating at room temperature

4.2.2. Screening of isolates for extracellular biosynthesis of metallic NPs

The 7 strains isolated were tested for their potential to synthesize different metallic nanoparticles viz, Fe, Ag, and Au. None of them produced Iron oxide Nanoparticles, while two showed silver nanoparticle-producing capability, and all seven produced Gold nanoparticles (Fig 4.2.2) (Table 4.2.1). The bacterial biomolecules can reduce Chloroauric acid ($HAuCl_4$) into $AuCl_4^-$ ions and aid the formation of AuNPs. The biomolecules such as proteins, enzymes, etc simulate the formation of AuNPs because of high standard electrode potential(Khan et al., 2022). Also, they reduce Ag^{+1} ion into Ag^0 and facilitate the formation of AgNPs. (Mikhailova, 2020) Since the bacterial by-products mediated the synthesis of the NPs, their properties, like morphology, size, and other physical, chemical, and biological properties, are greatly influenced by the active molecules in the culture supernatant. These molecules protect the NPs during the green synthesis processes and stabilize them. (Mohammed Fayaz et al., 2011)

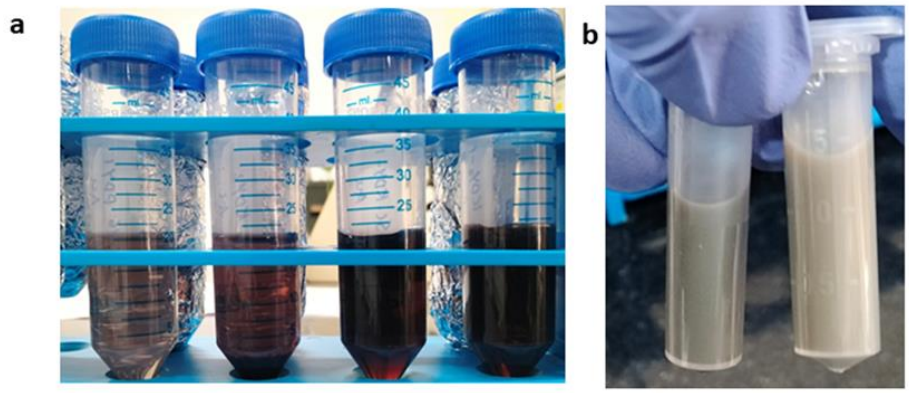

Fig. 4.2.2. Formation of Au and Ag NPs evidenced by the change in color: (a) yellow to deep purple **(b)** dark brown respectively

Table 4.2.1. List of Metallic NPs formed from different soil bacterial isolates

Au NPs formed	Ag NPs Formed
KDY1	KDY1
KDY2	PDY1
TP1	
TP2	
PDY1	
PDY2	
PDY3	

4.2.3. Screening the synthesized NPs for cytotoxic potential

The Gold and Silver Nanoparticles formed were screened for their cytotoxicity using MTT assays in Human colorectal cancer cells (HCT 116) and Human Adeno carcinoma cells (MCF-7). (Fig 4.2.3, 4.2.4). The KDY2 Au NPs showed comparable cytotoxicity in MCF-7 cells with an IC 50 value of 79.5±2.1 µg/mL (Fig 4.2.4) All other Au and Ag NPs showed IC 50 values greater than 100 µg/mL

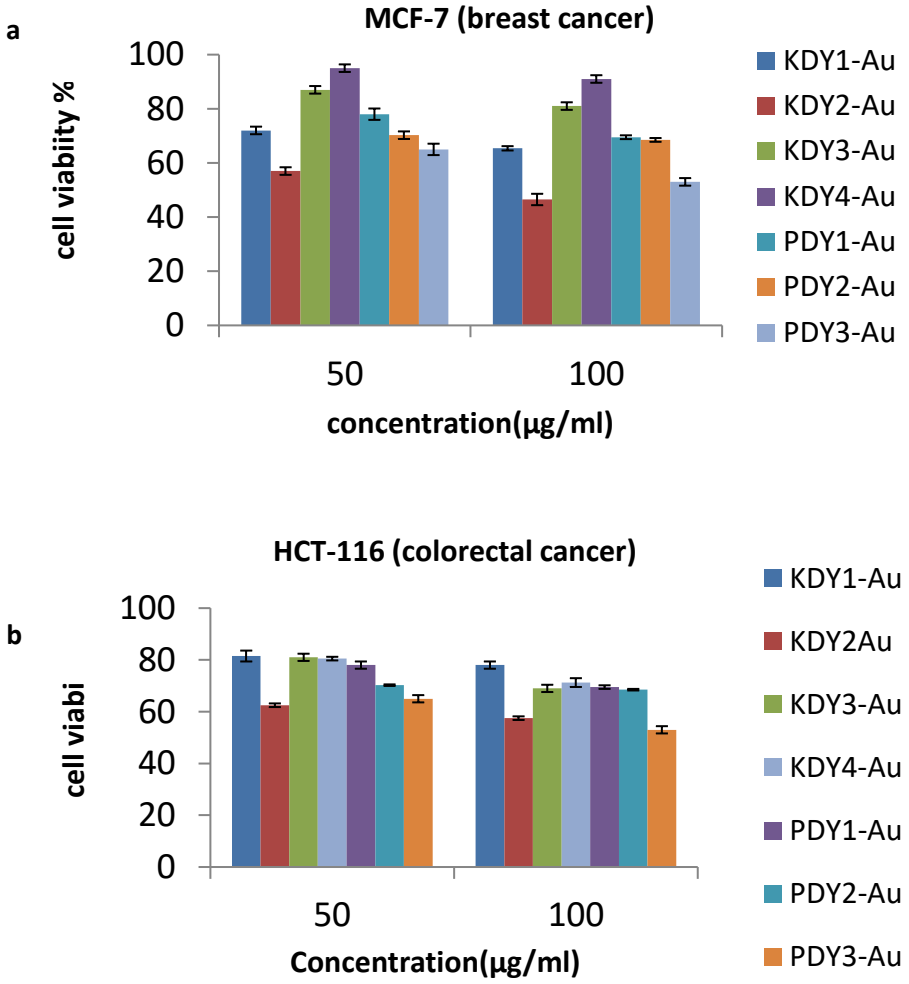

Fig. 4.2.3. Cytotoxicity of the Au NPs formed (a) Viability of breast cancer cells (MCF-7) when treated with two different concentrations of Au NPs. **(b)** Viability of colorectal cancer cells (HCT-116) when treated with two different concentrations of Au NPs. Values represent Mean ± SD (n=3); $P<0.01$

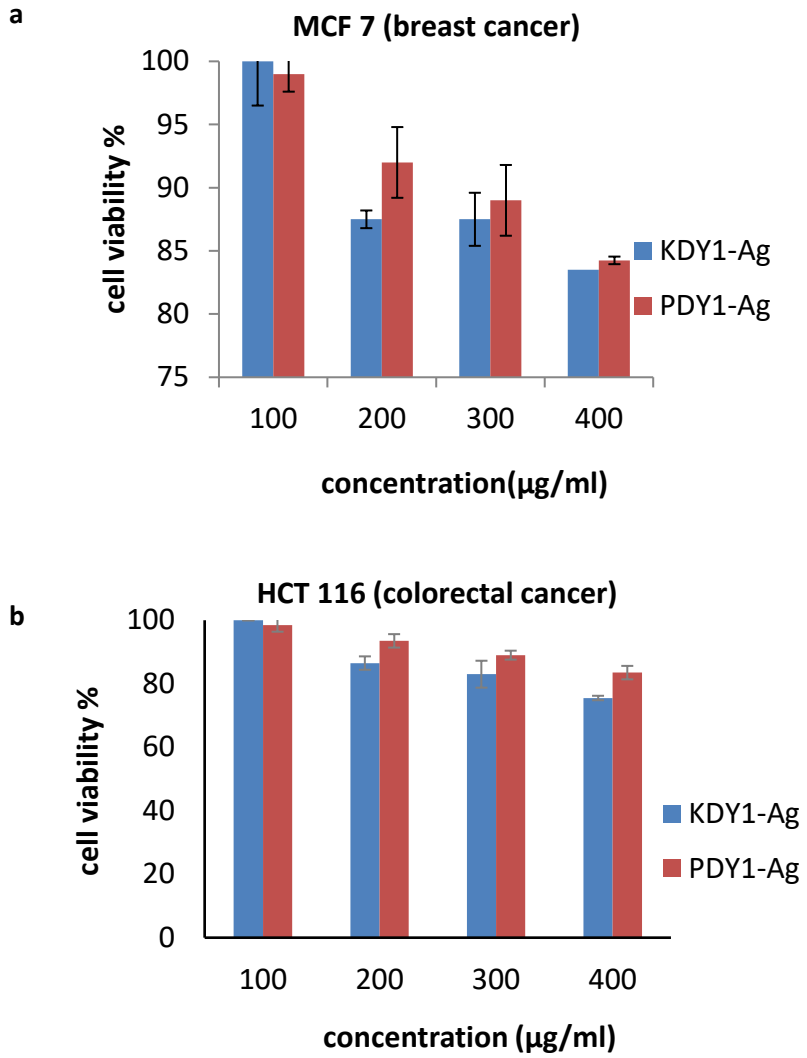

Fig. 4.2.4. Cytotoxicity of the Ag NPs formed (a) Viability of breast cancer cells (MCF-7) when treated with four different concentrations of Ag NPs. **(b)** Viability of colorectal cancer cells (HCT 116) when treated with four different concentrations of Ag NPs. Values represent Mean ± SD (n=3); $P<0.01$

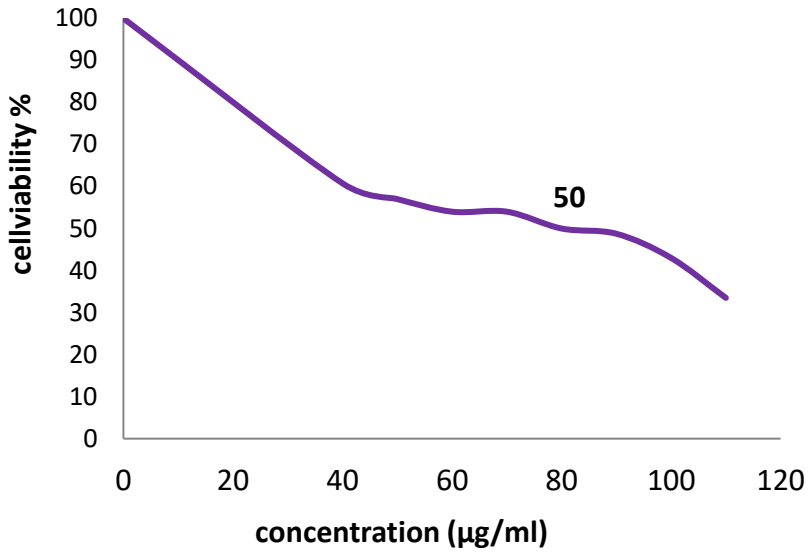

Fig. 4.2.5. Effect of Kdy 2 Au NPs on MCF-7 cell viability: The viability of MCF-7 cells when treated with different concentrations of KDY 2 Au NPs (0-120 µg/mL). An IC 50 value of 79.5±2.1 µg/mL was obtained. Values represent Mean ± SD (n=3); $P<0.01$

4.2.4. Molecular identification of the selected strain KDY2

The KDY2 strain was molecularly identified using the 16S rRNA sequencing method. Based on their homology and alignments with previously known bacterial 16S rRNA sequences obtained by BLAST search, the bacteria were identified as *Enterobacter hormaechei* strain. The data was reported to the NCBI GenBank database (accession No. PQ119951) (Fig 4.2.6 a). A phylogenetic tree was constructed using MEGA 11 (Fig 4.2.6 b).

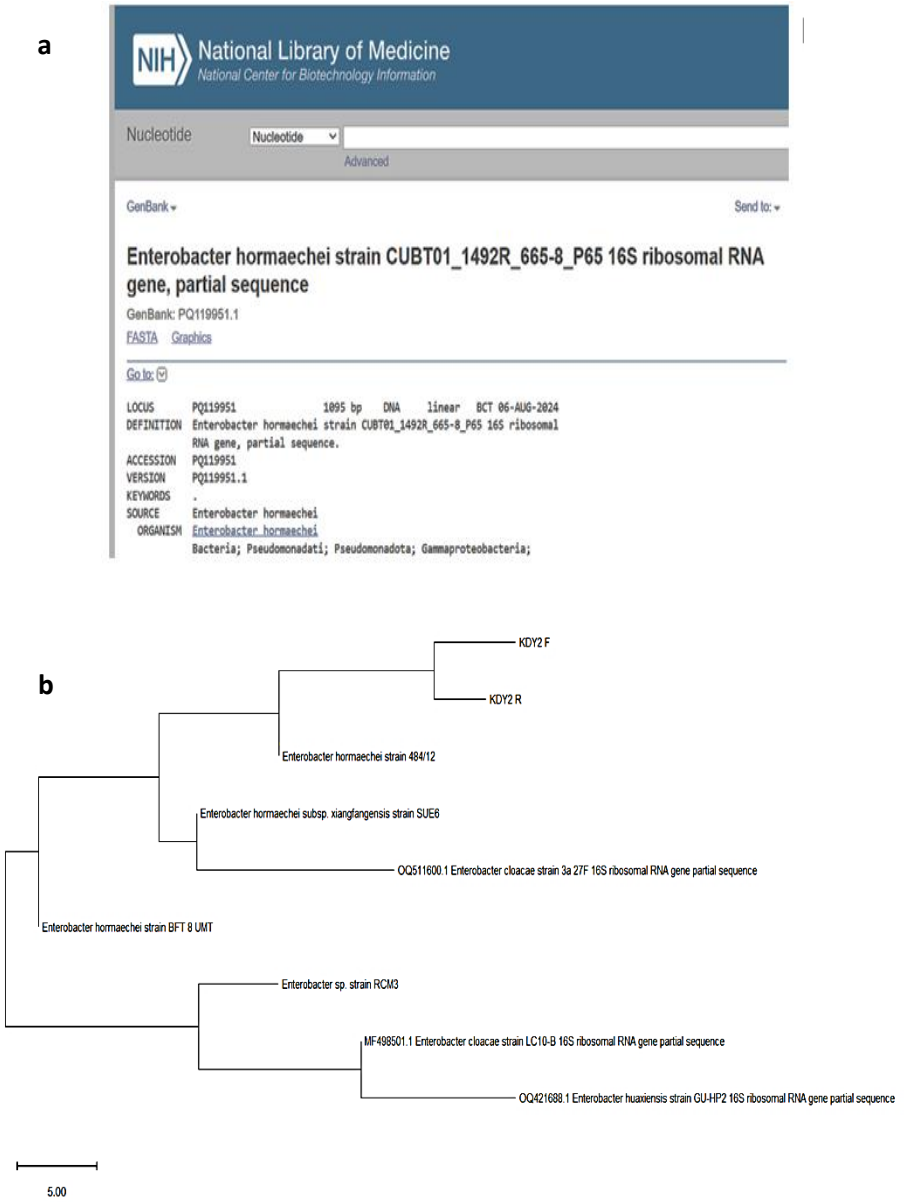

Fig 4.2.6. Molecular identification of the strain KDY 2 (a) The partial rRNA gene sequence of the KDY2 strain deposited in GenBank with accession number PQ119951 **(b)** The neighbor-joining approach was used to generate a phylogenetic tree Utilizing KDY2 16S rRNA gene sequence.

4.2.5. Characterization of KDY2 Au NPs

Scanning Electron Microscopy:

SEM was used to analyze the morphological features of the KDY 2 Au NPs, the NPs were found to be spherical within a diameter of 100 nm (Fig 4.2.7).

UV-VIS spectroscopy:

In UV-VIS spectroscopy, the KDY 2 Au NPs showed absorption peaks at 280 nm and 550 nm corresponding to the presence of proteins and Au NPs respectively (Biter et al., 2019) (Yi et al., 2013) (Fig4.2.8 a).

XRD:

The crystalline structure of synthesized KDY2 Au NPs was observed on the X-ray diffraction (XRD) pattern. Significant peaks were detected at 17.650°, 22.093° corresponding to amylopectin (a constituent of starch in the media used), and 38.190^0 corresponding to Gold (Fig 4.2.8 b, Table 4.2.2)

FTIR analysis:

The KDY2 Au NPs were subjected to Fourier transform infrared (FTIR) spectroscopy to trace the biomolecules present on their surface (Fig 4.2.9). Five prominent peaks were observed in the spectra at wavelengths 3433.15, 2927.89, 1643.53, 1156.59, and 1019.67 cm^{-1}. The peaks were analyzed using the Insta Nano- FTIR functional group

database table with search. The peak at 3433.15 cm^{-1}, distinguishes the O-H stretching involving the vibration of alcohols, which might be caused by the formation of NPs in the aqueous phase. The peak at 2927.89 cm^{-1} corresponds to alkane groups and amine salts, indicating the C−H stretch of methylene groups of protein and the N−H stretch of the amine salt. The C=O stretching of amino acid residues, C=N, C=C stretching, and N−H bending of amino acids and proteins are measured at 1643.53 cm^{-1}. The C−O stretching of alcohols, esters, carboxylic acids, and C−N stretching of aliphatic amines are recorded at 1156.59 cm^{-1}. C−F stretching of fluoride compounds is recorded at 1156.59 and 1019.67 cm^{-1} indicating the presence of Fluoroquinolones (Yadav & Talwar, 2019).

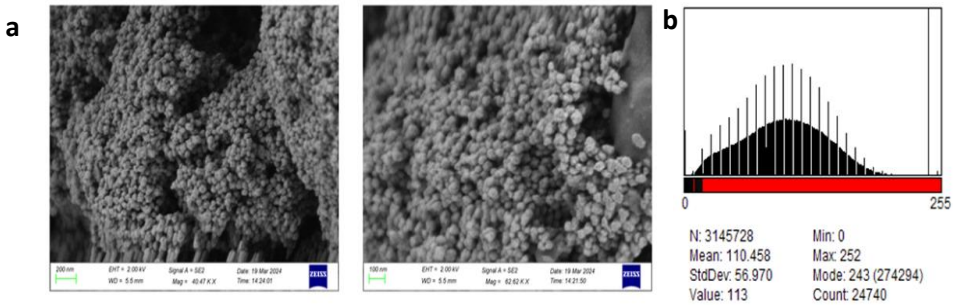

Fig. 4.2.7. (a) SEM images of KDY2 Au NPs. The NPs had a spherical shape with a smooth surface and very small size. Scale bars represent 200nm and 100nm respectively **(b)** Particle size distribution histogram of the NPs obtained from Image J software

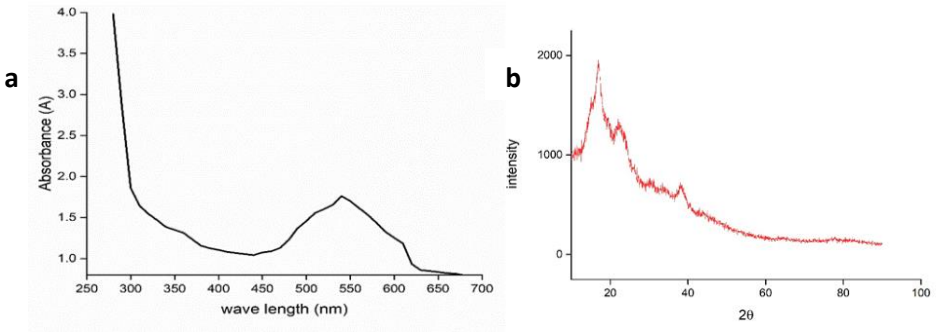

Fig. 4.2.8. Characterization of KDY2 Au NPs by UV-vis spectra and XRD: (a) UV-visible spectroscopy gave a peak at 545nm corresponding to Gold, implying the formation of gold nanoparticles, **(b)** the X-ray diffraction data gave evidence for the formation of gold nanoparticles by a peak at 38^{o} (2θ).

Table 4.2.2. Crystalline size of the KDY2 Au NPs obtained from XRD analysis

Peak (2θ)	Compound	Crystalline size (A^{o})
38.196	Gold (00-066-0091)	2.35432

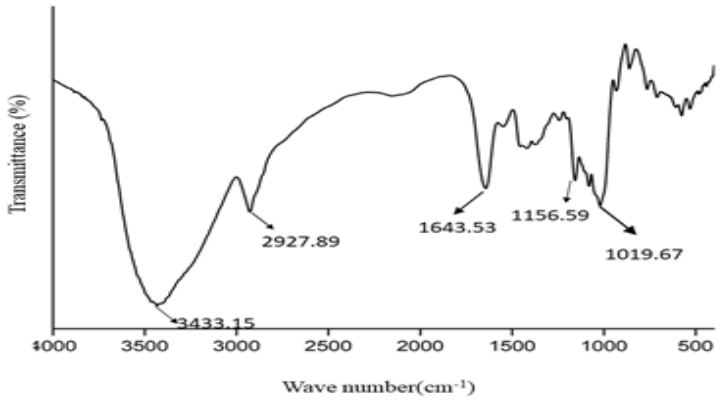

Fig. 4.2.9. FTIR spectra of KDY 2 Au NPs: The FTIR analysis gave insights into the composition of the KDY 2 Au NPs with peaks corresponding to proteins, amino acids, and a Fluorocompound.

4.2.6. Antioxidant activity assays of KDY 2 Au NPs

The anti-oxidant potential of KDY 2 Au NPs was tested using three different assays, DPPH radical scavenging assay, ABTS radical scavenging assay, and Metal chelating ability of ferrous ion. All three tests indicated that the KDY 2 Au NPs had no anti-oxidant property at the tested concentration range**.**

4.2.6.1. DPPH radical scavenging assay

The KDY2 Au NPs had negligible DPPH radical scavenging ability up to 1 mg/mL concentration compared to the positive control Ascorbic acid. (Figure 4.2.10 a)

4.2.6.2. ABTS radical scavenging activity

The KDY2 Au NPs exhibited no ABTS radical scavenging ability up to the tested concentration (1 mg/mL) when compared to the positive control Ascorbic acid. (Figure 4.2.10 b)

4.2.6.3. Metal chelating activity of Ferrous ion

The NPs had little or no metal chelation activity when compared to the positive control EDTA. (Figure 4.2.10 c)

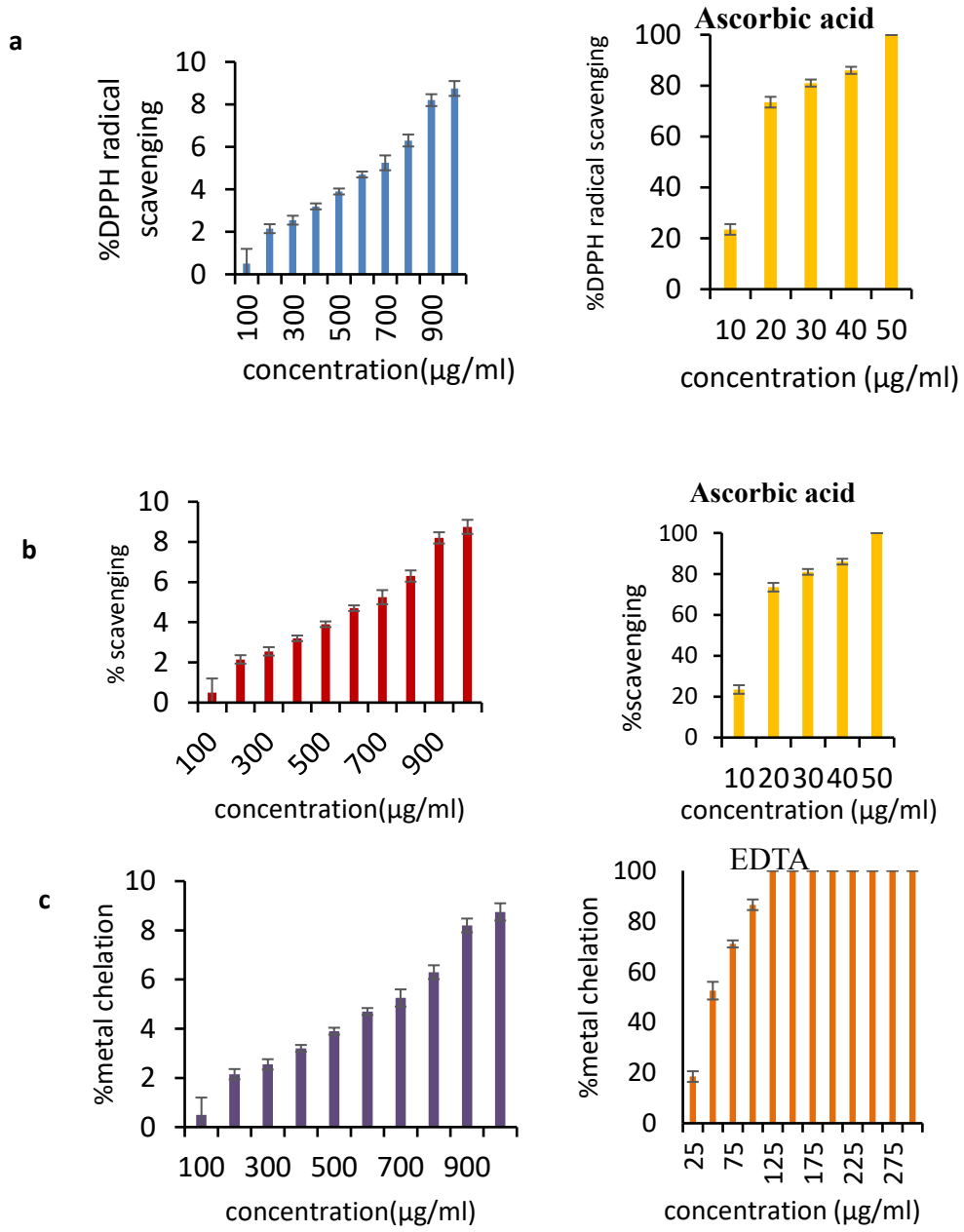

Fig. 4.2.10. Anti-oxidant activity of KDY2 Au NPs (a) DPPH free radical scavenging assay **(b)** ABTS radical scavenging activity **(c)** Metal chelation activity of ferrous ion. Values represent Mean ± SD (n=3); P<0.01

4.2.7. Anti-microbial assay

The anti-fungal activity of KDY2 Au NPs was tested in two pathogenic fungi (*Aspergillus niger*- NCIM 1004, *Candida albicans*- NCIM 3102) by agar well diffusion method. It showed little or nil anti-fungal activity in the concentrations tested (250-750 µg/mL) concentration tested (Fig 4.2.11).

The anti-bacterial activity of KDY2 Au NPs was tested against Two Gram-positive bacteria (*Staphylococcus aureus*-ATCC 29213, *Enterococcus faecalis*- ATCC 29212) and three Gram-negative bacteria (*Escherichia coli*- ATCC 25922, *Klebsiella pneumoniae*- ATCC 700603, *Pseudomonas aeruginosa*- ATCC 27853) by broth microdilution method. In this method, we can measure endpoints as the turbidity which indicates the concentration of viable microorganisms and hence helps to determine the IC 50 value.(Bubonja-Šonje et al., 2020) (Fig 4.2.12). The IC 50 values of the NPs are given in Table 4.2.3.

a

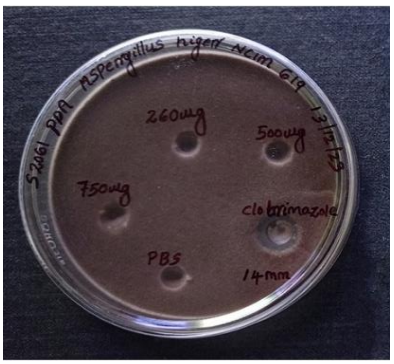

b

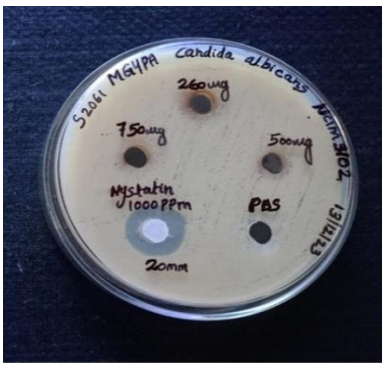

Fig. 4.2.11. Anti-fungal activity of KDY2 Au NPs in **(a)** *Aspergillus niger* **(b)** *Candida albicans*

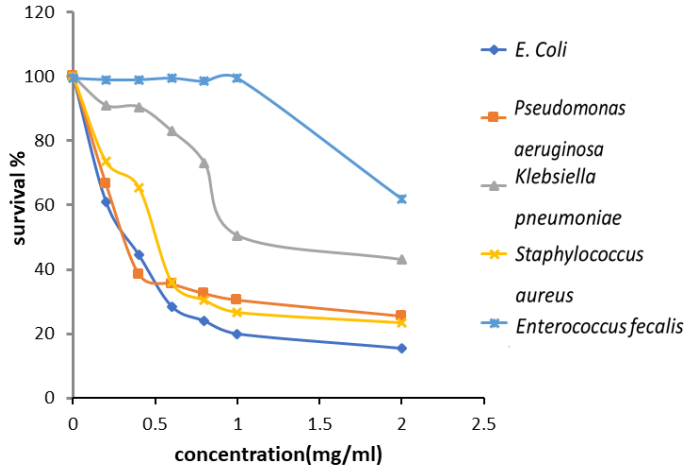

Fig. 4.2.12. Anti-bacterial activity of KDY2 Au NPs. Values represent Mean ± SD (n=3); P<0.05

Table 4.2.3. Antibacterial potential of KDY2 Au NPs. Values represents mean ±SD (n=3)

organism	**IC 50 (mg/mL)**
Escherichia coli	0.3±0.02
Pseudomonas aeruginosa	0.29±0.002
Klebsiella pneumoniae	0.9±0.04
Staphylococcus aureus	0.5±0.03
Enterococcus faecalis	>2.5

4.2.8. LC/Q-TOF/MS analysis of the KDY2 cell-free supernatant

LC/Q-TOF/MS analysis of the *E. hormaechei* supernatant gave evidence for the presence of a fluoroquinolone compound which is more identical to Norfloxacin and Moxifloxacin (Table 4.2.5) (Fig 4.2.13). This discovery made it easier to comprehend how KDY2 Au NPs work to combat bacteria and cancer. In bacterial cells, fluoroquinolones act by blocking the DNA gyrase (topoisomerase II)

and topoisomerase IV catalytic cycle, which are enzymes involved in bacterial transcription and replication. (Kloskowski et al., 2023). In cancer cells, they can cause mitochondrial malfunction, oxidative stress, and decreased glutathione levels. (Beberok, Rzepka, et al., 2018). Additionally, they cause apoptosis by raising BAX levels, mitochondrial depolarization, PARP cleavage, and the induction of Caspase-8, -9, and -3. They also induce cell cycle arrest by targeting Cyclin-CDK complexes. (Aranha et al., 2000) (Aranha et al., 2003)(Sousa et al., 2013) (Mukherjee et al., 2005) (Herald et al., 2002)

a

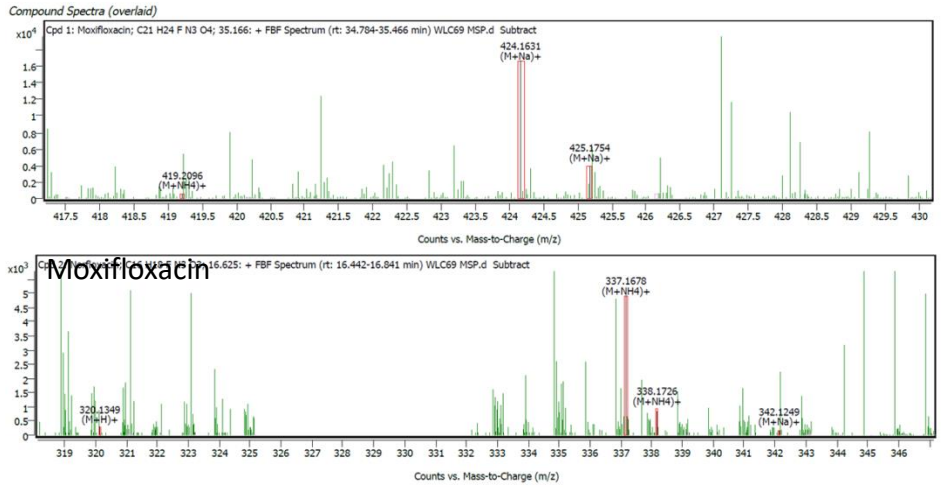

b

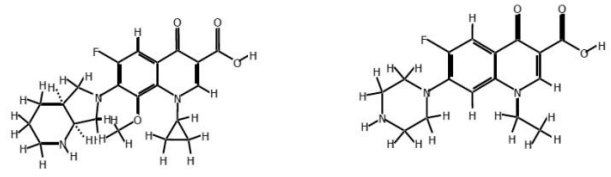

Moxifloxacin Norfloxacin

Fig 4.2.13. Results of the LC/Q-TOF/MS analysis of the *E. hormaechei* cell-free supernatant; (a) compound spectra overlaid (**b)** Structure of the identified compounds

Table. 4.2.4. Results from the LC/Q-TOF/MS analysis of the *E. hormaechei* cell-free supernatant

Sl. NO	Name	Formula	RT	Mass	Mass difference (ppm)	Score
1	Moxifloxacin	C21 H24 F N3 O4	35.166	401.1756	1.28	74.09
2	Norfloxacin	C16 H18 F N3 O3	16.625	319.1340	2.33	78.63

To summarize, the present study documents the successful synthesis of Iron Oxide Nanoparticles through the chemical co-precipitation method. Iron oxide Nanoparticles possess many favorable properties such as biocompatibility, and superparamagnetic properties. (Schneider et al., 2022). We utilized Gold and PEG to increase the bioavailability and stability of the IONPs because they have been shown to enhance the IONP-mediated delivery of numerous other compounds, such as Doxorubicin, EGF, Ce6, Sulforaphane, and Curcumin. (Danafar et al., 2018) (Nodoushan et al., 2023) (Cândido et al., 2023)(Peréz et al., 2024). The Gold coating protects the magnetic core, facilitates the conjugation of other molecules onto it, and increases the NPs' stability and bioavailability in physiological circumstances. (Lau et al., 2023) (Tonthat et al., 2023). By attaching PEG to biomolecules or nanoparticles via functional groups, a process known as PEG-ylation, the molecules become more hydrophilic, have a longer half-life, are less toxic, and are resistant to immune attacks. (L. Shi et al., 2021) Here, we could develop a drug delivery system combining Rapamycin with Gold-coated PEGylated iron oxide nanoparticles (R-Au-IONPs). The successful synthesis of IONPs and R-Au-IONPs was confirmed by SEM, XRD, and FTIR characterizations. Loading efficiency and the in vitro release of

Rapamycin from the nanoformulation were also examined. Further studies are recommended to test the enhanced activities of different drugs when administered through the IONP-delivery system.

Again, we did the first effective production of gold nanoparticles from the supernatant of the *E. hormaechei* KDY2-strain. The synthesis of Au NPs was validated by characterization techniques such as UV-Vis spectroscopy, SEM, and XRD. The results of the FTIR analysis showed that proteins and a fluoro compound were present in the produced nanoparticles, which may serve as the capping molecules in the NPs. The KDY2 Au NPs demonstrated significant cytotoxicity, antibacterial activity, and negligible or no antifungal and anti-oxidant activity. Again, we looked into identifying the principal constituent that is responsible for the cytotoxic properties of the KDY2 Au NPs utilizing LC/Q-TOF/MS analysis. The findings confirmed the existence of a fluoroquinolone compound that resembled Norfloxacin and Moxifloxacin. Fluoroquinolones interact with DNA Gyrase or topoisomerase II-DNA complexes in bacteria and prevent helix re-joining, which creates double-stranded DNA breaks. (Aldred et al. 2014). These enzymes are completely distinct from their mammalian counterparts, making Fluoroquinolones more susceptible to bacteria. (Zhao et al., 1997) Even though fluoroquinolones are synthetic molecules, many bacteria have been reported to produce their analogs. (Karatay et al., 2023) In addition to the Antibacterial properties, the KDY2 Au NPs showed cytotoxic potential in the Human adenocarcinoma cell line, MCF-7.

This indicates the need for further studies examining the anti-proliferative potential of the R-Au-IONPs and KDY2 Au NPs.

RESULTS II

5. ASSESSMENT OF THE ANTI-PROLIFERATIVE POTENTIAL OF SYNTHESIZED NANOPARTICLES

As Rapamycin is reported to have anti-proliferative effects in ER + breast cancer cells, (Chang et al., 2007) the R-Au-IONPs should possess significant cytotoxicity in an Estrogen receptor-positive (ER+) breast cancer cell line. So, we chose the MCF-7 cell line to evaluate its efficacy. The biologically produced KDY 2 gold nanoparticles also showed comparable activity in MCF-7 cells in the preliminary screening. The antiproliferative effects of R-Au-IONPs and KDY 2 Au NPs in MCF-7 cells are described in this section.

5.1. Cytotoxicity Assays

5.1.1. MTT Assay

Effect of R-Au-IONPs on MCF-7 cell viability:

The cell viabilities were assessed by MTT assay, the results are represented in terms of % cell viability and the IC 50 value. MCF-7 cells were treated with IONPs, Au-IONPs, PEG-Au-IONPs, R-Au-IONPs, and Pure Rapamycin at different concentrations (0 to 250 µg /mL) for 72 hours. IONPs, Au-IONPs, and PEG-Au-IONPs had little or no effect on MCF-7 cells. The R-Au-IONP treated cells showed a dose-dependent decrease in viability with an IC 50 value of 81±1.4 µg /mL (1.1±0.02 µg /mL concerning the loaded Rapamycin), at 72-hour treatment, pure Rapamycin showed an IC 50 value of 40±1.4 µg /mL. The results exhibited negligible cytotoxic activity of R – Au - IONPs in human peripheral blood lymphocytes. (Fig 5.1.1a,b)

IONPs are reported to have little cytotoxicity towards prostate cancer cell lines, PC 3, DU 145, and breast cancer cells. (Danafar et al., 2018; Kheiri Manjili et al., 2016). (Kojima et al., 2018) Rapamycin showed enhanced cytotoxic activity in the MDA-MB breast cancer cell line when administered through PLGA nanoparticles (11.39 µM)rather than in the free form (20.35 µM). (Katiyar et al., 2016) In another study, Rapamycin was administered using Fe_3O_4- Carboxy methyl chitosan nanoparticles and showed high cytotoxicity in hepatic carcinoma cells, HepG2, and LO2 cells. (G. Li et al., 2015)

Effect of KDY 2 Au NPs on MCF-7 cell viability:

The KDY2 Au NPs showed negligible cytotoxicity in normal cell lines, HEK 293, L929, and human peripheral blood lymphocytes. A dose-dependent decrease in cell viability was seen in MCF-7 cells with an IC 50 value of 79.5±2.12 µg/mL at 72-hour treatment (Fig 5.1.2 a). In a study involving the Gold nanoparticles generated from the cell-free supernatants of *Streptomyces cavouresis,* an IC 50 value of 49.82 µg /mL was reported in MCF-7 cells. (Lakshman Kumar et al., 2016)

The comparable IC 50 values of 81±1.4 µg /mL (R-Au-IONPs) and 79.5 µg /mL (KDY2 Au NPs) indicate that the biologically synthesized NPs are as effective as the chemically synthesized drug-loaded nanoformulation(Fig 5.1.2 b).

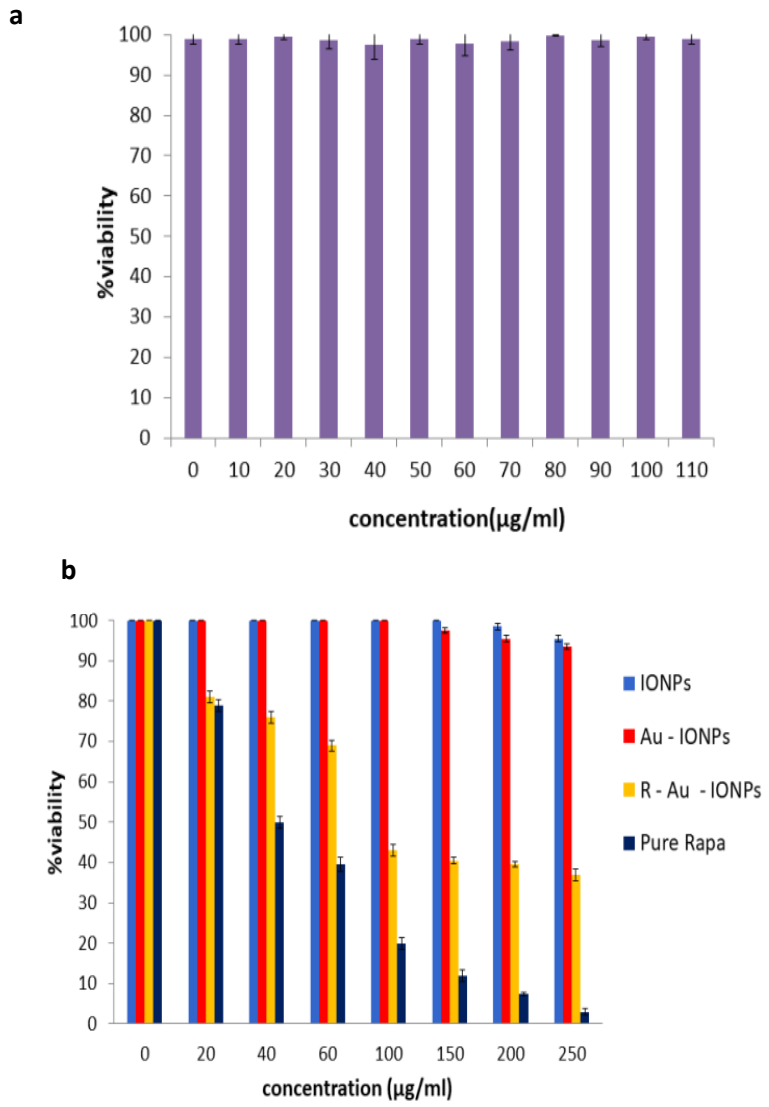

Fig 5.1.1. Cytotoxicity of R-Au-IONPs determined by MTT assay: **(a)** R-Au-IONPs' effect on the viability of human peripheral blood lymphocytes. Values represent Mean ± SD (n=3); $P<0.01$, **(b)** Cytotoxicity of IONPs, Au-IONPs, R-Au-IONPs, and pure Rapamycin in MCF-7 cells

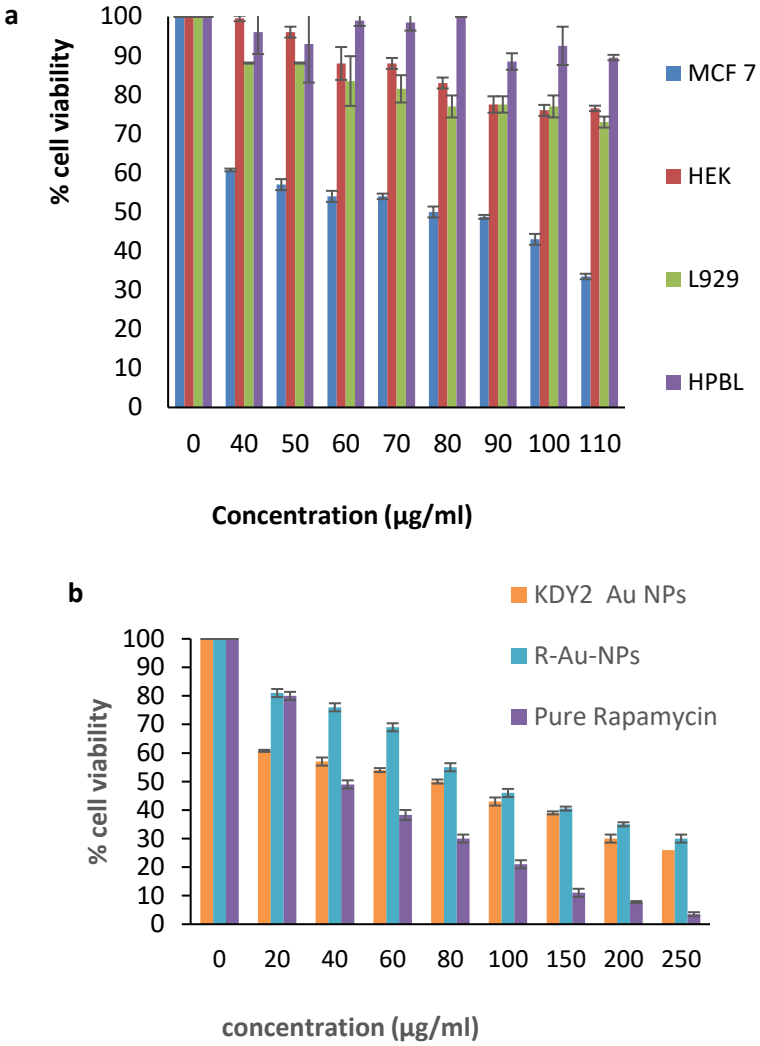

Fig 5.1.2. Cytotoxicity of KDY 2 Au NPs determined by MTT assay: (a) cytotoxic activity of KDY2 Au NPs in HEK, L929, MCF-7 cells, and human peripheral blood lymphocytes. **(b)** Cytotoxicity of R-Au-IONPs and KDY2 Au NPs on MCF-7 cells. Values represent Mean ± SD (n=3); $P<0.01$

5.1.2. Trypan Blue Dye Exclusion Assay

Other than the MTT assay, the Trypan blue dye exclusion assay was done to check the cytotoxicity of the NPs on MCF-7 cells. The live cells are distinguished from the dead ones by the ability to exclude acidic trypan blue dye with intact membranes. The damaged membranes in the non-viable cells let the dye in and stain the cytoplasm blue.

MCF-7 cells were treated with R-Au-IONPs and KDY 2 Au NPs for 72 hours and stained with trypan blue dye. The percentage of viable cells decreased by approximately 50% at the IC 50 concentration obtained from the MTT assay using the NPs. (Fig 5.1.3).

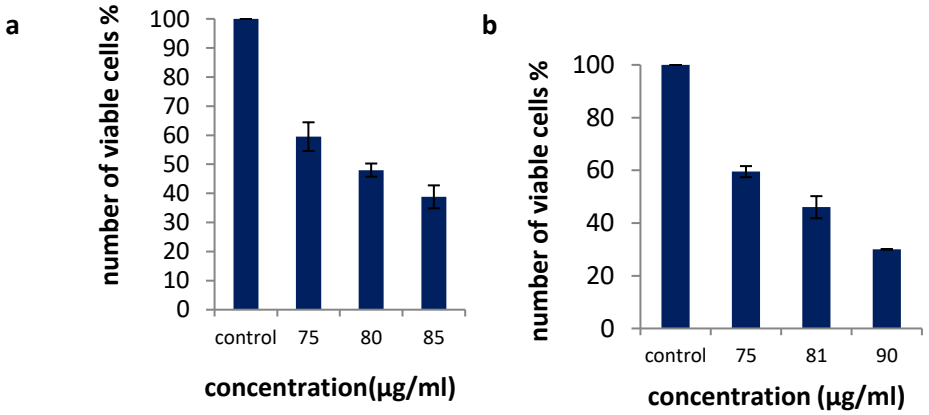

Fig. 5.1.3. Trypan blue dye exclusion assay: Effect of **(a)**R-Au-IONPs and **(b)** KDY 2 Au NPs on MCF-7 cells. The results are expressed as a percentage number of viable cells. Values represent the mean ± SD of three experiments. $P<0.001$

5.1.3. Hemolytic Assay

Hemolysis is considered crucial in evaluating the safety and functionality of the chemotherapeutic candidates. Here, PBS and 1 % Triton X-100 were used as negative and positive controls respectively. Conventionally, below 10% hemolysis is considered safe. The R-Au-IONPs and KDY 2 Au NPs exhibited a low hemolytic effect (< 10 %) toward human erythrocytes in the tested concentration range (10-100 µg/mL). The hemolytic percentage increased with the dose of the NPs (Fig 5.1.4).

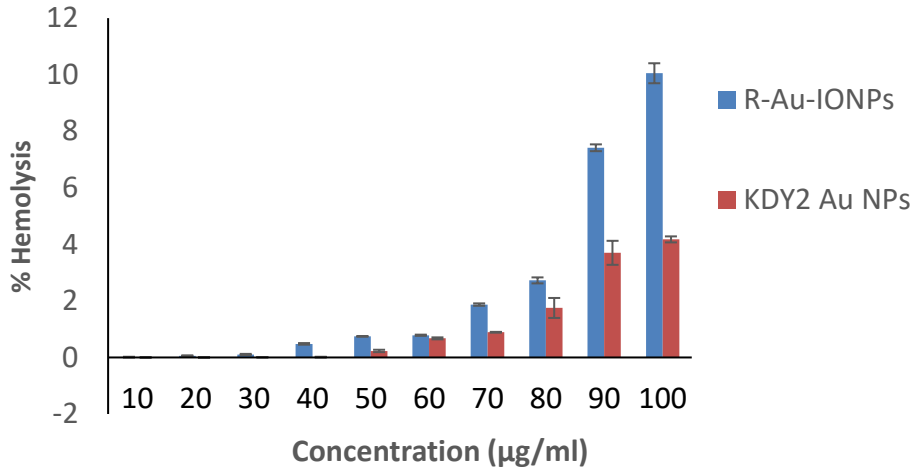

Fig 5.1.4. Hemolytic activity of R-Au-IONPs and KDY 2 Au NPs on human erythrocytes, Values represent Mean ± SD(n=3) P<0.05

5.2. Microscopic examination

5.2.1. Phase contrast microscopy

Microscopy revealed the morphological changes in the R-Au-IONP and KDY 2 Au NP-treated MCF-7 cells in a concentration-dependent manner. There was a noticeable drop in the number of cells, which suggests lower proliferation or increased cell death. The control cells looked normal as a confluent monolayer, while the treated cell population showed signs of apoptotic induction such as changes in cell shape, membrane blebbing, enlarged nuclei, etc. (Fig 5.2.1)

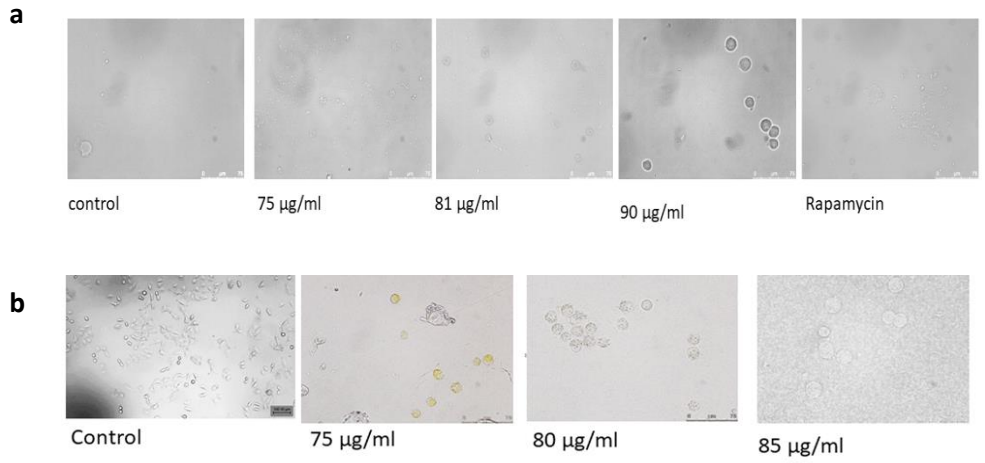

Fig 5.2.1. Phase contrast microscopy of R-Au-IONP and KDY 2 Au NP treated MCF-7 cells: Morphological changes in MCF-7 cells after treatment with (a) R-Au-IONPs, (b) KDY 2 Au NPs for 24 hr**.** Magnified images of cells undergoing apoptotic induction are also shown. Scale bars represent 75 µm**.**

5.2.2. AO-EtBr Dual staining

This simple and reliable staining method checks the apoptotic induction in cells and recognizes the early apoptotic, late apoptotic stages,(K. Liu et al., 2015) And necrosis. Acridine orange is permeable to intact membranes of viable cells and stains its nuclei green. At the same time, Ethidium bromide can only enter through disrupted cell membranes of apoptotic cells and bind DNA to emit yellow-to-orange fluorescence. Hence, normal cells appear with uniform bright green fluorescent nuclei; early apoptotic cells show green nuclei with bright patches of condensed nuclei or fragmented DNA; late apoptotic cells exhibit highly fragmented and condensed orange to red nuclei. Necrotic cells have uniformly stained bright orange nuclei. (K. Liu et al., 2015)

In R-Au-IONP and KDY 2 Au NP treated MCF-7 cells, the percentage of apoptotic cells with orange fluorescence was increased in a concentration-dependent manner compared to the control with bright green nuclei (Fig. 5.2.2 a, b). At the highest concentration of R-Au-IONP (90 µg/mL) and KDY 2 Au NPs (85 µg/mL), the apoptotic cell population was increased to 40.5 and 43.5% respectively in MCF-7 cells. The necrotic cell population was 28.5% and 30% in R-Au-IONP and KDY 2 Au NP-treated MCF-7 cells respectively.

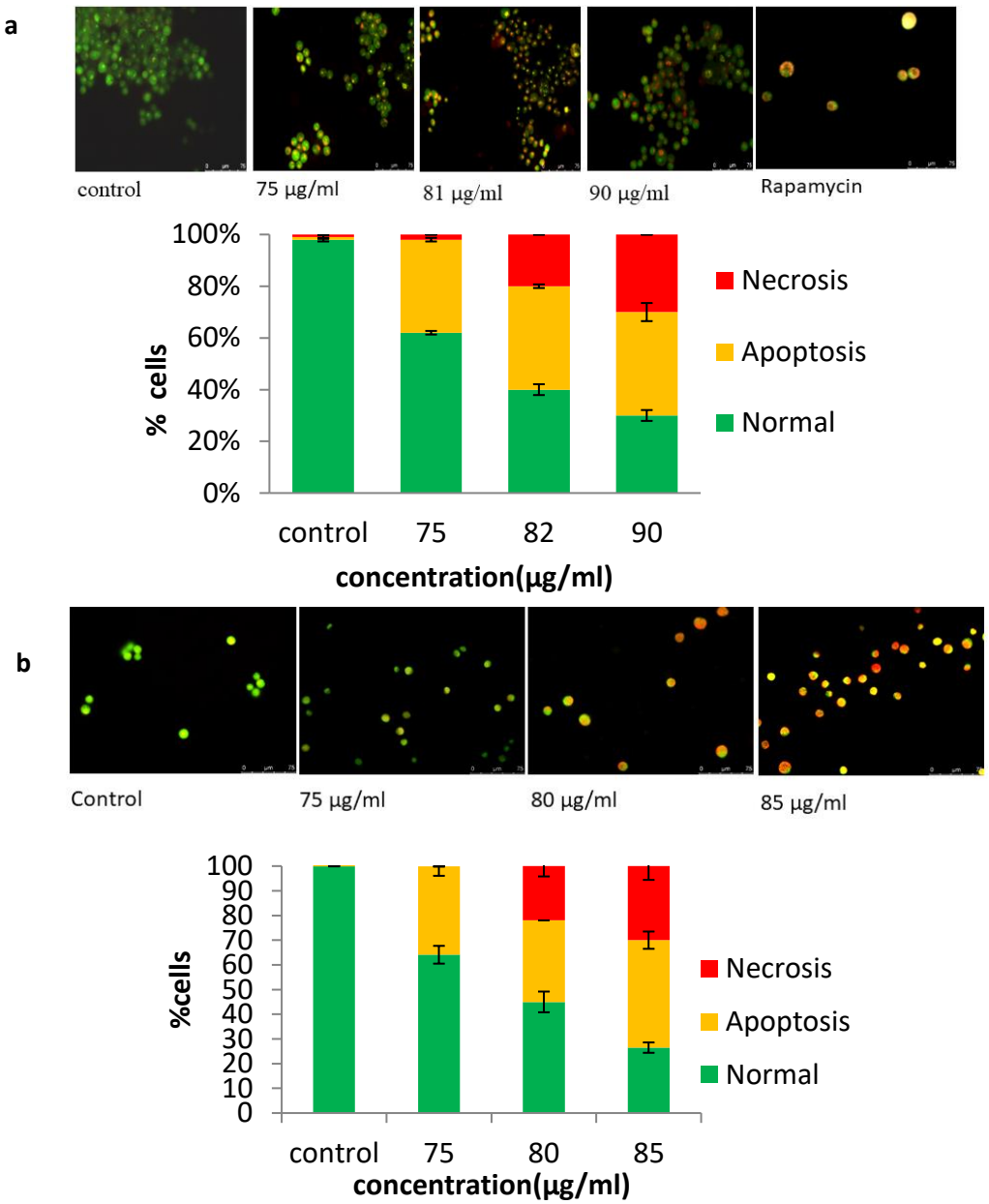

Fig 5.2.2. Fluorescence microscopy images of MCF-7 cells stained with acridine orange and ethidium bromide: After treatment for 24 hours with different concentrations of **(a)** R-Au-IONPs and **(b)** KDY 2 Au NPs. Scale bars represent 75 µm in all images. Quantitative values represent the mean ± SD of three experiments

5.2.3. Nuclear Hoechst 33258 Staining

DNA condensation and nuclei fragmentation give preliminary evidence of apoptosis in mammalian cells. These changes can be determined with the help of membrane-permeable DNA-binding fluorescent dyes. Here in the experiment, Hoechst 33258 is a dye that can bind to AT-rich regions in the minor grooves of DNA and is used to stain condensed nuclei of apoptotic cells. MCF-7 cells treated with R-Au-IONPs and KDY 2 Au NPs at different concentrations and stained with Hoechst 33258 showed a concentration-dependent increase in the number of cells with bright blue condensed nuclei compared to the uniformly stained untreated controls. The treated cells had condensed and fragmented nuclei indicating the induction of apoptosis and are marked with arrowheads. (Fig 5.2.3)

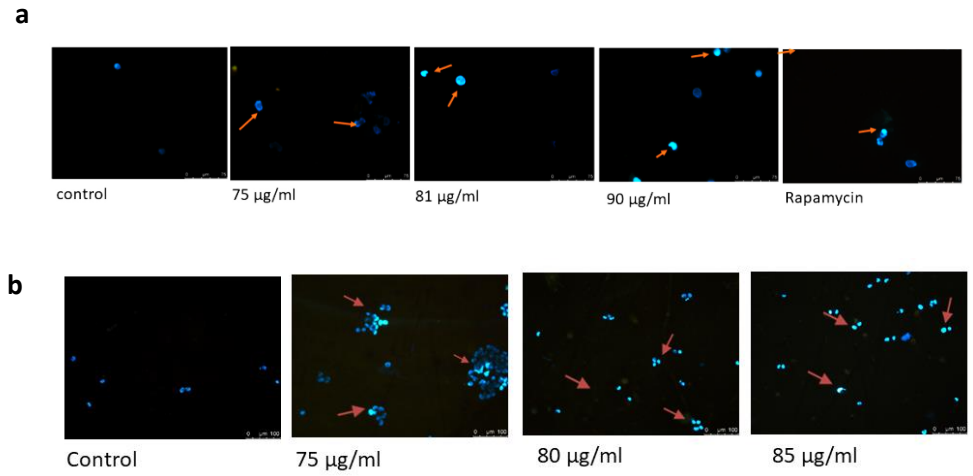

Fig 5.2.3. Hoechst 33258 staining: Fluorescence staining with Hoechst 33258 on MCF-7 cells following treatment 24-hour treatment with different concentrations of **(a)** R-Au-IONPs and **(b)** KDY 2 Au NPs. Arrowheads indicate apoptotic nuclear condensation and DNA fragmentation; scale bars represent 75 µm in all images)

5.2.4. Propidium Iodide staining

Propidium iodide is impermeable to live cells but can enter dead cells, bind to the DNA, and give red fluorescence. The nuclear morphology analysis of R-Au-IONP and KDY 2 Au NP treated MCF-7 cells confirmed the presence of apoptotic cells with fragmented nuclei and the percentage of apoptotic nuclei increased up to 68% and 63% respectively as shown in Fig (5.2.4).

a

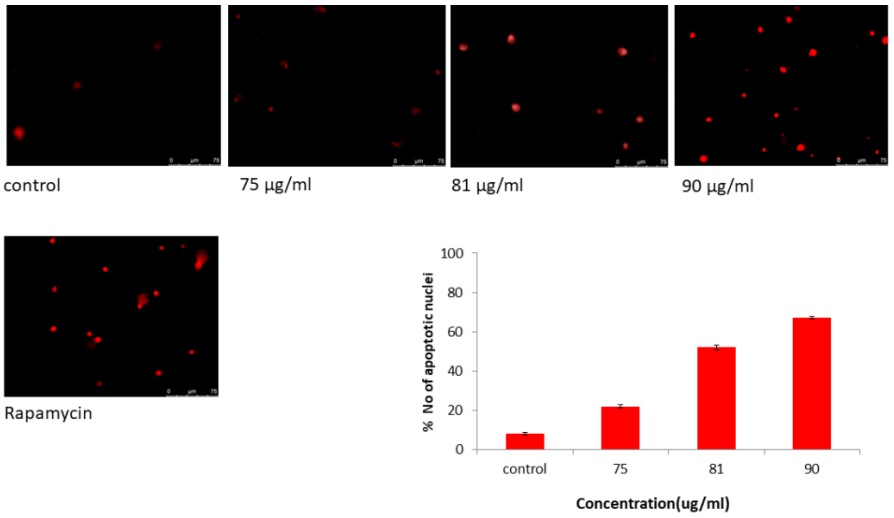

b

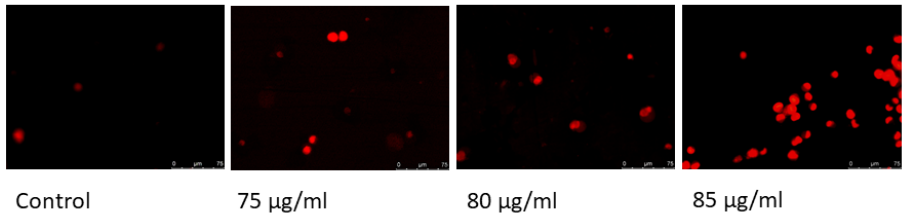

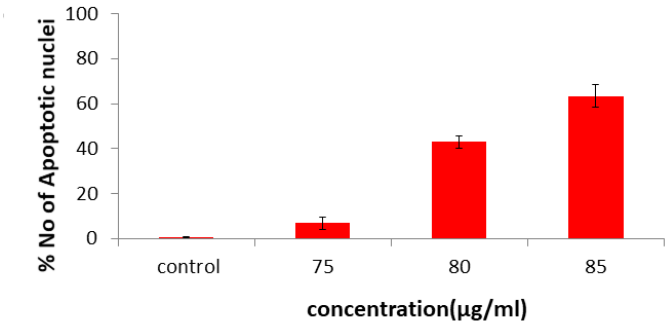

Fig 5.2.4. Fluorescence microscopy images of MCF-7 cells stained with propidium iodide: (a) Effect of R-Au-IONPs and **(b)** KDY 2 Au NPs on cells following 24 h treatment and Quantitative analysis of apoptotic cells. Scale bars represent 75 um, and Quantitative values represent the mean ± SD of three experiments. P<0.001

5.3. Clonogenic assay

Clonogenic assay checks the reproductive integrity of drug-treated cells over time to disclose the phenotypic effects that may take time to develop. The cells were treated with R-Au-IONPs and KDY 2 Au NPs at their different concentrations, the results show a concentration-dependent decrease in colony formation compared to the untreated control cells. A 70% and 30 % reduction in colony number was observed in MCF-7 cells treated with R-Au-IONPs and KDY 2 Au NPs respectively at IC 50 concentration. The NPs significantly affected the clonogenic survival of the cell. The results demonstrated that the

NP formulations have a cytostatic effect on the cell thus interfering with the colony formation ability. (Fig 5.3)

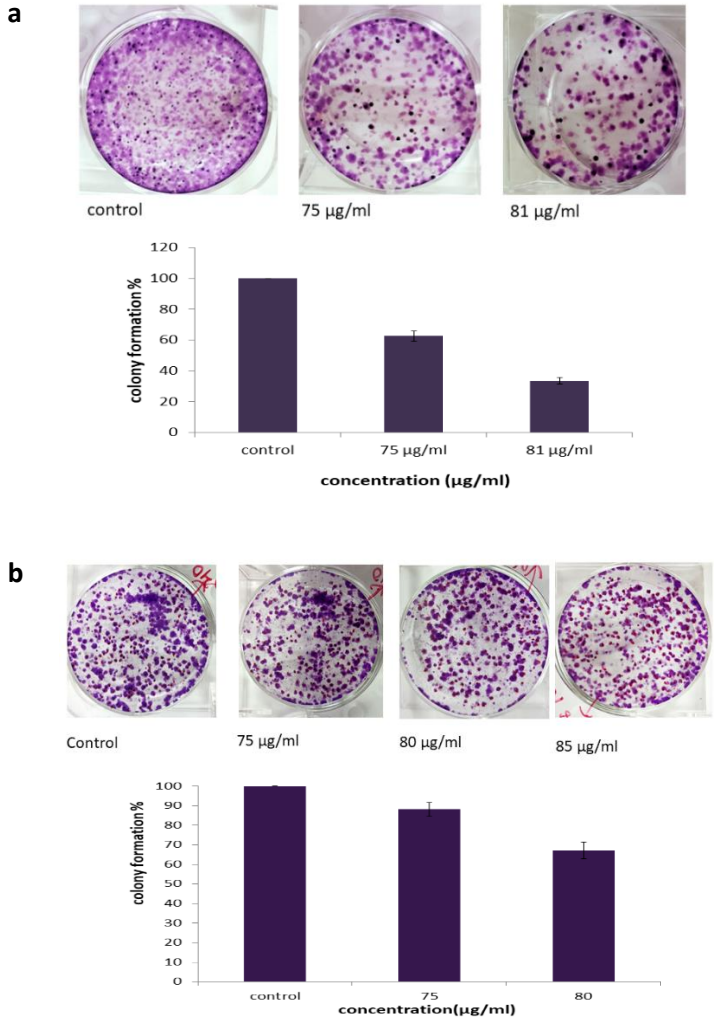

Fig. 5.3. Clonogenic assay of MCF-7 cells: (a) R-Au-IONPs and **(b)** KDY 2 Au NPs treated MCF-7 cells. Colonies stained with crystal violet. The number of colonies reduced when compared to untreated controls. The colonies were counted manually and expressed as a percentage of treatment relative to the control. values represent the mean ± SD of three experiments

5.4. Apoptosis Assays

5.4.1. Evaluation of Mitochondrial membrane potential change (ΔΨm)-Rhodamine 123 staining

Membrane depolarization of mitochondria is a hallmark of apoptosis, The MMP reduction initiates cell apoptosis irreversibly. ΔΨm changes can be detected using lipophilic cationic dyes permeable through the cell membrane to accumulate in the mitochondrial matrix. Rhodamine123 is a cationic fluorescence dye used as an indicator for transmembrane potential. R-Au-IONP and KDY 2 Au NP treated MCF-7 cells showed an increase in fluorescence compared to the control, indicating the changes in mitochondrial membrane potentials. (Fig 5.4.1)

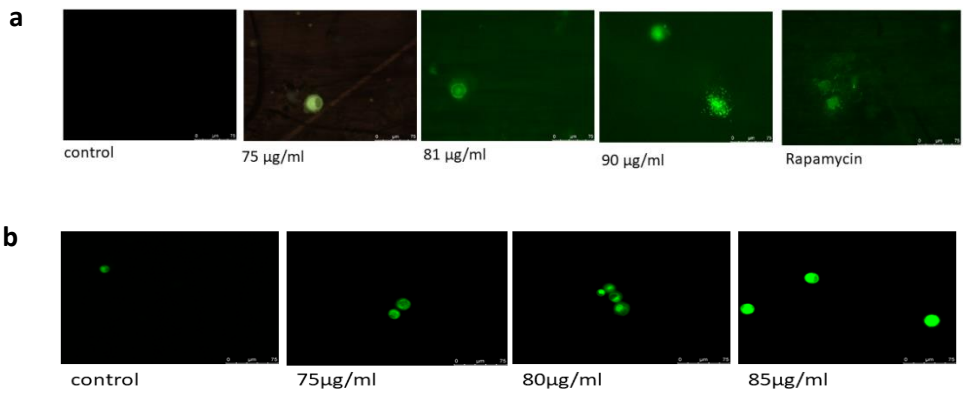

Fig 5.4.1. Measurement of mitochondrial membrane potential in MCF-7 cells using Rhodamine 123: Following 24 hr treatment with **(a)** R-Au-IONPs and **(b)** KDY 2 Au NPs. scale bars represent 75 µm

5.4.2. Assessment of Phosphatidyl Serine externalization (Annexin V-FITC-PI staining)

A biochemical hallmark of early apoptosis, Phosphatidylserine externalization can be detected by Annexin V / Propidium iodide staining and flow cytometric analysis. Annexin V/Propidium iodide co-staining differentially detects late apoptotic/necrotic cells from early apoptotic cells due to Propidium iodide's ability to only enter into disrupted cells to bind with DNA and Annexin V to bind phosphatidylserine.(Crowley et al., 2016)

Assessment of PS externalization in MCF-7 cells treated with R-Au-IONPs and KDY 2 Au NPs for 24 hours. Flow cytometry showed an increase in the late apoptotic and necrotic cells up to 16% and 5% respectively in the R-Au-IONP treated cells (Fig 5.4.2a) and 10% and 3% respectively in the KDY 2 Au NP treated cells (Fig 5.4.2b).

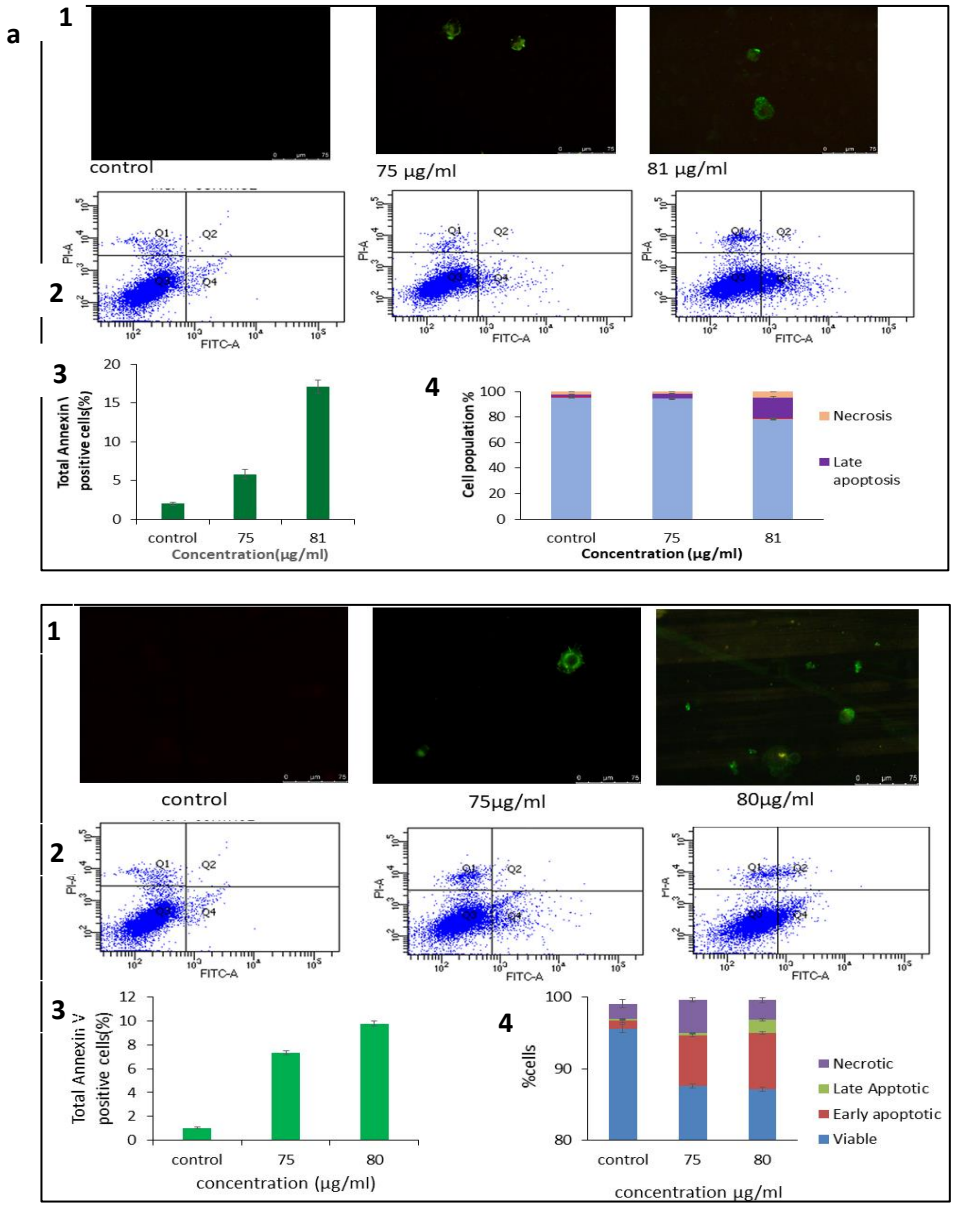

Fig. 5.4.2. Apoptosis induction in MCF-7 cells stained with Alexa Fluor®annexin V-FITC / PI following 24 hr treatment with NPs: (a) R-Au-IONPs and **(b)** KDY 2 Au NPs treated MCF-7 cells detected using Annexin V-FITC/PI staining (1) displays the fluorescence microscopy images; (2) the flow cytometric fluorescence patterns; (3) The bar chart shows the percentage of Annexin V positive cells; (4) The bar chart summarizes the percentage of viable, early apoptotic, late apoptotic and necrotic cells. Scale bars represent 75 µm in all images

5.4.3. Immunoblotting

The induction of apoptosis was confirmed by PARP (Poly (ADP-ribose) Polymerase-1) cleavage detected by western blot analysis in R-Au-NP and KDY 2 Au NP treated MCF-7 cells. PARP-1 is a nuclear enzyme, specifically proteolyzed by caspases to a 24 kDa (DNA-binding domain) and 89 kDa (catalytic fragment) during apoptosis. The results indicated the diminished expression of the PARP protein in the R-Au-IONP treated cells, whereas, the KDY 2 Au NP treated cells showed the cleavage of PARP protein. β- Actin was used as the loading control. (Fig 5.4.3)

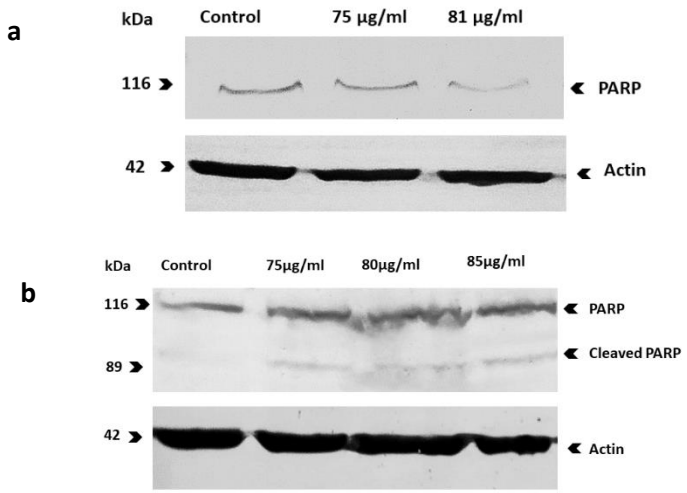

Fig. 5.4.3. Western blot analysis of PARP protein in MCF-7 cells: (a) R-Au-IONPs and **(b)** KDY 2 Au NPs treated cells (24 hr). Immunostaining to monitor the expression of cleaved PARP (visualized using TMB-HRP-H_2O_2 reaction). The protein was normalized against β-actin taken as the loading control

5.5. Cell Cycle Assay

The cell cycle phase-specific distribution of R-Au-IONP and KDY 2 Au NP treated MCF-7 cells was studied by flow cytometric analysis on staining with DNA binding fluorescent dye, propidium iodide (PI). Cell cycle analysis shows the changes in the DNA molecules in reaction to drug treatments. The distribution of cells in three major phases of the cycle- G1, S, and G2/M, and a subpopulation of cells- sub-G0 phase representing cells with fractional DNA content are obtained. A prominent dose-dependent increase in the G1 phase was observed in R-Au-IONP treated cells, which was in accordance with the loaded drug, Rapamycin. (Chatterjee et al., 2015) (Din et al., 2014)

A prominent dose-dependent increase in the Sub G0 phase was observed in KDY 2 Au NP-treated cells. Indicating that the cells are not progressing through the cell cycle events and accumulating in the G0 state, implying the presence of fragmented nuclei due to the apoptosis/cell death. (Hasanzadeh et al., 2017) A subsequent decrease in G1, S, and G2 populations is also seen. (Fig 5.5).

In a study involving Moxifloxacin and its derivatives, cell cycle arrest in the G0/G1 phase was observed. (F. Yu et al., 2020) Also, Gold complexes with Norfloxacin, Levofloxacin, and other fluoroquinolones are reported to inhibit the cell cycle in the G0/G1 phase and trigger apoptosis. (Gouvea et al., 2012)

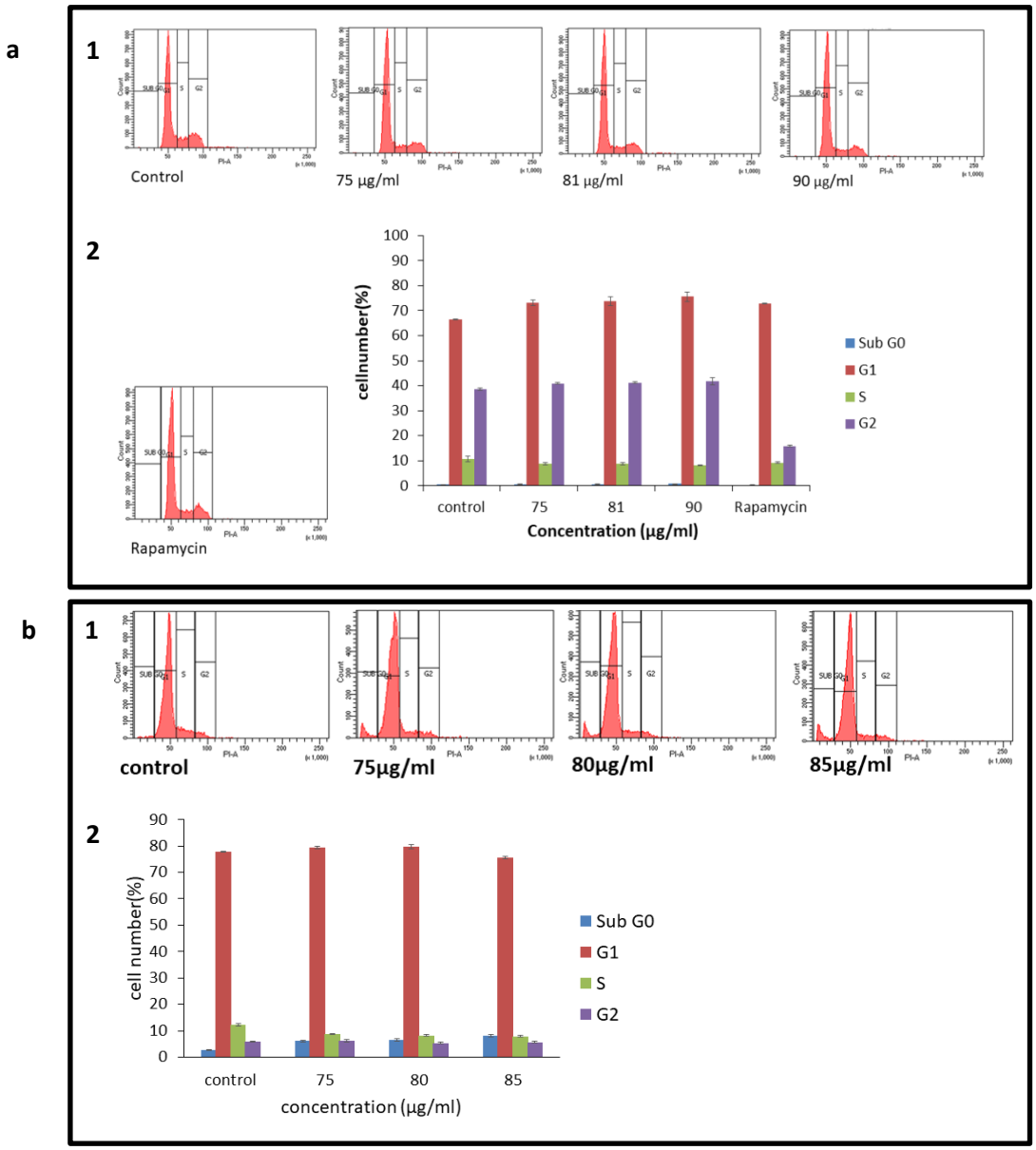

Fig. 5.5. Effect of R-Au-IONPs and KDY 2 Au NPs on the cell cycle distribution of MCF-7 cells. **(a)** R-Au-IONPs and **(b)** KDY 2 Au NPs treated MCF-7 cells after 12 hours**;1.** Flow cytometric analysis following PI staining **2.** quantification of cells in different cell cycle phases. Data represents the mean ± SD of three independent experiments. $P<0.01$

Rapamycin on R-Au-IONPs showed enhanced activity of Rapamycin in the Nano formulation on MCF-7 cells with an IC 50 value of 1.1 µg/mL when compared to the free Rapamycin which was 40µg/mL. There was a considerable increase in apoptosis and cell death rates when using R-Au-IONPs compared to free Rapamycin or bare iron oxide nanoparticles on MCF-7 cells. Accordingly, the loading of Rapamycin onto the PEGylated- Gold coated Fe3O4 NPs is a substantial modification to boost the effect of Rapamycin on cancer cells to induce apoptosis.

A significant rise in the sub-G0 population was revealed by cell cycle analysis in KDY 2 Au NP-treated cells, suggesting the existence of fragmented nuclei in the KDY 2 Au NPs treated cells. Again, we looked into the mechanism of action of KDY 2 Au NPs utilizing LC/Q-TOF/MS analysis. The findings confirmed the existence of a fluoroquinolone compound that resembled Norfloxacin and Moxifloxacin, indicating that apoptosis was caused by the pPI3k/pPAKT/mTOR and Bax/Bcl2 pathways. Consequently, it can be concluded that the E. hormaechei KDY2 strain can be used to produce KDY 2 Au NPs, which would be an effective nanoformulation for the treatment of breast cancer and an excellent antibacterial agent. However, we suggest additional research, particularly using in vivo models.

The cytotoxicity assays confirmed the Onset of cell death by the chemical and biogenic nanoparticles. The MTT, trypan blue, and hemolytic assays were used to check the cytotoxic potentials of the

nanoparticles. Additionally, several cell viability tests, such as microscopy, fluorescence labeling, and clonogenic assay, were used to confirm the cytotoxicity. Western blotting, mitochondrial membrane potential, and the PS-externalization assay demonstrated that the NPs caused apoptosis in the MCF-7 cell line. The cell cycle analysis confirmed the cell cycle arrest in the NP-treated cells leading to the inhibition of their proliferation.

6. SUMMARY AND CONCLUSIONS

The present study explored the utilization of nanoparticles in cancer treatment, particularly breast cancer. Both chemical and biological approaches were used to synthesize the nanoparticles. The NPs were characterized using SEM, RD, FTIR, and UV/Vis spectroscopy, and their anti-proliferative properties in the Human breast adenocarcinoma cell line, MCF-7 were assessed.

In the chemical synthesis approach, an effective drug delivery system using Iron oxide- Gold-core-shell nanoparticles (IONPs) was developed; the successful delivery of a bacterial macrolide-derived compound, Rapamycin, using this nano-delivery system was achieved for the first time. Rapamycin has already proven its anti-proliferative ability in breast cancer cells and is used here to check the efficiency of the chemically synthesized nanocarrier system. This nanoformulation (R-Au-IONPs) with an IC 50 value of 81.0±1.4 µg /ml enhanced Rapamycin's cytotoxicity (IC 50, 1.10±0.02 µg/mL) compared to the free Rapamycin (IC 50, 40±1.4 µg/mL) in MCF-7 cells. Also, the induction of apoptosis in the R-Au-IONP-treated MCF-7 cells was confirmed using different viability assays and apoptosis assays including western blotting and cell cycle analysis.

In the biological synthesis approach, the cell-free supernatant of *E. hormaechei* soil isolate, KDY 2 was used for the generation of Gold nanoparticles. The KDY 2 Au NPs showed comparable

cytotoxicity as R-Au-IONPs in the breast cancer cell line, MCF-7 with an IC 50 value of 79.50±2.12 µg/mL. The KDY 2 Au NPs induced apoptosis in MCF-7 cells as evidenced by the different apoptosis assays and viability assays. Also, they exhibited significant anti-bacterial properties. While examining the constituents of the NPs, the FTIR spectroscopy indicated the presence of proteins, amino acids, and a Fluorocompound. When delved further by LC/Q-TOF/MS analysis, a fluoroquinolone-like molecule similar to Moxifloxacin and Norfloxacin was identified. This helped to understand the mechanism behind the anti-cancer and anti-bacterial properties of the KDY 2 Au NPs.

To conclude, the results of the current study have successfully culminated in the development of a nanoparticle-based drug delivery system through chemical synthesis. This is the first report on the successful delivery of Rapamycin using the Au-IONP delivery system with enhanced activity of Rapamycin. However, we suggest further analysis including pre-clinical studies to check the applicability of this nanocarrier system containing Rapamycin.

Also, this study paved the way for the discovery of a potent biogenic nanoformulation (KDY2 Au NPs) containing a fluoroquinolone molecule with exceptional anticancer and anti-bacterial potentials. This reports the first-ever production of gold nanoparticles from *E. hormaechei* soil isolates. This approach could be considered an efficient, cost-effective, and facile technique to generate

nanoparticles with comparable effects to the chemically synthesized drug-loaded nanoparticles.

The biological synthesis of nanoparticles with substantial bio activities emphasized the way to establish a more effective production system for biomolecule-capped nanoparticle generation. This will in fact reduce the lengthy and tedious procedure of coating an already available pure compound which is purified from a bacterial extract. Here, this approach would be considered effortless when the biomolecule of interest's origin is known and can be directly converted to nanoparticles easily. However, we recommend more research including production optimization, and in vivo studies.

RECOMMENDATIONS

This research work has demonstrated the efficacy of nanoparticle-based therapeutic approaches for combating breast cancer. Both chemical and biological synthesis methods were utilized here to evaluate their efficacy to create nanoparticles as potent anti-cancer agents. The chemical synthesis involved the production of PEG-ylated iron oxide gold core-shell nanoparticles. Being biocompatible and superparamagnetic, they amplified the effect of the therapeutic agent, Rapamycin, loaded on them. The substantial induction of apoptosis in breast cancer cells, MCF-7 was evidenced by different viability tests and apoptosis assays, implying the benefit of the nano-drug carrier system. On the other hand, the biological synthesis method utilized bacterial cell-free supernatant to produce nanoparticles and succeeded in generating Gold nanoparticles with remarkable anti-cancer effects in MCF-7 cells. They also displayed matching effects as the chemically synthesized nanoparticles. Different cytotoxicity and apoptosis assays elaborated on their effect.

However, more emphasis is to be given to pre-clinical studies when regarding the applicability of these nanoformulations. The efficacy of PEG-ylated iron oxide gold core-shell nanoparticles in delivering different therapeutic agents for treating different disease conditions is to be explored. Their further modifications for fitting different functional groups are also to be examined. When coming to

the biologically synthesized KDY2 Gold nanoparticles, their production optimization for large-scale synthesis is to be done. Their targeted delivery using photothermal therapy could be explored. The possibility of generating nanoparticles containing already available therapeutics of biological origin utilizing the biological method could be explored. This will help reduce the lengthy procedure of isolating and loading the compound onto different nanoparticles.

Concerning the more sophisticated treatment options, 3D bio-printed scaffolds could be used to implement these nanoformulations in disease models and clinical trials. Additionally, the modification of the NPs with different metals/compounds could be studied to attain more desirable effects.

REFERENCES

Abishad, P., Vergis, J., Unni, V., Ram, V. P., Niveditha, P., Yasur, J., Juliet, S., John, L., Byrappa, K., Nambiar, P., Kurkure, N. V., Barbuddhe, S. B., & Rawool, D. B. (2022). Green Synthesized Silver Nanoparticles Using Lactobacillus Acidophilus as an Antioxidant, Antimicrobial, and Antibiofilm Agent Against Multi-drug Resistant Enteroaggregative Escherichia Coli. *Probiotics and Antimicrobial Proteins*, *14*(5). https://doi.org/10.1007/s12602-022-09961-1

Aboeleneen, S. B., Scully, M. A., Harris, J. C., Sterin, E. H., & Day, E. S. (2022). Membrane-wrapped nanoparticles for photothermal cancer therapy. In *Nano Convergence* (Vol. 9, Issue 1). https://doi.org/10.1186/s40580-022-00328-4

Ahmad, F., Ashraf, N., Ashraf, T., Zhou, R. Bin, & Yin, D. C. (2019). Biological synthesis of metallic nanoparticles (MNPs) by plants and microbes: their cellular uptake, biocompatibility, and biomedical applications. In *Applied Microbiology and Biotechnology* (Vol. 103, Issue 7). https://doi.org/10.1007/s00253-019-09675-5

Ahmad, F., Salem-Bekhit, M. M., Khan, F., Alshehri, S., Khan, A., Ghoneim, M. M., Wu, H. F., Taha, E. I., & Elbagory, I. (2022). Unique Properties of Surface-Functionalized Nanoparticles for Bio-Application: Functionalization Mechanisms and Importance in Application. In *Nanomaterials* (Vol. 12, Issue 8). https://doi.org/10.3390/nano12081333

Ahmad, N., Albassam, A. A., Faiyaz Khan, M., Ullah, Z., Mohammed Buheazah, T., Salman AlHomoud, H., & Ali Al-Nasif, H. (2022). A novel 5-Fluorocuracil multiple-nanoemulsion used for the enhancement of oral bioavailability in the treatment of colorectal cancer. *Saudi Journal of Biological Sciences*, *29*(5). https://doi.org/10.1016/j.sjbs.2022.02.017

Aldred, K. J., Kerns, R. J., & Osheroff, N. (2014). Mechanism of quinolone action and resistance. In *Biochemistry* (Vol. 53, Issue 10). https://doi.org/10.1021/bi5000564

Altammar, K. A. (2023). A review on nanoparticles: characteristics, synthesis, applications, and challenges. In *Frontiers in Microbiology* (Vol. 14). https://doi.org/10.3389/fmicb.2023.1155622

Amin, K., & Dannenfelser, R. M. (2006). In vitro hemolysis: Guidance for the pharmaceutical scientist. *Journal of Pharmaceutical Sciences*, *95*(6). https://doi.org/10.1002/jps.20627

Anand, U., Dey, A., Chandel, A. K. S., Sanyal, R., Mishra, A., Pandey, D. K., De Falco, V., Upadhyay, A., Kandimalla, R., Chaudhary, A., Dhanjal, J. K., Dewanjee, S., Vallamkondu, J., & Pérez de la Lastra, J. M. (2023). Cancer chemotherapy and beyond: Current status, drug candidates, associated risks and progress in targeted therapeutics. In *Genes and Diseases* (Vol. 10, Issue 4). https://doi.org/10.1016/j.gendis.2022.02.007

Ansari, M. J. (2019). Transport Phenomenon of Nanoparticles in Animals and Humans. *Diffusion Foundations*, *23*. https://doi.org/10.4028/www. scientific. net/df.23.173

Aranha, O., Grignon, R., Fernandes, N., McDonnell, T. J., Wood, D. P., & Sarkar, F. H. (2003). Suppression of human prostate cancer cell growth by ciprofloxacin is associated with cell cycle arrest and apoptosis. *International Journal of Oncology*, *22*(4). https://doi.org/10.3892/ijo.22.4.787

Aranha, O., Wood, D. P., & Sarkar, F. H. (2000). Ciprofloxacin mediated cell growth inhibition, S/G2-M cell cycle arrest, and apoptosis in a human transitional cell carcinoma of the bladder cell line. *Clinical Cancer Research*, *6*(3).

Arnold, M., Morgan, E., Rumgay, H., Mafra, A., Singh, D., Laversanne, M., Vignat, J., Gralow, J. R., Cardoso, F., Siesling, S., & Soerjomataram, I. (2022). Current and future burden of breast cancer: Global statistics for 2020 and 2040. *Breast*, *66*. https://doi.org/10.1016/j.breast.2022.08.010

Arshad, M., Alyousef, A., Ahmad, I., Khan, J. M., & Shahzad, S. A. (2018). Low temperature synthesis of superparamagnetic iron oxide (Fe3O4) nanoparticles and their ROS mediated inhibition of biofilm formed by food-associated bacteria. *Frontiers in Microbiology*, *9*(NOV). https://doi.org/10.3389/fmicb.2018.02567

Asmathunisha, N., & Kathiresan, K. (2013). A review on biosynthesis of nanoparticles by marine organisms. In *Colloids and Surfaces B: Biointerfaces* (Vol. 103). https://doi.org/10.1016/j.colsurfb.2012.10.030

Attard, G., Casadesús, M., MacAskie, L. E., & Deplanche, K. (2012). Biosynthesis of platinum nanoparticles by Escherichia coli MC4100: Can such nanoparticles exhibit intrinsic surface enantioselectivity? *Langmuir*, *28*(11). https://doi.org/10.1021/la204495z

Averous, J., & Proud, C. G. (2006). When translation meets transformation: The mTOR story. In *Oncogene* (Vol. 25, Issue 48). https://doi.org/10.1038/ sj.onc.1209887

Baig, N., Kammakakam, I., Falath, W., & Kammakakam, I. (2021). Nanomaterials: A review of synthesis methods, properties, recent progress, and challenges. In *Materials Advances* (Vol. 2, Issue 6). https://doi.org/10.1039/ d0ma00807a

Banerjee, A. N., Krishna, R., & Das, B. (2008). Size controlled deposition of Cu and Si nano-clusters by an ultra-high vacuum sputtering gas aggregation technique. *Applied Physics A: Materials Science and Processing*, *90*(2). https://doi.org/10.1007/s00339-007-4271-7

Baskić, D., Popović, S., Ristić, P., & Arsenijević, N. N. (2006). Analysis of cycloheximide-induced apoptosis in human leukocytes: Fluorescence microscopy using annexin V/propidium iodide versus acridin orange/ethidium bromide. *Cell Biology International*, *30*(11). https://doi.org/10.1016/j.cellbi.2006.06.016

Beaver, J. A., & Park, B. H. (2012). The BOLERO-2 trial: The addition of everolimus to exemestane in the treatment of postmenopausal hormone receptor-positive advanced breast cancer. *Future Oncology*, *8*(6). https://doi.org/10.2217/fon.12.49

Beberok, A., Rzepka, Z., Respondek, M., Rok, J., Sierotowicz, D., & Wrześniok, D. (2018). GSH depletion, mitochondrial membrane breakdown, caspase-3/7 activation and DNA fragmentation in U87MG glioblastoma cells: New insight into the mechanism of cytotoxicity induced by fluoroquinolones. *European Journal of Pharmacology*, *835*. https://doi.org/10.1016/j.ejphar.2018.08.002

Beberok, A., Rzepka, Z., Respondek, M., Rok, J., Stradowski, M., & Wrześniok, D. (2019). Moxifloxacin as an inducer of apoptosis in melanoma cells: A study at the cellular and molecular level. *Toxicology in Vitro*, *55*. https://doi.org/10.1016/j.tiv.2018.12.002

Beberok, A., Wrześniok, D., Minecka, A., Rok, J., Delijewski, M., Rzepka, Z., Respondek, M., & Buszman, E. (2018). Ciprofloxacin-mediated induction of S-phase cell cycle arrest and apoptosis in COLO829 melanoma cells. *Pharmacological Reports*, *70*(1). https://doi.org/10.1016/j.pharep.2017.07.007

Beberok, A., Wrześniok, D., Rok, J., Rzepka, Z., Respondek, M., & Buszman, E. (2018). Ciprofloxacin triggers the apoptosis of human triple-negative breast cancer MDA-MB-231 cells via the p53/Bax/Bcl-2 signaling pathway. *International Journal of Oncology*, *52*(5), 1727–1737. https://doi.org/10.3892/ijo.2018.4310

Ben-Sahra, I., Howell, J. J., Asara, J. M., & Manning, B. D. (2013). Stimulation of de novo pyrimidine synthesis by growth signaling through mTOR and S6K1. *Science*, *339*(6125). https://doi.org/10.1126/science.1228792

Ben-Sahra, I., Hoxhaj, G., Ricoult, S. J. H., Asara, J. M., & Manning, B. D. (2016). mTORC1 induces purine synthesis through control of the mitochondrial tetrahydrofolate cycle. *Science*, *351*(6274). https://doi.org/10.1126/science.aad0489

Betz, C., & Hall, M. N. (2013). Where is mTOR and what is it doing there? *Journal of Cell Biology*, *203*(4). https://doi.org/10.1083/jcb.201306041

Bhardwaj, H., & Jangde, R. K. (2023). Current updated review on preparation of polymeric nanoparticles for drug delivery and biomedical applications. *Next Nanotechnology*, *2*. https://doi.org/10.1016/j.nxnano.2023.100013

Bing, W., Sun, H., Wang, F., Song, Y., & Ren, J. (2018). Hydrogen-producing hyperthermophilic bacteria synthesized size-controllable fine gold nanoparticles with excellence for eradicating biofilm and antibacterial applications. *Journal of Materials Chemistry B*, *6*(28). https://doi.org/10.1039/c8tb00549d

Biter, A. B., Pollet, J., Chen, W. H., Strych, U., Hotez, P. J., & Bottazzi, M. E. (2019). A method to probe protein structure from UV absorbance spectra. *Analytical Biochemistry*, *587*. https://doi.org/10.1016/j.ab.2019.113450

Blagosklonny, M. V. (2022). Rapamycin treatment early in life reprograms aging: hyperfunction theory and clinical practice. *Aging*, *14*(20). https://doi.org/10.18632/aging.204354

Blagosklonny, M. V. (2023). Cancer prevention with rapamycin. In *Oncotarget* (Vol. 14, Issue 1). https://doi.org/10.18632/oncotarget.28410

Bonnie, J. (2020). Características clínicas , diagnóstico y estadificación del cáncer de mama recién diagnosticado . *UpToDate*.

Boulares, A. H., Yakovlev, A. G., Ivanova, V., Stoica, B. A., Wang, G., Iyer, S., & Smulson, M. (1999). Role of poly(ADP-ribose) polymerase (PARP) cleavage in apoptosis. Caspase 3-resistant PARP mutant increases rates of apoptosis in transfected cells. *Journal of Biological Chemistry*, *274*(33). https://doi.org/10.1074/jbc.274.33.22932

Brand-Williams, W., Cuvelier, M. E., & Berset, C. (1995). Use of a free radical method to evaluate antioxidant activity. In *LWT - Food Science and Technology* (Vol. 28, Issue 1). https://doi.org/10.1016/S0023-6438(95)80008-5

Bubonja-Šonje, M., Knezević, S., & Abram, M. (2020). Challenges to antimicrobial susceptibility testing of plant-derived polyphenolic compounds. In *Arhiv za Higijenu Rada i Toksikologiju* (Vol. 71, Issue 4). https://doi.org/10.2478/aiht- 2020-71-3396

Campaña, A. L., Saragliadis, A., Mikheenko, P., & Linke, D. (2023). Insights into the bacterial synthesis of metal nanoparticles. In *Frontiers in Nanotechnology* (Vol. 5). https://doi.org/10.3389/fnano.2023.1216921

Cândido, M., Vieira, P., Campos, A., Soares, C., & Raniero, L. (2023). Gold-Coated Superparamagnetic Iron Oxide Nanoparticles Functionalized to EGF and Ce6 Complexes for Breast Cancer Diagnoses and Therapy. *Pharmaceutics*, *15*(1). https://doi.org/10.3390/pharmaceutics15010100

Cao, Z., Cui, L., Liu, Q., Liu, F., Zhao, Y., Guo, K., Hu, T., Zhang, F., Sheng, X., Wang, X., Peng, Z., & Dai, M. (2022). Phenotypic and Genotypic Characterization of Multidrug-Resistant Enterobacter hormaechei Carrying qnrS Gene Isolated from Chicken Feed in China . *Microbiology Spectrum*, *10*(3). https://doi.org/10.1128/spectrum.02518-21

Castillo-Henríquez, L., Alfaro-Aguilar, K., Ugalde-álvarez, J., Vega-Fernández, L., de Oca-Vásquez, G. M., & Vega-Baudrit, J. R. (2020). Green synthesis of gold and silver nanoparticles from plant extracts and their possible applications as antimicrobial agents in the agricultural area. In *Nanomaterials* (Vol. 10, Issue 9). https://doi.org/10.3390/nano10091763

Chandrakala, V., Aruna, V., & Angajala, G. (2022). Review on metal nanoparticles as nanocarriers: current challenges and perspectives in drug delivery systems. In *Emergent Materials* (Vol. 5, Issue 6). https://doi.org/10.1007/s42247-021-00335-x

Chang, S. B., Miron, P., Miron, A., & Iglehart, J. D. (2007). Rapamycin Inhibits Proliferation of Estrogen-Receptor-Positive Breast Cancer Cells. *Journal of Surgical Research*, *138*(1). https://doi.org/10.1016/j.jss.2006.07.003

Chatterjee, A., Mukhopadhyay, S., Tung, K., Patel, D., & Foster, D. A. (2015). Rapamycin-induced G1 cell cycle arrest employs both TGF-β and Rb pathways. *Cancer Letters*, *360*(2). https://doi.org/10.1016/j.canlet.2015.01.043

Chaurasia, M., Singh, R., Sur, S., & Flora, S. J. S. (2023). A review of FDA approved drugs and their formulations for the treatment of breast cancer. In *Frontiers in Pharmacology* (Vol. 14). https://doi.org/10.3389/fphar.2023.1184472

Chavda, V. P., Nalla, L. V., Balar, P., Bezbaruah, R., Apostolopoulos, V., Singla, R. K., Khadela, A., Vora, L., & Uversky, V. N. (2023). Advanced Phytochemical-Based Nanocarrier Systems for the Treatment of Breast Cancer. In *Cancers* (Vol. 15, Issue 4). https://doi.org/10.3390/cancers15041023

Chen, C. Y., Chang, Y. C., Tsai, T. H., Liu, M. H., & Chung, Y. C. (2021). Multifunctional activities of gold nanoparticles biosynthesized using bacteria isolated from mining areas. *Applied Sciences (Switzerland)*, *11*(8). https://doi.org/10.3390/app11083670

Cheng, X., Xie, Q., & Sun, Y. (2023). Advances in nanomaterial-based targeted drug delivery systems. In *Frontiers in Bioengineering and Biotechnology* (Vol. 11). https://doi.org/10.3389/fbioe.2023.1177151

Chitgupi, U., Qin, Y., & Lovell, J. F. (2017). Targeted nanomaterials for phototherapy. In *Nanotheranostics* (Vol. 1, Issue 1). https://doi.org/10.7150/ntno.17694

Choudhary, N., Hwang, S., & Choi, W. (2014). Carbon nanomaterials: a review. Handbook of nanomaterials properties. In *Handbook of nanomaterials properties*.

Cobley, C. M., Chen, J., Chul Cho, E., Wang, L. V., & Xia, Y. (2011). Gold nanostructures: A class of multifunctional materials for biomedical applications. *Chemical Society Reviews*, *40*(1). https://doi.org/10.1039/b821763g

Colombo, M., Carregal-Romero, S., Casula, M. F., Gutiérrez, L., Morales, M. P., Böhm, I. B., Heverhagen, J. T., Prosperi, D., & Parak, W. J. (2012). Biological applications of magnetic nanoparticles. *Chemical Society Reviews*, *41*(11). https://doi.org/10.1039/c2cs15337h

Comanescu, C. (2023). Recent Advances in Surface Functionalization of Magnetic Nanoparticles. *Coatings*, *13*(10). https://doi.org/10.3390/COATINGS13101772

Comşa, Ş., Cîmpean, A. M., & Raica, M. (2015). The story of MCF-7 breast cancer cell line: 40 Years of experience in research. In *Anticancer Research* (Vol. 35, Issue 6).

Cornu, M., Albert, V., & Hall, M. N. (2013). MTOR in aging, metabolism, and cancer. *Current Opinion in Genetics and Development*, *23*(1), 53–62. https://doi.org/10.1016/j.gde.2012.12.005

Crespo, K. A., Baronetti, J. L., Quinteros, M. A., Páez, P. L., & Paraje, M. G. (2017). Intra- and Extracellular Biosynthesis and Characterization of Iron Nanoparticles from Prokaryotic Microorganisms with Anticoagulant Activity. *Pharmaceutical Research*, *34*(3). https://doi.org/10.1007/s11095-016-2084-0

Crowley, L. C., Marfell, B. J., Scott, A. P., & Waterhouse, N. J. (2016). Quantitation of apoptosis and necrosis by annexin V binding, propidium iodide uptake, and flow cytometry. *Cold Spring Harbor Protocols*, *2016*(11). https://doi.org/10.1101/pdb.prot087288

Danafar, H., Sharafi, A., Kheiri, S., & Manjili, H. K. (2018). Co -delivery of sulforaphane and curcumin with pegylated iron oxide-gold core shell

nanoparticles for delivery to breast cancer cell line. *Iranian Journal of Pharmaceutical Research*, *17*(2).

Datta, S. R., Dudek, H., Xu, T., Masters, S., Haian, F., Gotoh, Y., & Greenberg, M. E. (1997). Akt phosphorylation of BAD couples survival signals to the cell-intrinsic death machinery. *Cell*, *91*(2). https://doi.org/10.1016/S0092-8674(00)80405-5

Desai, M. P., Patil, R. V., & Pawar, K. D. (2020). Selective and sensitive colorimetric detection of platinum using Pseudomonas stutzeri mediated optimally synthesized antibacterial silver nanoparticles. *Biotechnology Reports*, *25*. https://doi.org/10.1016/j.btre.2019.e00404

Din, T. A. D. A. A. T., Seeni, A., Khairi, W. N. M., Shamsuddin, S., & Jaafar, H. (2014). Effects of rapamycin on cell apoptosis in MCF-7 human breast cancer cells. *Asian Pacific Journal of Cancer Prevention*, *15*(24). https://doi.org/10.7314/APJCP.2014.15.24.10659

Di Stefano, A. (2023). Nanotechnology in Targeted Drug Delivery. In *International Journal of Molecular Sciences* (Vol. 24, Issue 9). https://doi.org/10.3390/ijms24098194

Dos, D. S., Ali, S. M., Kim, D. H., Guertin, D. A., Latek, R. R., Erdjument-Bromage, H., Tempst, P., & Sabatini, D. M. (2004). Rictor, a novel binding partner of mTOR, defines a rapamycin-insensitive and raptor-independent pathway that regulates the cytoskeleton. *Current Biology*, *14*(14). https://doi.org/10.1016/j.cub.2004.06.054

Dowling, R. J. O., Topisirovic, I., Fonseca, B. D., & Sonenberg, N. (2010). Dissecting the role of mTOR: Lessons from mTOR inhibitors. In *Biochimica et Biophysica Acta - Proteins and Proteomics* (Vol. 1804, Issue 3). https://doi.org/10.1016/j.bbapap.2009.12.001

Düvel, K., Yecies, J. L., Menon, S., Raman, P., Lipovsky, A. I., Souza, A. L., Triantafellow, E., Ma, Q., Gorski, R., Cleaver, S., Vander Heiden, M. G., MacKeigan, J. P., Finan, P. M., Clish, C. B., Murphy, L. O., & Manning, B. D. (2010). Activation of a Metabolic Gene Regulatory Network Downstream of mTOR Complex 1. *Molecular Cell*, *39*(2), 171–183. https://doi.org/10.1016/J.MOLCEL.2010.06.022

Elahi, N., Kamali, M., & Baghersad, M. H. (2018). Recent biomedical applications of gold nanoparticles: A review. In *Talanta* (Vol. 184). https://doi.org/10.1016/j.talanta. 2018.02.088

Fan, M., Chen, S., Weng, Y., Li, X., Jiang, Y., Wang, X., Bie, M., An, L., Zhang, M., Chen, B., Huang, G., Wu, J., Zhu, M., & Shi, Q. (2020). Ciprofloxacin promotes polarization of CD86+CD206- macrophages to suppress liver cancer. *Oncology Reports*, *44*(1). https://doi.org/10.3892/or.2020.7602

Fatemi, M., Mollania, N., Momeni-Moghaddam, M., & Sadeghifar, F. (2018). Extracellular biosynthesis of magnetic iron oxide nanoparticles by Bacillus cereus strain HMH1: Characterization and in vitro cytotoxicity analysis on MCF-7 and 3T3 cell lines. *Journal of Biotechnology*, *270*. https://doi.org/10.1016/j.jbiotec.2018.01.021

Feng, Y., Chen, X., Cassady, K., Zou, Z., Yang, S., Wang, Z., & Zhang, X. (2021). The Role of mTOR Inhibitors in Hematologic Disease: From Bench to Bedside. In *Frontiers in Oncology* (Vol. 10). https://doi.org/10.3389/fonc.2020.611690

Ferrario, N., Marras, E., Vivona, V., Randisi, F., Fallica, A. N., Marrazzo, A., Perletti, G., & Gariboldi, M. B. (2024). Mechanisms of the Antineoplastic Effects of New Fluoroquinolones in 2D and 3D Human Breast and Bladder Cancer Cell Lines. *Cancers*, *16*(12). https://doi.org/10.3390/cancers16122227

Foster, K. G., & Fingar, D. C. (2010). Mammalian target of rapamycin (mTOR): Conducting the cellular signaling symphony. In *Journal of Biological Chemistry* (Vol. 285, Issue 19). https://doi.org/10.1074/jbc.R109.094003

Franken, N. A. P., Rodermond, H. M., Stap, J., Haveman, J., & van Bree, C. (2006). Clonogenic assay of cells in vitro. *Nature Protocols*, *1*(5). https://doi.org/10.1038/nprot.2006.339

Gan, X., Wang, J., Wang, C., Sommer, E., Kozasa, T., Srinivasula, S., Alessi, D., Offermanns, S., Simon, M. I., & Wu, D. (2012). PRR5L degradation promotes mTORC2-mediated PKC-δ phosphorylation and cell migration downstream of Gα 12. *Nature Cell Biology*, *14*(7). https://doi.org/10.1038/ncb2507

García-Martínez, J. M., & Alessi, D. R. (2008). mTOR complex 2 (mTORC2) controls hydrophobic motif phosphorylation and activation of serum- and glucocorticoid-induced protein kinase 1 (SGK1). *Biochemical Journal*, *416*(3). https://doi.org/10.1042/BJ20081668

Gopinath, V., Priyadarshini, S., Loke, M. F., Arunkumar, J., Marsili, E., MubarakAli, D., Velusamy, P., & Vadivelu, J. (2017). Biogenic synthesis, characterization of antibacterial silver nanoparticles and its cell cytotoxicity. *Arabian Journal of Chemistry*, *10*(8). https://doi.org/10.1016/j.arabjc.2015.11.011

Gousias, K., Theocharous, T., & Simon, M. (2022). Mechanisms of Cell Cycle Arrest and Apoptosis in Glioblastoma. In *Biomedicines* (Vol. 10, Issue 3). https://doi.org/10.3390/biomedicines10030564

Gouvea, L. R., Garcia, L. S., Lachter, D. R., Nunes, P. R., De Castro Pereira, F., Silveira-Lacerda, E. P., Louro, S. R. W., Barbeira, P. J. S., & Teixeira, L. R.

(2012). Atypical fluoroquinolone gold(III) chelates as potential anticancer agents: Relevance of DNA and protein interactions for their mechanism of action. *European Journal of Medicinal Chemistry*, *55*. https://doi.org/10.1016/j.ejmech.2012.07.004

Guduru, S. K. R., & Arya, P. (2018). Synthesis and biological evaluation of rapamycin-derived, next generation small molecules. In *MedChemComm* (Vol. 9, Issue 1). https://doi.org/10.1039/c7md00474e

Guertin, D. A., & Sabatini, D. M. (2009). The pharmacology of mTOR inhibition. In *Science Signaling* (Vol. 2, Issue 67). https://doi.org/10.1126/scisignal.267pe24

Hagiwara, A., Cornu, M., Cybulski, N., Polak, P., Betz, C., Trapani, F., Terracciano, L., Heim, M. H., Rüegg, M. A., & Hall, M. N. (2012). Hepatic mTORC2 activates glycolysis and lipogenesis through Akt, glucokinase, and SREBP1c. *Cell Metabolism*, *15*(5). https://doi.org/10.1016/j.cmet.2012.03.015

Haleem, A., Javaid, M., Singh, R. P., Rab, S., & Suman, R. (2023). Applications of nanotechnology in medical field: a brief review. In *Global Health Journal* (Vol. 7, Issue 2). https://doi.org/10.1016/j.glohj.2023.02.008

Hammami, I., Alabdallah, N. M., jomaa, A. Al, & kamoun, M. (2021). Gold nanoparticles: Synthesis properties and applications. In *Journal of King Saud University - Science* (Vol. 33, Issue 7). https://doi.org/10.1016/j.jksus.2021.101560

Hanker, A. B., Sudhan, D. R., & Arteaga, C. L. (2020). Overcoming Endocrine Resistance in Breast Cancer. In *Cancer Cell* (Vol. 37, Issue 4). https://doi.org/10.1016/j.ccell.2020.03.009

Han, Z., Tang, Z., Jiang, K., Huang, Q., Meng, J., Nie, D., & Zhao, Z. (2020). Dual-target electrochemical aptasensor based on co-reduced molybdenum disulfide and Au NPs (rMoS2-Au) for multiplex detection of mycotoxins. *Biosensors and Bioelectronics*, *150*. https://doi.org/10.1016/j.bios.2019.111894

Hasanzadeh, D., Mahdavi, M., Dehghan, G., & Charoudeh, H. N. (2017). Farnesiferol C induces cell cycle arrest and apoptosis mediated by oxidative stress in MCF-7 cell line. *Toxicology Reports*, *4*. https://doi.org/10.1016/j.toxrep. 2017.07.010

Hazra, B., Biswas, S., & Mandal, N. (2008). Antioxidant and free radical scavenging activity of Spondias pinnata. *BMC Complementary and Alternative Medicine*, *8*. https://doi.org/10.1186/1472-6882-8-63

Herald, C., Occur, M., Ganslmayer, M., Gerauer, H., Hahn, E. G., & Schuppan, D. (2002). Ciprofloxacin induces apoptosis and inhibits proliferation of human colorectal carcinoma cells. *British Journal of Cancer*, *86*(3). https://doi.org/10.1038/sj.bjc.6600079

He, X., Yao, Q., Hall, D. D., Song, Z., Fan, D., You, Y., Lian, W., Zhou, Z., Duan, L., & Chen, B. (2022). Levofloxacin exerts broad-spectrum anticancer activity via regulation of THBS1, LAPTM5, SRD5A3, MFAP5 and P4HA1. *Anti-Cancer Drugs*, *33*(1). https://doi.org/10.1097/CAD.0000000000001194

Holmannova, D., Borsky, P., Svadlakova, T., Borska, L., & Fiala, Z. (2022). Carbon Nanoparticles and Their Biomedical Applications. In *Applied Sciences (Switzerland)* (Vol. 12, Issue 15). https://doi.org/10.3390/app12157865

Holz, M. K., Ballif, B. A., Gygi, S. P., & Blenis, J. (2005). mTOR and S6K1 mediate assembly of the translation preinitiation complex through dynamic protein interchange and ordered phosphorylation events. *Cell*, *123*(4). https://doi.org/10.1016/j.cell.2005.10.024

Howland, J. L. (1996). Short protocols in molecular biology, third edition: Edited by F Ausubel, R Brent, R E Kingston, D D Moore, J G Seidman, J A Smith and K Struhl. P 836. John Wiley & Sons, New York. 1995. $74.95. ISBN 0-471-13781-2. *Biochemical Education*, *24*(1). https://doi.org/10.1002/bmb.1996.5690240143

Huang, C., Jiang, J., Muangphat, C., Sun, X., & Hao, Y. (2011). Trapping Iron Oxide into Hollow Gold Nanoparticles. *Nanoscale Research Letters*, *6*(1). https://doi.org/10.1007/s11671-010-9792-x

Hwang, S. K., & Kim, H. H. (2011). The functions of mTOR in ischemic diseases. In *BMB Reports* (Vol. 44, Issue 8). https://doi.org/10.5483/BMBRep.2011.44.8.506

Ibrahim, S., Ahmad, Z., Manzoor, M. Z., Mujahid, M., Faheem, Z., & Adnan, A. (2021). Optimization for biogenic microbial synthesis of silver nanoparticles through response surface methodology, characterization, their antimicrobial, antioxidant, and catalytic potential. *Scientific Reports*, *11*(1). https://doi.org/10.1038/s41598-020-80805-0

Idowu, T., & Schweizer, F. (2017). Ubiquitous nature of fluoroquinolones: The oscillation between antibacterial and anticancer activities. In *Antibiotics* (Vol. 6, Issue 4). https://doi.org/10.3390/antibiotics6040026

Iravani, S., Korbekandi, H., Mirmohammadi, S. V., & Zolfaghari, B. (2014). Synthesis of silver nanoparticles: Chemical, physical and biological methods. In *Research in Pharmaceutical Sciences* (Vol. 9, Issue 6).

Jacinto, E., & Lorberg, A. (2008). TOR regulation of AGC kinases in yeast and mammals. In *Biochemical Journal* (Vol. 410, Issue 1). https://doi.org/10.1042/BJ20071518

Jacob, P. J., Masarudin, M. J., Hussein, M. Z., & Rahim, R. A. (2017). Facile aerobic construction of iron based ferromagnetic nanostructures by a novel microbial nanofactory isolated from tropical freshwater wetlands. *Microbial Cell Factories*, *16*(1). https://doi.org/10.1186/s12934-017-0789-3

Jemel-Oualha, I., Elloumi-Mseddi, J., Beji, A., Hakim, B., & Aifa, S. (2016). Controversial effect on Erk activation of some cytotoxic drugs in human LOVO colon cancer cells. *Journal of Receptors and Signal Transduction*, *36*(1). https://doi.org/10.3109/10799893.2014.975246

Jun, Y. W., Seo, J. W., & Cheon, J. (2008). Nanoscaling laws of magnetic nanoparticles and their applicabilities in biomedical sciences. *Accounts of Chemical Research*, *41*(2). https://doi.org/10.1021/ar700121f

Kadhum, W. R., Majeed, A. A., Saleh, R. O., Ali, E., Alhajlah, S., Alwaily, E. R., Mustafa, Y. F., Ghildiyal, P., Alawadi, A., & Alsalamy, A. (2024). Overcoming drug resistance with specific nano scales to targeted therapy: Focused on metastatic cancers. In *Pathology Research and Practice* (Vol. 255). https://doi.org/10.1016/j.prp.2024.155137

Kapoor, R. T., Salvadori, M. R., Rafatullah, M., Siddiqui, M. R., Khan, M. A., & Alshareef, S. A. (2021). Exploration of Microbial Factories for Synthesis of Nanoparticles – A Sustainable Approach for Bioremediation of Environmental Contaminants. In *Frontiers in Microbiology* (Vol. 12). https://doi.org/10.3389/fmicb.2021.658294

Karatay, K. B., Gungor, N. D., Colak, B., Muftuler, F. Z. B., & Aras, O. (2023). Bacterial production of ciprofloxacin and potential usage as a radiotracer. *PLoS ONE*, *18*(11 November). https://doi.org/10.1371/journal.pone.0291342

Kari, S., Subramanian, K., Altomonte, I. A., Murugesan, A., Yli-Harja, O., & Kandhavelu, M. (2022). Programmed cell death detection methods: a systematic review and a categorical comparison. In *Apoptosis* (Vol. 27, Issues 7–8). https://doi.org/10.1007/s10495-022-01735-y

Kassab, A. E., Gomaa, R. M., & Gedawy, E. M. (2024). Drug repurposing of fluoroquinolones as anticancer agents in 2023. In *RSC Advances* (Vol. 14, Issue 50, pp. 37114–37130). Royal Society of Chemistry. https://doi.org/10.1039/d4ra03571b

Katiyar, S. S., Muntimadugu, E., Rafeeqi, T. A., Domb, A. J., & Khan, W. (2016). Co-delivery of rapamycin- and piperine-loaded polymeric nanoparticles for

breast cancer treatment. *Drug Delivery*, *23*(7). https://doi.org/10.3109/10717544. 2015.1039667

Kerr, A. J., Dodwell, D., McGale, P., Holt, F., Duane, F., Mannu, G., Darby, S. C., & Taylor, C. W. (2022). Adjuvant and neoadjuvant breast cancer treatments: A systematic review of their effects on mortality. In *Cancer Treatment Reviews* (Vol. 105). https://doi.org/10.1016/j.ctrv.2022.102375

Khan, M. A. R., Al Mamun, M. S., Habib, M. A., Islam, A. B. M. N., Mahiuddin, M., Karim, K. M. R., Naime, J., Saha, P., Dey, S. K., & Ara, M. H. (2022). A review on gold nanoparticles: Biological synthesis, characterizations, and analytical applications. In *Results in Chemistry* (Vol. 4). https://doi.org/10.1016/j.rechem.2022.100478

Kheiri Manjili, H., Ma'mani, L., Tavaddod, S., Mashhadikhan, M., Shafiee, A., & Naderi-Manesh, H. (2016). D, l-sulforaphane loaded Fe3O4@ gold core shell nanoparticles: A potential sulforaphane delivery system. *PLoS ONE*, *11*(3). https://doi.org/10.1371/journal.pone.0151344

Kikuchi, F., Kato, Y., Furihata, K., Kogure, T., Imura, Y., Yoshimura, E., & Suzuki, M. (2016). Formation of gold nanoparticles by glycolipids of Lactobacillus casei. *Scientific Reports*, *6*. https://doi.org/10.1038/srep34626

Kim, D. H., Sarbassov, D. D., Ali, S. M., Latek, R. R., Guntur, K. V. P., Erdjument-Bromage, H., Tempst, P., & Sabatini, D. M. (2003). GβL, a positive regulator of the rapamycin-sensitive pathway required for the nutrient-sensitive interaction between raptor and mTOR. *Molecular Cell*, *11*(4). https://doi.org/10.1016/S1097-2765(03)00114-X

Kim, J., Kundu, M., Viollet, B., & Guan, K. L. (2011). AMPK and mTOR regulate autophagy through direct phosphorylation of Ulk1. *Nature Cell Biology*, *13*(2). https://doi.org/10.1038/ncb2152

Kloskowski, T., Fekner, Z., Szeliski, K., Paradowska, M., Balcerczyk, D., Rasmus, M., Dąbrowski, P., Kaźmierski, Ł., Drewa, T., & Pokrywczyńska, M. (2023). Effect of four fluoroquinolones on the viability of bladder cancer cells in 2D and 3D cultures. *Frontiers in Oncology*, *13*. https://doi.org/10.3389/fonc.2023.1222411

Kloskowski, T., Szeliski, K., Fekner, Z., Rasmus, M., Dąbrowski, P., Wolska, A., Siedlecka, N., Adamowicz, J., Drewa, T., & Pokrywczyńska, M. (2021). Ciprofloxacin and levofloxacin as potential drugs in genitourinary cancer treatment—the effect of dose–response on 2D and 3D cell cultures. *International Journal of Molecular Sciences*, *22*(21). https://doi.org/10.3390/ijms222111970

Kohler, B. A., Sherman, R. L., Howlader, N., Jemal, A., Ryerson, A. B., Henry, K. A., Boscoe, F. P., Cronin, K. A., Lake, A., Noone, A. M., Henley, S. J.,

Eheman, C. R., Anderson, R. N., & Penberthy, L. (2015). Annual report to the nation on the status of cancer, 1975-2011, featuring incidence of breast cancer subtypes by race/ethnicity, poverty, and state. *Journal of the National Cancer Institute*, *107*(6). https://doi.org/10.1093/jnci/djv048

Kojima, K., Takahashi, S., Saito, S., Endo, Y., Nittami, T., Nozaki, T., Sobti, R. C., & Watanabe, M. (2018). Combined effects of Fe3O4 nanoparticles and chemotherapeutic agents on prostate cancer cells in vitro. *Applied Sciences (Switzerland)*, *8*(1). https://doi.org/10.3390/app8010134

Kumar, A., Nautiyal, U., Kaur, C., Goel, V., & Piarchand, N. (2017). Targeted Drug Delivery System : Current and Novel Approach. *International Journal of Pharmaceutical and Medicinal Research Journal*, *5*(2).

Kumari, S. C., Dhand, V., & Padma, P. N. (2021). Green synthesis of metallic nanoparticles: a review. In *Nanomaterials: Application in Biofuels and Bioenergy Production Systems*. https://doi.org/10.1016/B978-0-12-822401-4.00022-2

Kumar, R., Singh, R. K., Dubey, P. K., Kumar, P., Tiwari, R. S., & Oh, I. K. (2013). Pressure-dependent synthesis of high-quality few-layer graphene by plasma-enhanced arc discharge and their thermal stability. *Journal of Nanoparticle Research*, *15*(9). https://doi.org/10.1007/s11051-013-1847-3

Kumar, S., Bhushan, P., & Bhattacharya, S. (2018). Fabrication of Nanostructures with Bottom-up Approach and Their Utility in Diagnostics, Therapeutics, and Others. In *Energy, Environment, and Sustainability*. https://doi.org/10.1007/978-981-10-7751-7_8

Kumar, S., Sandhir, R., & Ojha, S. (2014). Evaluation of antioxidant activity and total phenol in different varieties of Lantana camara leaves. *BMC Research Notes*, *7*(1). https://doi.org/10.1186/1756-0500-7-560

Kuppusamy, P., Yusoff, M. M., Maniam, G. P., & Govindan, N. (2016). Biosynthesis of metallic nanoparticles using plant derivatives and their new avenues in pharmacological applications – An updated report. In *Saudi Pharmaceutical Journal* (Vol. 24, Issue 4). https://doi.org/10.1016/j.jsps.2014.11.013

Lakshman Kumar, B., Ranjith, D. S., Kumar, S., Narendhran, S., & Kumar, P. S. (2016). A Novel Streptomyces sp. Mediated Gold Nanoparticle Synthesis and Its Efficacy on Antibiogram and Cytotoxic Activity on Breast Cancer (MCF-7) Cell Line. *Journal of Scientific Research*, *11*(3). https://doi.org/10.5829/idosi.aejsr.2016.11.3.22798

Lalitha, M. K. (2007). Manual on Antimicrobial Susceptibility Testing. *Indian Association of Medical Microbiologists)*.

Laplante, M., & Sabatini, D. M. (2012). MTOR signaling in growth control and disease. In *Cell* (Vol. 149, Issue 2). https://doi.org/10.1016/j.cell.2012.03.017

Lassoued, A., Dkhil, B., Gadri, A., & Ammar, S. (2017). Control of the shape and size of iron oxide (α-Fe2O3) nanoparticles synthesized through the chemical precipitation method. *Results in Physics*, *7*. https://doi.org/10.1016/j.rinp.2017.07.066

Lau, E. C. H. T., Åhlén, M., Cheung, O., Ganin, A. Y., Smith, D. G. E., & Yiu, H. H. P. (2023). Gold-iron oxide (Au/Fe3O4) magnetic nanoparticles as the nanoplatform for binding of bioactive molecules through self-assembly. *Frontiers in Molecular Biosciences*, *10*. https://doi.org/10.3389/fmolb.2023.1143190

Laurent, S., Forge, D., Port, M., Roch, A., Robic, C., Vander Elst, L., & Muller, R. N. (2008). Magnetic iron oxide nanoparticles: Synthesis, stabilization, vectorization, physicochemical characterizations and biological applications. *Chemical Reviews*, *108*(6). https://doi.org/10.1021/cr068445e

Law, B. K. (2005). Rapamycin: An anti-cancer immunosuppressant? In *Critical Reviews in Oncology/Hematology* (Vol. 56, Issue 1 SPEC. ISS.). https://doi.org/10.1016/j.critrevonc.2004.09.009

Lee Ventola, C. (2017). Cancer immunotherapy, part 3: Challenges and future trends. *P and T*, *42*(8).

Lee, Y. C., & Moon, J. Y. (2020). Introduction to bionanotechnology. In *Introduction to Bionanotechnology*. https://doi.org/10.1007/978-981-15-1293-3

Let's talk about lipid nanoparticles. (2021). In *Nature Reviews Materials* (Vol. 6, Issue 2). https://doi.org/10.1038/s41578-021-00281-4

Li, G., Cao, L., Zhou, Z., Chen, Z., Huang, Y., & Zhao, Y. (2015). Rapamycin loaded magnetic Fe3O4/carboxymethylchitosan nanoparticles as tumor-targeted drug delivery system: Synthesis and in vitro characterization. *Colloids and Surfaces B: Biointerfaces*, *128*. https://doi.org/10.1016/j.colsurfb. 2015.02.035

Li, J., Kim, S. G., & Blenis, J. (2014). Rapamycin: One drug, many effects. In *Cell Metabolism*. https://doi.org/10.1016/j.cmet.2014.01.001

Ling, D., & Hyeon, T. (2013). Chemical design of biocompatible iron oxide nanoparticles for medical applications. In *Small* (Vol. 9, Issues 9–10). https://doi.org/10.1002/smll.201202111

Liu, B., Zhou, H., Tan, L., Siu, K. T. H., & Guan, X. Y. (2024). Exploring treatment options in cancer: Tumor treatment strategies. In *Signal Transduction and*

Targeted Therapy (Vol. 9, Issue 1). Springer Nature. https://doi.org/ 10.1038/ s41392-024-01856-7

Liu, K., Liu, P. cheng, Liu, R., & Wu, X. (2015). Dual AO/EB staining to detect apoptosis in osteosarcoma cells compared with flow cytometry. *Medical Science Monitor Basic Research*, *21*. https://doi.org/10.12659/MSMBR. 893327

Li, X., & Gao, T. (2014). MTORC2 phosphorylates protein kinase Cζ to regulate its stability and activity. *EMBO Reports*, *15*(2). https://doi.org/10.1002/embr. 201338119

Lyu, H., Gao, B., He, F., Ding, C., Tang, J., & Crittenden, J. C. (2017). Ball-Milled Carbon Nanomaterials for Energy and Environmental Applications. In *ACS Sustainable Chemistry and Engineering* (Vol. 5, Issue 11). https://doi.org/10.1021/ acssuschemeng.7b02170

Machac, P., Cichon, S., Lapcak, L., & Fekete, L. (2020). Graphene prepared by chemical vapour deposition process. *Graphene Technology*, *5*(1–2). https://doi.org/10.1007/s41127-019-00029-6

Malhotra, S. P. K., & Alghuthaymi, M. A. (2021). Biomolecule-assisted biogenic synthesis of metallic nanoparticles. In *Agri-Waste and Microbes for Production of Sustainable Nanomaterials*. https://doi.org/10.1016/B978-0-12-823575-1.00011-1

Marinelli, L., Ciulla, M., Ritsema, J. A. S., van Nostrum, C. F., Cacciatore, I., Dimmito, M. P., Palmerio, F., Orlando, G., Robuffo, I., Grande, R., Puca, V., & Di Stefano, A. (2022). Preparation, Characterization, and Biological Evaluation of a Hydrophilic Peptide Loaded on PEG-PLGA Nanoparticles. *Pharmaceutics*, *14*(9). https://doi.org/10.3390/pharmaceutics14091821

Martin, S. J., Reutelingsperger, C. P. M., McGahon, A. J., Rader, J. A., Van Schie, R. C. A. A., LaFace, D. M., & Green, D. R. (1995). Early redistribution of plasma membrane phosphatidylserine is a general feature of apoptosis regardless of the initiating stimulus: Inhibition by overexpression of Bcl-2 and Abl. *Journal of Experimental Medicine*, *182*(5). https://doi.org/10.1084/jem.182.5.1545

Mathew, T., Kreis, H., & Friend, P. (2004). Two-year incidence of malignancy in sirolimus-treated renal transplant recipients: Results from five multicenter studies. *Clinical Transplantation*, *18*(4). https://doi.org/10.1111/j.1399-0012.2004.00188.x

Ma, X. M., & Blenis, J. (2009). Molecular mechanisms of mTOR-mediated translational control. In *Nature Reviews Molecular Cell Biology* (Vol. 10, Issue 5). https://doi.org/10.1038/nrm2672

Mikhailova, E. O. (2020). Silver Nanoparticles: Mechanism of Action and Probable Bio-Application. In *Journal of Functional Biomaterials* (Vol. 11, Issue 4). https://doi.org/10.3390/jfb11040084

Min, H. Y., & Lee, H. Y. (2022). Molecular targeted therapy for anticancer treatment. In *Experimental and Molecular Medicine* (Vol. 54, Issue 10). https://doi.org/10.1038/s12276-022-00864-3

Mishra, A., Kumar, J., & Melo, S. (2020). Silica Based Bio-hybrid Materials and their Relevance to Bionanotechnology. *Austin J Plant Biol*, *6*(1).

Mody, V. V., Nounou, M. I., & Bikram, M. (2009). Novel nanomedicine-based MRI contrast agents for gynecological malignancies. In *Advanced Drug Delivery Reviews* (Vol. 61, Issue 10). https://doi.org/10.1016/j.addr.2009.04.020

Mogana, R., Adhikari, A., Tzar, M. N., Ramliza, R., & Wiart, C. (2020). Antibacterial activities of the extracts, fractions and isolated compounds from canarium patentinervium miq. Against bacterial clinical isolates. *BMC Complementary Medicine and Therapies*, *20*(1). https://doi.org/10.1186/s12906-020-2837-5

Mohammed Fayaz, A., Girilal, M., Rahman, M., Venkatesan, R., & Kalaichelvan, P. T. (2011). Biosynthesis of silver and gold nanoparticles using thermophilic bacterium Geobacillus stearothermophilus. *Process Biochemistry*, *46*(10). https://doi.org/10.1016/j.procbio.2011.07.003

Mondal, E. R., Das, S. K., & Mukherjee, P. (2004). Comparative evaluation of antiproliferative activity and induction of apoptosis by some fluoroquinolones with a human non-small cell lung cancer cell line in culture. *Asian Pacific Journal of Cancer Prevention*, *5*(2).

Monowar, T., Rahman, M. S., Bhore, S. J., & Sathasivam, K. V. (2021). Endophytic bacteria enterobacter hormaechei fabricated silver nanoparticles and their antimicrobial activity. *Pharmaceutics*, *13*(4). https://doi.org/10.3390/pharmaceutics13040511

Mossmann, D., Park, S., & Hall, M. N. (2018). mTOR signalling and cellular metabolism are mutual determinants in cancer. *Nature Reviews Cancer*, *18*(12), 744–757. https://doi.org/10.1038/s41568-018-0074-8

Mourdikoudis, S., Pallares, R. M., & Thanh, N. T. K. (2018). Characterization techniques for nanoparticles: Comparison and complementarity upon studying nanoparticle properties. In *Nanoscale* (Vol. 10, Issue 27). https://doi.org/10.1039/c8nr02278j

Mukherjee, P., Mandal, E. R., & Das, S. K. (2005). Evaluation of Antiproliferative Activity of Enoxacin on a Human Breast Cancer Cell Line. *International*

Journal of Human Genetics, *5*(1). https://doi.org/10.1080/09723757.2005.11885917

Nakai, S., Imaizumi, T., Watanabe, T., Iwase, Y., Nishi, K., Okudaira, K., & Yumita, N. (2017). Photodynamically-induced apoptosis due to ultraviolet a in the presence of lomefloxacin in human promyelocytic leukemia cells. *Anticancer Research*, *37*(11). https://doi.org/10.21873/anticanres.12094

Nao Hosokawa, †, Taichi Hara, †, Takeshi Kaizuka, C. K., Akito Takamura,* Yutaka Miura, S. I., Natsume, T., Kenji Takehana,§ Naoyuki Yamada, 储, Guan, J.-L., & Noriko Oshiro, @ and Noboru Mizushima*. (2009). Nutrient-dependent mTORC1 Association with the ULK1–Atg13–FIP200 Complex Required for Autophagy. *Molecular Biology of the Cell*, *20*(m).

Neufeld, T. P. (2010). TOR-dependent control of autophagy: Biting the hand that feeds. In *Current Opinion in Cell Biology* (Vol. 22, Issue 2). https://doi.org/10.1016/j.ceb.2009.11.005

Nitha, B., De, S., Adhikari, S. K., Devasagayam, T. P. A., & Janardhanan, K. K. (2010). Evaluation of free radical scavenging activity of morel mushroom, Morchella esculenta mycelia: A potential source of therapeutically useful antioxidants. *Pharmaceutical Biology*, *48*(4). https://doi.org/10.3109/13880200903170789

Nodoushan, F. S., Hakimian, F., & Haghiralsadat, B. F. (2023). Magnetic Iron Oxide Nanoparticles Coated with Polyethylene and Gold as a Suitable Carrier for Doxorubicin and its Effect on Mcf-7 Breast Cancer Cells. *Journal of Shahid Sadoughi University of Medical Sciences*. https://doi.org/10.18502/ssu.v31i10.14567

Omajali, J. B., Gomez-Bolivar, J., Mikheenko, I. P., Sharma, S., Kayode, B., Al-Duri, B., Banerjee, D., Walker, M., Merroun, M. L., & Macaskie, L. E. (2019). Novel catalytically active Pd/Ru bimetallic nanoparticles synthesized by Bacillus benzeovorans. *Scientific Reports*, *9*(1). https://doi.org/10.1038/s41598-019-40312-3

Organization, W. H. (2024). Cancer today globocan 2022: lung. *The Global Cancer Observatory* |.

Osial, M., Rybicka, P., Pękała, M., Cichowicz, G., Cyrański, M. K., & Krysiński, P. (2018). Easy synthesis and characterization of holmium-doped SPIONs. *Nanomaterials*, *8*(6). https://doi.org/10.3390/nano8060430

Padín-González, E., Lancaster, P., Bottini, M., Gasco, P., Tran, L., Fadeel, B., Wilkins, T., & Monopoli, M. P. (2022). Understanding the Role and Impact of Poly (Ethylene Glycol) (PEG) on Nanoparticle Formulation: Implications

for COVID-19 Vaccines. In *Frontiers in Bioengineering and Biotechnology* (Vol. 10). https://doi.org/10.3389/fbioe.2022.882363

Parashar, M., Shukla, V. K., & Singh, R. (2020). Metal oxides nanoparticles via sol–gel method: a review on synthesis, characterization and applications. In *Journal of Materials Science: Materials in Electronics* (Vol. 31, Issue 5). https://doi.org/10.1007/s10854-020-02994-8

Parker, A. L., Benguigui, M., Fornetti, J., Goddard, E., Lucotti, S., Insua-Rodríguez, J., & Wiegmans, A. P. (2022). Current challenges in metastasis research and future innovation for clinical translation. *Clinical and Experimental Metastasis*, *39*(2). https://doi.org/10.1007/s10585-021-10144-5

PATIL, N., BHASKAR, R., VYAVHARE, V., DHADGE, R., KHAIRE, V., & PATIL, Y. (2021). OVERVIEW ON METHODS OF SYNTHESIS OF NANOPARTICLES. *International Journal of Current Pharmaceutical Research*. https://doi.org/10.22159/ijcpr.2021v13i2.41556

Peréz, D. Ll., Puentes, I., Romero, G. A. M., Gaona, I. M. S., Vargas, C. A. P., & Rincón, R. J. (2024). Synthesis of superparamagnetic iron oxide nanoparticles coated with polyethylene glycol as potential drug carriers for cancer treatment. *Journal of Nanoparticle Research*, *26*(1). https://doi.org/10.1007/s11051-023-05900-5

Pérez-Tijerina, E., Gracia Pinilla, M., Mejía-Rosales, S., Ortiz-Méndez, U., Torres, A., & José-Yacamán, M. (2008). Highly size-controlled synthesis of Au/Pd nanoparticles by inert-gas condensation. *Faraday Discussions*, *138*. https://doi.org/10.1039/b705913m

Perucca, P., Savio, M., Cazzalini, O., Mocchi, R., Maccario, C., Sommatis, S., Ferraro, D., Pizzala, R., Pretali, L., Fasani, E., Albini, A., & Stivala, L. A. (2014). Structure-activity relationship and role of oxygen in the potential antitumour activity of fluoroquinolones in human epithelial cancer cells. *Journal of Photochemistry and Photobiology B: Biology*, *140*. https://doi.org/10.1016/j.jphotobiol.2014.07.006

Peterson, T. R., Sengupta, S. S., Harris, T. E., Carmack, A. E., Kang, S. A., Balderas, E., Guertin, D. A., Madden, K. L., Carpenter, A. E., Finck, B. N., & Sabatini, D. M. (2011). MTOR complex 1 regulates lipin 1 localization to control the srebp pathway. *Cell*, *146*(3). https://doi.org/10.1016/j.cell.2011.06.034

Pham, T. D. M., Ziora, Z. M., & Blaskovich, M. A. T. (2019). Quinolone antibiotics. In *MedChemComm* (Vol. 10, Issue 10). https://doi.org/10.1039/c9md00120d

Porstmann, T., Santos, C. R., Griffiths, B., Cully, M., Wu, M., Leevers, S., Griffiths, J. R., Chung, Y. L., & Schulze, A. (2008). SREBP Activity Is Regulated by

mTORC1 and Contributes to Akt-Dependent Cell Growth. *Cell Metabolism*, *8*(3). https://doi.org/10.1016/j.cmet.2008.07.007

Pourali, P., Badiee, S. H., Manafi, S., Noorani, T., Rezaei, A., & Yahyaei, B. (2017). Biosynthesis of gold nanoparticles by two bacterial and fungal strains, Bacillus cereus and Fusarium oxysporum, and assessment and comparison of their nanotoxicity in vitro by direct and indirect assays. *Electronic Journal of Biotechnology*, *29*. https://doi.org/10.1016/j.ejbt.2017.07.005

Quinteros, M. A., Bonilla, J. O., Alborés, S. V., Villegas, L. B., & Páez, P. L. (2019). Biogenic nanoparticles: Synthesis, stability and biocompatibility mediated by proteins of Pseudomonas aeruginosa. *Colloids and Surfaces B: Biointerfaces*, *184*. https://doi.org/10.1016/j.colsurfb.2019.110517

Rai, M., Yadav, A., & Gade, A. (2009). Silver nanoparticles as a new generation of antimicrobials. In *Biotechnology Advances* (Vol. 27, Issue 1). https://doi.org/10.1016/j.biotechadv.2008.09.002

Rani, K., & Paliwal, S. (2014). A Review on Targeted Drug Delivery: its Entire Focus on Advanced Therapeutics and Diagnostics. *Scholars Journal of Applied Medical Sciences*, *2*(1).

Rarokar, N., Yadav, S., Saoji, S., Bramhe, P., Agade, R., Gurav, S., Khedekar, P., Subramaniyan, V., Wong, L. S., & Kumarasamy, V. (2024). Magnetic nanosystem a tool for targeted delivery and diagnostic application: Current challenges and recent advancement. In *International Journal of Pharmaceutics: X* (Vol. 7). https://doi.org/10.1016/j.ijpx.2024.100231

Rizwan, M., Faisal, S., Tariq, M. H., Zafar, S., Khan, A., & Ahmad, F. (2023). Enterobacter hormaechei-Driven Novel Biosynthesis of Tin Oxide Nanoparticles and Evaluation of Their Anti-aging, Cytotoxic, and Enzyme Inhibition Potential. *ACS Omega*, *8*(30). https://doi.org/10.1021/acsomega.3c02932

Rodriguez, M. J., Perrone, M. C., Riggio, M., Palafox, M., Salinas, V., Elia, A., Salgueiro, N. D., Werbach, A. E., Marks, M. P., Kauffman, M. A., Vellón, L., Serra, V., & Novaro, V. (2023). Targeting mTOR to overcome resistance to hormone and CDK4/6 inhibitors in ER-positive breast cancer models. *Scientific Reports*, *13*(1). https://doi.org/10.1038/s41598-023-29425-y

Sadhasivam, S., Shanmugam, P., Veerapandian, M., Subbiah, R., & Yun, K. (2012). Biogenic synthesis of multidimensional gold nanoparticles assisted by Streptomyces hygroscopicus and its electrochemical and antibacterial properties. *BioMetals*, *25*(2). https://doi.org/10.1007/s10534-011-9506-6

Sæbø, I. P., Bjørås, M., Franzyk, H., Helgesen, E., & Booth, J. A. (2023). Optimization of the Hemolysis Assay for the Assessment of Cytotoxicity.

International Journal of Molecular Sciences, *24*(3). https://doi.org/10.3390/ijms24032914

Sajid, M., & Płotka-Wasylka, J. (2020). Nanoparticles: Synthesis, characteristics, and applications in analytical and other sciences. In *Microchemical Journal* (Vol. 154). https://doi.org/10.1016/j.microc.2020.104623

Salehirozveh, M., Dehghani, P., & Mijakovic, I. (2024). Synthesis, Functionalization, and Biomedical Applications of Iron Oxide Nanoparticles (IONPs). In *Journal of Functional Biomaterials* (Vol. 15, Issue 11). Multidisciplinary Digital Publishing Institute (MDPI). https://doi.org/10.3390/jfb15110340

Sanad, M. F., Meneses-Brassea, B. P., Blazer, D. S., Pourmiri, S., Hadjipanayis, G. C., & El-Gendy, A. A. (2021). Superparamagnetic fe/au nanoparticles and their feasibility for magnetic hyperthermia. *Applied Sciences (Switzerland)*, *11*(14). https://doi.org/10.3390/app11146637

Saravanan, A., Kumar, P. S., Karishma, S., Vo, D. V. N., Jeevanantham, S., Yaashikaa, P. R., & George, C. S. (2021). A review on biosynthesis of metal nanoparticles and its environmental applications. *Chemosphere*, *264*. https://doi.org/10.1016/j.chemosphere.2020.128580

Sarbassov, D. D., Guertin, D. A., Ali, S. M., & Sabatini, D. M. (2005). Phosphorylation and regulation of Akt/PKB by the rictor-mTOR complex. *Science*, *307*(5712). https://doi.org/10.1126/science.1106148

Sawyers, C. (2004). Targeted cancer therapy. In *Nature* (Vol. 432, Issue 7015, pp. 294–297). https://doi.org/10.1038/nature03095

Saxton, R. A., & Sabatini, D. M. (2017). mTOR Signaling in Growth, Metabolism, and Disease. In *Cell* (Vol. 168, Issue 6). https://doi.org/10.1016/j.cell.2017.02.004

Schneider, M. G. M., Martín, M. J., Otarola, J., Vakarelska, E., Simeonov, V., Lassalle, V., & Nedyalkova, M. (2022). Biomedical Applications of Iron Oxide Nanoparticles: Current Insights Progress and Perspectives. In *Pharmaceutics* (Vol. 14, Issue 1). https://doi.org/10.3390/pharmaceutics14010204

Schwaminger, S. P., Syhr, C., & Berensmeier, S. (2020). Controlled synthesis of magnetic iron oxide nanoparticles: Magnetite or maghemite? *Crystals*, *10*(3). https://doi.org/10.3390/cryst10030214

Shah, A., Aftab, S., Nisar, J., Ashiq, M. N., & Iftikhar, F. J. (2021). Nanocarriers for targeted drug delivery. In *Journal of Drug Delivery Science and Technology* (Vol. 62). https://doi.org/10.1016/j.jddst.2021.102426

Shi, L., Zhang, J., Zhao, M., Tang, S., Cheng, X., Zhang, W., Li, W., Liu, X., Peng, H., & Wang, Q. (2021). Effects of polyethylene glycol on the surface of nanoparticles for targeted drug delivery. In *Nanoscale* (Vol. 13, Issue 24). https://doi.org/10.1039/d1nr02065j

Shi, Y., Frankel, A., Mills, G. B., Radvanyi, L. G., Miller, R. G., & Penn, L. Z. (1995). Rapamycin Enhances Apoptosis and Increases Sensitivity to Cisplatin in Vitro. *Cancer Research*, *55*(9), 1982–1988.

Singh, N. A., Narang, J., Garg, D., Jain, V., Payasi, D., Suleman, S., & Swami, R. K. (2023). Nanoparticles synthesis via microorganisms and their prospective applications in agriculture. In *Plant Nano Biology* (Vol. 5). https://doi.org/10.1016/j.plana.2023.100047

Sin, S. H., Roy, D., Wang, L., Staudt, M. R., Fakhari, F. D., Patel, D. D., Henry, D., Harrington, W. J., Damania, B. A., & Dittmer, D. P. (2007). Rapamycin is efficacious against primary effusion lymphoma (PEL) cell lines in vivo by inhibiting autocrine signaling. *Blood*, *109*(5). https://doi.org/10.1182/blood-2006-06-028092

Soulard, A., Cohen, A., & Hall, M. N. (2009). TOR signaling in invertebrates. *Current Opinion in Cell Biology*, *21*(6), 825–836. https://doi.org/10.1016/j.ceb. 2009.08.007

Sousa, E. J., Graça, I., Baptista, T., Vieira, F. Q., Palmeira, C., Henrique, R., & Jerónimo, C. (2013). Enoxacin inhibits growth of prostate cancer cells and effectively restores microRNA processing. *Epigenetics*, *8*(5). https://doi.org/10.4161/epi.24519

Spirescu, V. A., Chircov, C., Grumezescu, A. M., & Andronescu, E. (2021). Polymeric nanoparticles for antimicrobial therapies: An up-to-date overview. In *Polymers* (Vol. 13, Issue 5). https://doi.org/10.3390/polym13050724

S. S., P., BHAT, M. P., & NAYAKA, S. (2021). MICROBIAL SYNTHESIS OF SILVER NANOPARTICLES USING STREPTOMYCES SP. PG12 AND THEIR CHARACTERIZATION, ANTIMICROBIAL ACTIVITY AND CYTOTOXICITY ASSESSMENT AGAINST HUMAN LUNG (A549) AND BREAST (MCF-7) CANCER CELL LINES. *International Journal of Pharmacy and Pharmaceutical Sciences*. https://doi.org/10.22159/ijpps.2021v13i8.41876

Sterner, R. C., & Sterner, R. M. (2021). CAR-T cell therapy: current limitations and potential strategies. In *Blood Cancer Journal* (Vol. 11, Issue 4). https://doi.org/10.1038/s41408-021-00459-7

Strober, W. (2015). Trypan Blue Exclusion Test of Cell Viability. *Current Protocols in Immunology*, *111*(1). https://doi.org/10.1002/0471142735.ima03bs111

Tenchov, R., Bird, R., Curtze, A. E., & Zhou, Q. (2021). Lipid Nanoparticles from Liposomes to mRNA Vaccine Delivery, a Landscape of Research Diversity and Advancement. In *ACS Nano* (Vol. 15, Issue 11). https://doi.org/10.1021/acsnano.1c04996

Thanki, K., Gangwal, R. P., Sangamwar, A. T., & Jain, S. (2013). Oral delivery of anticancer drugs: Challenges and opportunities. In *Journal of Controlled Release* (Vol. 170, Issue 1). https://doi.org/10.1016/j.jconrel.2013.04.020

Thiruppathi, R., Mishra, S., Ganapathy, M., Padmanabhan, P., & Gulyás, B. (2017). Nanoparticle functionalization and its potentials for molecular imaging. *Advanced Science*, *4*(3). https://doi.org/10.1002/advs.201600279

Thomanetz, V., Angliker, N., Cloëtta, D., Lustenberger, R. M., Schweighauser, M., Oliveri, F., Suzuki, N., & Rüegg, M. A. (2013). Ablation of the mTORC2 component rictor in brain or Purkinje cells affects size and neuron morphology. *Journal of Cell Biology*, *201*(2). https://doi.org/10.1083/jcb.201205030

Tonthat, L., Kimura, M., Ogawa, T., Kitamura, N., Kobayashi, Y., Gonda, K., & Yabukami, S. (2023). Development of gold-coated magnetic nanoparticles as a theranostic agent for magnetic hyperthermia and CT imaging applications. *AIP Advances*, *13*(2). https://doi.org/10.1063/9.0000592

Torino, F., Barnabei, A., Paragliola, R., Baldelli, R., Appetecchia, M., & Corsello, S. M. (2013). Thyroid dysfunction as an unintended side effect of anticancer drugs. In *Thyroid* (Vol. 23, Issue 11). https://doi.org/10.1089/thy.2013.0241

Tortora, G. J., Funke, B. R., & Case, C. L. (2010). Microbiology an Introduction 10th ed. *Pearson Education. Inc, USA*, *578*.

Unni, N., & Arteaga, C. L. (2019). Is Dual mTORC1 and mTORC2 Therapeutic Blockade Clinically Feasible in Cancer? In *JAMA Oncology* (Vol. 5, Issue 11). https://doi.org/10.1001/jamaoncol.2019.2525

Upadhyay, K., Tamrakar, R. K., Thomas, S., & Kumar, M. (2023a). Surface functionalized nanoparticles: A boon to biomedical science. In *Chemico-Biological Interactions* (Vol. 380). https://doi.org/10.1016/j.cbi.2023.110537

Upadhyay, K., Tamrakar, R. K., Thomas, S., & Kumar, M. (2023b). Surface functionalized nanoparticles: A boon to biomedical science. *Chemico-Biological Interactions*, *380*, 110537. https://doi.org/10.1016/J.CBI.2023.110537

Vander Heiden, M. G., & DeBerardinis, R. J. (2017). Understanding the Intersections between Metabolism and Cancer Biology. In *Cell* (Vol. 168, Issue 4). https://doi.org/10.1016/j.cell.2016.12.039

Van Meerloo, J., Kaspers, G. J. L., & Cloos, J. (2011). Cell sensitivity assays: The MTT assay. *Methods in Molecular Biology*, *731*. https://doi.org/10.1007/978-1-61779-80-5_20

Venkatas, J., Daniels, A., & Singh, M. (2022). The Potential of Curcumin-Capped Nanoparticle Synthesis in Cancer Therapy: A Green Synthesis Approach. In *Nanomaterials* (Vol. 12, Issue 18). https://doi.org/10.3390/nano12183201

Vijayaram, S., Razafindralambo, H., Sun, Y. Z., Vasantharaj, S., Ghafarifarsani, H., Hoseinifar, S. H., & Raeeszadeh, M. (2024). Applications of Green Synthesized Metal Nanoparticles — a Review. In *Biological Trace Element Research* (Vol. 202, Issue 1). https://doi.org/10.1007/s12011-023-03645-9

Wang, L., Luo, J., Fan, Q., Suzuki, M., Suzuki, I. S., Engelhard, M. H., Lin, Y., Kim, N., Wang, J. Q., & Zhong, C. J. (2005). Monodispersed core-shell Fe 3O 4@Au nanoparticles. *Journal of Physical Chemistry B*, *109*(46), 21593–21601. https://doi.org/10.1021/jp0543429

Wang, W., Wei, Q. Q., Wang, J., Wang, B. C., Zhang, S. hui, & Yuan, Z. (2013). Role of thiol-containing polyethylene glycol (thiol-PEG) in the modification process of gold nanoparticles (AuNPs): Stabilizer or coagulant? *Journal of Colloid and Interface Science*, *404*, 223–229. https://doi.org/10.1016/J.JCIS.2013.04.020

Xie, J., Yang, Z., Zhou, C., Zhu, J., Lee, R. J., & Teng, L. (2016). Nanotechnology for the delivery of phytochemicals in cancer therapy. In *Biotechnology Advances* (Vol. 34, Issue 4). https://doi.org/10.1016/j.biotechadv.2016.04.002

Xi, J., & Ma, C. X. (2020). Sequencing Endocrine Therapy for Metastatic Breast Cancer: What Do We Do After Disease Progression on a CDK4/6 Inhibitor? In *Current Oncology Reports* (Vol. 22, Issue 6). https://doi.org/10.1007/s11912-020-00917-8

Yadav, V., Sultana, S., Yadav, J., & Saini, N. (2012). Gatifloxacin Induces S and G2-Phase Cell Cycle Arrest in Pancreatic Cancer Cells via p21/p27/p53. *PLoS ONE*, *7*(10). https://doi.org/10.1371/journal.pone.0047796

Yadav, V., & Talwar, P. (2019). Repositioning of fluoroquinolones from antibiotic to anti-cancer agents: An underestimated truth. In *Biomedicine and Pharmacotherapy* (Vol. 111). https://doi.org/10.1016/j.biopha.2018.12.119

Yadav, V., Varshney, P., Sultana, S., Yadav, J., & Saini, N. (2015). Moxifloxacin and ciprofloxacin induces S-phase arrest and augments apoptotic effects of cisplatin in human pancreatic cancer cells via ERK activation. *BMC Cancer*, *15*(1). https://doi.org/10.1186/s12885-015-1560-y

Yazdani, F., & Seddigh, M. (2016). Magnetite nanoparticles synthesized by co-precipitation method: The effects of various iron anions on specifications. *Materials Chemistry and Physics*, *184*. https://doi.org/10.1016/j.matchemphys.2016.09.058

Yi, S., Xia, L., Lenaghan, S. C., Sun, L., Huang, Y., Burris, J. N., Stewart, C. N., & Zhang, M. (2013). Bio-synthesis of gold nanoparticles using English ivy (hedera helix). *Journal of Nanoscience and Nanotechnology*, *13*(3). https://doi.org/10.1166/jnn.2013.7183

Yoon, M. S. (2017). The role of mammalian target of rapamycin (mTOR) in insulin signaling. In *Nutrients* (Vol. 9, Issue 11). https://doi.org/10.3390/nu9111176

Yu, F., Zhang, Z., Li, W., Tian, H., Xu, J., & Bao, Y. (2020). Synthesis and evaluation of moxifloxacin derivatives for effects on proliferation and apoptosis of NCI-H1299 cells. *Tetrahedron Letters*, *61*(21). https://doi.org/10.1016/j.tetlet.2020.151873

Yu, M., Li, R., & Zhang, J. (2016). Repositioning of antibiotic levofloxacin as a mitochondrial biogenesis inhibitor to target breast cancer. *Biochemical and Biophysical Research Communications*, *471*(4). https://doi.org/10.1016/j.bbrc.2016.02.072

Zhang, C., Zeng, C. C., Lai, S. H., Xing, D. G., Li, W., Han, B. J., & Liu, Y. J. (2016). Synthesis, cytotoxicity in vitro, apoptosis, cell cycle arrest and comet assay of asymmetry ruthenium(II) complexes. *Polyhedron*, *106*. https://doi.org/10.1016/j.poly.2015.12.058

Zhao, X., Xu, C., Domagala, J., & Drlica, K. (1997). DNA topoisomerase targets of the fluoroquinolones: A strategy for avoiding bacterial resistance. *Proceedings of the National Academy of Sciences of the United States of America*, *94*(25). https://doi.org/10.1073/pnas.94.25.13991

Zhu, L., Li, X. X., Shi, L., Wu, J., Qian, J. Y., Xia, T. S., Zhou, W. Bin, Sun, X., Zhou, X. J., Wei, J. F., & Ding, Q. (2019). Rapamycin enhances the sensitivity of ER-positive breast cancer cells to tamoxifen by upregulating p73 expression. *Oncology Reports*, *41*(1). https://doi.org/10.3892/or.2018.6842

Zielinska, A., Carreiró, F., Oliveira, A. M., Neves, A., Pires, B., Nagasamy Venkatesh, D., Durazzo, A., Lucarini, M., Eder, P., Silva, A. M., Santini, A., & Souto, E. B. (2020). Polymeric Nanoparticles: Production, Characterization, Toxicology and Ecotoxicology. In *Molecules* (Vol. 25, Issue 16). https://doi.org/10.3390/molecules25163731

Zugazagoitia, J., Guedes, C., Ponce, S., Ferrer, I., Molina-Pinelo, S., & Paz-Ares, L. (2016). Current Challenges in Cancer Treatment. In *Clinical Therapeutics* (Vol. 38, Issue 7). https://doi.org/10.1016/j.clinthera.2016.03.026

APPENDIX

1. Starch Casein (SC) Agar (1000mL)

Starch soluble	10g
Casein	1g
Sea water	37mL
Agar	15g
Amphotericin B	10mg
Erythromycin	25mg

2. Glycerol Yeast Extract (GYE) Agar (1000mL)

Yeast extract	2g
glycerol	10mL
Agar	15g
Amphotericin B	10mg
Erythromycin	25mg

2. Malt Extractglucose Yeast Extract Peptone (MGYP) agar (1000mL)

malt extract	3g
glucose	10g
Yeast extract	3g
Peptone	5g
Agar	20g

4. PI staining solution for flow cytometry

DNase-free RNase A	2mg/mL

Propidium iodide	500 µg/mL

5. RPMI – 1640medium

RPMI powder	10.4g
FBS	10% v/v
Sodium bicarbonate	2g
Streptomycin	100 µg/mL
Penicillin	100 U/mL

6. TBE (1000mL)

Tris base	54g
Boric acid	27.5g
EDTA (0.5m)	20mL

7. Phosphate Buffered Saline (1X, pH 7.4)

NaCl	8g
KCl	0.2g
Na_2HPO_4	1.44g
KH_2PO_4	0.25g
Distilled water	1000mL

8. Bradford reagent

Coomassie blueg-250	10mg
95% ethanol	5mL
85% phosphoric acid	10mL
Distilled water	85mL (final volume)

9. Acrylamide (30%, pH < 7.0)

Acrylamide	29g
Bis acrylamide	1g
Distilled water	100mL (final volume)

Note: Filtered before use.

10. Tris HCl (1.5m, pH 8.8)

Tris base	18.171g
Distilled water	100mL

Note: Adjusted to required pH with concentrated HCl.

11. Tris HCl (0.5m, pH 6.8)

Tris base	6.057g
Distilled water	100mL

Note: Adjusted to required pH with concentrated HCl.

12. SDS Running buffer/ Laemmli buffer (pH 8.3, 10X)

Tris base	15g
Glycine	72g
SDS	5g
Distilled water	500mL

13. SDS sample buffer (4X, 10ml)

Tris HCl (pH 6.8)	0.25M (5mL from the0.5M stock)
SDS	8% (0.8g)
2-ME	10% (100µL/900µL of sample buffer)
Glycerol	30% (3mL)
Bromophenol blue	0.02% (2mg)
Distilled water	1mL

14. Gel recipe for SDS-PAGE

14.1. Resolving gel (12.5%)

30% Acrylamide	3.33mL
1.5mM Tris HCl (pH, 8.8)	2mL
Distilled water	2.5mL

SDS	80 µL
APS	80 µL
TEMED	8 µL

14.2. Stackinggel (6%)

30% Acrylamide	0.5mL
0.5mM Tris HCl (pH 6.8)	0.625mL
Distilled water	1.3mL
SDS	25 µL
APS	25 µL
TEMED	2.5 µL

15. Dulbecco'smodified Eaglemedium (DMEM)

DMEM powder	10g
FBS	100mL (10% v/v)
Sodium bicarbonate	3.7g
Streptomycin	100mg
Penicillin	66mg
Gentamycin	50mg
Amphotericin	2.5mg
Distilled water	900mL

16. PBS-EDTA (1X, pH 7.4)

NaCl	8g
KCl	0.2g
Na_2HPO_4	1.44g
KH_2PO_4	0.25g
EDTA	0.4g
Distilled water	1000mL

17. Trypsin-EDTA

Hanks BSS	2.375g
$NaHCO_3$	0.0875g
Trypsin	62mg
EDTA	39mg
Streptomycin	25mg
Penicillin	16.5mg
Gentamycin	125mg
Distilled water	250mL

18. Alexa Fluor® Annexin V binding buffer (pH 7.4)

HEPES	10mM
NaCl	140mM
$CaCl_2 .2H_2O$	2.5mM

19. WCL buffer

Tris HCl (1M, pH 7.4)	20 µL
NaCl (5m)	50 µL
EDTA (0.5m)	4 µL
DTT (0.1m)	10 µL
Triton X (10% v/v)	10 µL
AP (10mg/mL)	5 µL
LP (1mg/mL)	5 µL
PMSF (17.4mg/mL in ethanol)	5 µL
NaV (1.83mg/mL)	8 µL
Distilled water	916 µL

20. Tris buffered saline (TBS, 10X, pH 7.6)

Tris base	12.1g

NaCl	40g
Distilled water	500mL (final volume)

21. TBST (1X)

TBS (10X)	50mL
Tween 20	2mL
Distilled water	450mL

22. Blotting buffer (Towbin buffer/Transfer buffer)

Tris base	3.03g
Glycine	14.4g
Methanol	200mL

LIST OF PUBLICATIONS

Journal

1. Koothradan, S. & Elyas, K.K. Biogenically produced gold nanoparticles containing a Fluoroquinolone molecule from the cell-free extract of E. hormaechei soil isolates with anti-bacterial and anti-cancer properties. Inorganic Chemistry Communications (178-2025). https://doi.org/10.1016/j.inoche. 2025.114536

2. Koothradan, S., Nayeem, S. & Elyas, K.K. PEGylated iron oxide-gold core-shell nanoparticles for tumor-targeted delivery of Rapamycin. 3 biotech 15, 23 (2025). https://doi.org/10.1007/s 13205-024- 04189-y

3. Koothradan S, Elyas K.K. Immunoinformatic evaluation of the cross-presentation of donor major histocompatibility derived epitopes by recipient major histocompatibility class I molecules in transplantation rejection. Indian J Transplant 2023; 17:418 24. https://doi.org/10.4103/ijot.ijot_4_22

Book chapter

1. **Suhana Koothradan** and K K Elyas (2023), Nanotechnology and Nanobiotechnology for a sustainable environment, Fundamental Applications of Biochemistry in the Environment, PG Department of Chemistry, KAHM Unity Women's College, Manjeri, Kerala-676122, India. **ISBN: 978-93-5737-783-6**

CONFERENCES

1. **Suhana Koothradan,** Safia Nayeem, Elyas K. K. PEGylated iron oxide-gold core-shell nanoparticles as tumor-targeted drug delivery system; a study using Rapamycin- National conference on Omics in redefining healthcare-ORAH -August 2024, held at Jubilee center for Medical Research, Thrissur, Kerala.

2. **Suhana Koothradan,** Safia Nayeem, Elyas K. K. Tumor-targeted drug delivery system based on PEGylated Iron oxide-gold core-shell nanoparticles; a study using Rapamycin- International conference on advanced research, INSIGHT– February 2024, held at MES KEYVEEYAM College, Valancheri, Kerala

3. **Suhana Koothradan**, Feroz Aziz, k Elyas K. K. Analysis of donor MHC antigen cross-presentation by recipient MHC class I molecules in organ transplantation; an immunoinformatics approach- The international conference on agriculture, climate change & life sciences – march 2021, held by IMRF, Andhra Pradesh

4. **Suhana Koothradan** and Elyas K. K. Identification of MHC-class I epitopes from spike protein of Severe Acute Respiratory Syndrome-Coronavirus-2 (SARS-Cov-2) in Kerala population: an Immunoinformatics method. 33rd Kerala Science Congress, January 2021.